U 790 289
COPY 1

NSWC TR 79-289

AN EXPERIMENTAL STUDY OF TWO-DIMENSIONAL SUPERSONIC JET IMPINGEMENT ON A FLAT PLATE

BY T. F. ZIEN R. T. DRIFTMYER

RESEARCH AND TECHNOLOGY DEPARTMENT

24 AUGUST 1979

NAVAL SURFACE WEAPONS CENTER

Dahlgren, Virginia 22448 • Silver Spring, Maryland 20910

UNCLASSIFIED

SECURITY CLASSIFICATION OF THIS PAGE (When Data Entered)

REPORT DOCUMENTATION PAGE		READ INSTRUCTIONS BEFORE COMPLETING FORM
1. REPORT NUMBER NSWC TR 79-289	2. GOVT ACCESSION NO.	3. RECIPIENT'S CATALOG NUMBER
4. TITLE (and Subtitle) AN EXPERIMENTAL STUDY OF TWO-DIMENSIONAL SUPERSONIC JET IMPINGEMENT ON A FLAT PLATE		5. TYPE OF REPORT & PERIOD COVERED 6. PERFORMING ORG. REPORT NUMBER
7. AUTHOR(s) T. F. Zien and R. T. Driftmyer		8. CONTRACT OR GRANT NUMBER(s)
9. PERFORMING ORGANIZATION NAME AND ADDRESS Naval Surface Weapons Center White Oak Silver Spring, Maryland 20910		10. PROGRAM ELEMENT, PROJECT, TASK AREA & WORK UNIT NUMBERS 61153N; A320 320C/004A/ 9R-23-02-003; 0; 0
11. CONTROLLING OFFICE NAME AND ADDRESS		12. REPORT DATE 24 Aug 1979 13. NUMBER OF PAGES 95
14. MONITORING AGENCY NAME & ADDRESS(if different from Controlling Office)		15. SECURITY CLASS. (of this report) Unclassified 15a. DECLASSIFICATION/DOWNGRADING SCHEDULE

16. DISTRIBUTION STATEMENT (of this Report)

Approved for public release, distribution unlimited

17. DISTRIBUTION STATEMENT (of the abstract entered in Block 20, if different from Report)

18. SUPPLEMENTARY NOTES

19. KEY WORDS (Continue on reverse side if necessary and identify by block number)

Jet Flow, Jet Impingement, Pressure Measurement, Two-dimensional Flows

20. ABSTRACT (Continue on reverse side if necessary and identify by block number)

An experimental study of the flow field associated with a two-dimensional, supersonic jet impinging normally on a flat plate is reported. Two wedge nozzles manufactured at the design Mach numbers of 1.75 and 2.75, respectively, were used to provide the jet. Extensive pitot surveys of the free jet were first conducted to determine the quality of the free jet. Results indicate that the simple wedge nozzles were adequate in providing the desired two-dimensional jet in the free expansion configuration. Results of

surface pressure measurements and schlieren photographs of the impingement flow indicating the shock patterns are then presented and discussed. Although the results are principally reported for the case of the jet at isentropic exit conditions, some results of underexpanded and overexpanded jets are also included. Some discrepancies between the experiment and the simple theory based in the method of integral relations and the inviscid flow model are noted and discussed. An "effective" jet Mach number is introduced which accounts largely for the discrepancy between experiments and theory, and its determination is based on the measured stagnation point pressure on the plate surface.

SUMMARY

This work represents the continuing efforts in the study of shock interference heating phenomena associated with the operation of most Navy tactical missiles. It was supported by the Naval Air Systems Command, AIR 320C Airtask No. A320320C/004A/9R023-02-003, under the cognizance of Mr. W. C. Volz whose encouragement is greatly appreciated. The authors also gratefully acknowledged some enlightening discussions with Dr. B. L. Hunt of the University of Bristol, England.

Paul R. Wessel

PAUL R. WESSEL
By direction

CONTENTS

ILLUSTRATIONS

ILLUSTRATIONS (Cont.)

1. INTRODUCTION

The primary motivation of the present study is to gain some basic understanding of the anomalous heating experienced by many tactical missiles flying at supersonic speeds, generally known as the shock-interference heating. When an extraneous shock wave impinges on a body in supersonic flight, it interferes with the basic bow shock of the body. This interference is believed to be responsible for the severe heating and sharp pressure rise observed in the experiments (see, for example, References 1-5). The incident shock may originate from an external source, or it may be generated within the flow field of the aerodynamic body itself, such as the shock caused by boundary-layer separation ahead of a compression ramp. The problem is obviously of practical importance because most aerodynamic configurations in practical use are, to a varying degree, susceptible to such interference phenomena. Examples include space shuttle, winged bodies, missile with control fins, etc.

After a careful and extensive experimental study of the problem, Edney[1] has classified the shock-interference patterns into six possible types depending on the orientation of the incident shock and the position of the impingement point relative to the basic bow shock. Among them, the type IV interference is found to lead to the most severe heating and pressure peaks. A peak heating rate as high as 17 times the interference-free stagnation point value together with a peak pressure of about 8 times the free-stream pitot pressure has been measured by Hains and Keyes[2] in a configuration where the type IV interference pattern is expected to occur. Characteristic to the type IV interference is the impingement of a supersonic jet on the body where the jet is produced by the interference between the impinging shock and the bow shock.

It is therefore clear that a good understanding of the supersonic jet-impingement problem is essential to the understanding of the overall aerodynamic heating associated with the shock-interference phenomena. In the present project, effort was first expended in developing a simple, approximate theory for the flow

1. Edney, B., "Anomalous Heat Transfer and Pressure Distributions on Blunt Bodies at Hypersonic Speeds in the Presence of an Impinging Shock," FFA Report 115, The Aeronautical Research Institute of Sweden, Stockholm, 1968.
2. Hains, F. D. and Keyes, J. W., "Shock Interference Heating in Hypersonic Flows," AIAA Journal, Vol. 10, No. 11, Nov 1972, pp. 1441-1447.
3. Heirs, R. S. and Loubsky, W. J., "Effects of Shock-Wave Impingement on the Heat Transfer on a Cylindrical Leading Edge," NASA TN D-3859, Ames Research Center, Moffet Field, Calif., 1967.
4. Kaufman, L. G., III, Karkegi, R. H. and Morton, L. C., "Shock Impingement Caused by Boundary Layer Separation Ahead of Blunt Fins," ARL TR 72-0118, Aerospace Research Laboratories, WPAFB, Ohio, 1972.
5. Gillerlain, J. D., Jr., "Experimental Investigation of a Fin-Cone Interface Flow Field at Mach 5," NSWC/WOL/TR 75-63, Naval Surface Weapons Center, White Oak Laboratory, Silver Spring, Md., 1976.

associated with the supersonic jet impingement on a flat plate. The flow was assumed inviscid and the jet was assumed to be uniform and isentropic. A detailed description of the theoretical work can be found in Chien[6].

The present report contains the detailed results of an experimental study of the jet-impingement flow field. The experiment was intended as a verification of the approximate theory. The jet was produced by two simple wedge-nozzles at two design Mach numbers of 1.75 and 2.75, respectively, and the experiment was conducted in a two-dimensional configuration. Results reported here include the survey of the free jet, surface pressure distribution on the plate, and schlieren photographs of the shock wave pattern. Comparison with theory is made whenever appropriate. Although the results are mainly presented and discussed for the case of an isentropic jet, some surface pressure measurements made with underexpanded and overexpanded jets are also reported here.

Related experiments of supersonic jet impingement flows previously reported include the work of Hunt and others[7,8] for the axisymmetric jet and Pollard and Bradbury[9] for the two-dimensional jet. The work of Ref. (9) was carried out in relation to V/STOL applications, and the emphasis was placed on the case of relatively large nozzle-to-surface distances when turbulent mixing and viscous entrainment by the jet were important. On the other hand, we are concerned with the situation where the ratio of the nozzle-to-surface distance to the nozzle exit width is about unity and the viscous effects are believed to be of secondary importance.

It is noted here that the highlights of the results included in this report were presented earlier as Ref. 10 where a brief description of the theoretical work was also given.

---

6. Chien, K.-Y., "Normal Impingement of a Supersonic Jet on a Plane--A Basic Study of Shock-Interference Heating," NSWC/WOL/TR 75-195, Naval Surface Weapons Center, White Oak Laboratory, Silver Spring, Md., 1975.
7. Gummer, J. H. and Hunt, B. L., "The Impingement of a Uniform, Axisymmetric, Supersonic Jet on a Perpendicular Flat Plate," The Aeronautical Quarterly, Vol. 22, Pt. 4, Nov 1971, pp. 403-420.
8. Carling, J. C. and Hunt, B. L., "The Near Wall Jet of a Normally Impinging, Uniform, Axisymmetric, Supersonic Jet," Journal of Fluid Mechanics, Vol. 66, Pt. 1, 1974, pp. 159-176.
9. Pollard, D. J. and Bradbury, L. J. S., "Impingement of a Two-Dimensional Supersonic Jet upon a Normal Ground Surface," AIAA Journal, Vol. 14, No. 8, Aug 1976, pp. 1095-1098.
10. Zien, T. F., Chien, K.-Y. and Driftmyer, R. T., "Two-Dimensional Supersonic Jet Impingement on a Flat Plate," AIAA Paper 78-208, AIAA 16th Aerospace Sciences Meeting, Huntsville, Alabama, Jan 1978. Also, AIAA Journal, Vol. 17, No. 1, Jan 1979, pp. 4-5.

2. DESCRIPTION OF EXPERIMENT

2.1 EXPERIMENTAL HARDWARE AND SETUP. Two stainless steel wedge nozzles were manufactured at the design Mach numbers of 1.75 and 2.75, respectively, to provide for the supersonic jets used in the experiment. The aerodynamic design of the nozzle was based on the simple inviscid, one-dimensional flow model for air (perfect gas, $\gamma = 1.405$). The nozzles have the same exit width of 3.81 cm (1½ in.) and the same exit area of 3.81 cm x 5.08 cm (1½ in. x 2 in.). The semi-wedge angle was 2° 13' for the Mach 1.75 nozzle, and 5° 34' for the Mach 2.75 nozzle. A sketch of the nozzle is shown in Fig. 1, and the drawing of the Mach 1.75 nozzle block holder is shown in Fig. 2.

The test plate used in the jet-impingement experiment was made of stainless steel, and instrumented with a row of five pressure taps evenly spaced across a 2.54 cm (1 in.) span in the center portion of the plate (entire plate width = 5.74 cm (2.26 in.))*. The pressure taps were aligned in the depth direction of the nozzle block in order to determine the two-dimensionality of the impingement flow field in the experiment. The end view of the test plate showing the pressure taps is given in Fig. 3. Two glass ported side plates were rigidly fixed to the edges of test plate to constrain the flow in order to achieve the desired two-dimensionality. These side plates were made of schlieren quality glass so that photographs could be taken of the impinging jet and the associated shock system. The clearance between the outside of the nozzle block holder and the inside of the glass ported side plates was on the order of the thickness of a sheet of tablet paper. The entire test plate/side plates assembly was connected to an axial traverse mechanism with controlled translational motion, and the assembly was made to slide relative to the (stationary) nozzle during the measurement. A continuous pressure signature on the test plate was thus recorded. Because of the relative motion between the walls of the nozzle block and the glass side plate anticipated in the run and the small clearance in the contact surfaces, special care was exercised in aligning the nozzle block with the side plates to ensure a non-interfering relative motion. The plate/nozzle package used in the experiment is shown in Fig. 4a (only one side plate is shown). Also shown in Fig. 4a are two static pressure probes in their respective positions during the run. There were two pairs of such probes located symmetrically with respect to the nozzle symmetry plane. P_{e1} measured the exit pressure of the jet, and was used in determining the exit conditions (isentropic, underexpanded, or overexpanded) of the jet, and P_{e2} was taken also to give some idea of the pressure gradient existing in the test chamber during each run. This pressure gradient is significant in interpreting the experimental data because it is indicative of the nonuniformity in the ambient conditions unaccounted for by the theory. The nonuniformity was expected especially in the surface pressure tests where it was conceivably difficult for the semi-confined flow field to accommodate the added mass of air from the jet while maintaining a constant and uniform ambient condition as required by the theory. A more complete view of the nozzle-mate-side-mate assembly is shown in Fig. 4b.

---

*The plate width was made to be the same as the nozzle block depth which was necessarily larger than the nozzle exit depth (5.08 cm) because of the thickness of the block. Only a minor three-dimensionality of the impingement flow near the edges of the test plate is expected, and this will be discussed in light of the experimental results (Section 3).

The nozzle/plate assembly was installed in the test section of the Supersonic Wind Tunnel No. 2 at the Naval Surface Weapons Center with the nozzle axis aligned in the vertical direction perpendicular to the (horizontal) test plate. An overall view of the experimental apparatus is shown in Fig. 5. We note that the primary reason for choosing this facility to conduct our experiment was to take advantage of the existing vacuum capacity of the tunnel to control the back pressure of the jet. Other mechanical and optical accessories for routine tunnel operations provided the additional convenience, but the original aerodynamic characteristics of the wind tunnel were largely irrelevant to the present experiment.

The test air was supplied from bottle-filled air normally stored at pressures up to 3000 psia. The stagnation chamber pressure in this experiment was controlled by a dome loader control valve located outside the wind tunnel test cell. In the Mach 2.75 test series, an electric resistance heater was installed in the piping system between the control valve and the stagnation chamber so that the stagnation temperature of the air could be raised sufficiently to eliminate possible condensation problems in the expansion through the nozzle.

A pitot rake assembly was designed and manufactured with five 0.159 cm (1/16 in.) O.D. stainless steel tubes as pitot probes. The five probes were aligned in the same direction as the pressure taps on the test plate. The probes extended vertically upward and were spaced 0.635 cm (1/4 in.) apart, center to center. The pitot rake was used to survey the free jet, in the absence of the test plate/side plate package. When surveying the free jet, the rake was fastened to the axial traverse mechanism of the wind tunnel, and was moved across the width of the nozzle exit in a controlled manner.

All pressure measurements were made with the strain gage type pressure transducers. The stagnation temperature was measured with a copper-constantan thermocouple referenced to 0°C.

2.2 EXPERIMENTAL PROCEDURE

2.2.1 Pitot Survey. The experiment with each nozzle began with a pitot survey of the free jet, using the pitot rake described in section 2.1, to establish the actual Mach number and to determine the uniformity and quality of the two-dimensional jet. The survey was made at two distances downstream of the nozzle exit, Δ_2 = 0.3175 cm (1/8 in.) and Δ_2 = 2.54 cm (1 in.), in an effort to determine any possible changes in the properties of the jet during its passage through the quiescent air.

In the pitot survey of the free jet, the test plate and the side plates were removed, and the pitot rake was carefully installed at the desired distance below the nozzle exit plane. The jet was free to expand and exhaust into a large opening. The stagnation chamber pressure was first set at a desired value, and the vacuum pump was turned on to reduce the pressure in the test cell of the wind tunnel until the reading of P_{e1} reached the value approximately equal to the exit pressure for an (one-dimensional) isentropic expansion of the stagnant air to the design Mach number. P_0 and P_{e1} were held constant when the rake traversed the width of the nozzle exit at a speed of 1.905 cm/min (0.75 in./min). The survey was conducted at two values of the stagnation pressure, P_0, for each value of Δ_2. The test cell was then opened, and the rake was moved manually to a new position corresponding to the second value of Δ_2. The stagnation pressure, P_0, was reset and the vacuum operation was repeated in preparation of the pitot survey at the new value of Δ_2. The pitot traverse covered the entire width of the nozzle exit plane, i.e., 3.81 cm (1½ in.) for each value of Δ_2, and schlieren photographs were taken at selected positions of the pitot rake during its traverse.

2.2.2 Surface Pressure Distribution. Upon completion of the pitot survey of a wedge nozzle, the pitot rake was removed from the test cell of the wind tunnel, and the test plate/side plate package was carefully assembled and installed in the test chamber. The distance between the nozzle exit plane and the surface of the test plate, Δ_1, was predetermined using the theoretical predictions of Ref. (6) as a guide. The value of Δ_1 was selected such that the plate shock would appear within the distance Δ_1. Note that too large a value of Δ_1 would introduce unwanted complications into the jet-impingement flow field, such as viscous entrainment, and hence caused unnecessary difficulties in analyzing the data. For each jet Mach number, two values of Δ_1 were used in the surface pressure measurements. The adjustment of Δ_1 was achieved by moving the stagnation chamber-nozzle block assembly along a vertical slot located in the stagnation chamber mounting bracket while the test plate remained in its fixed elevation.

An important parameter of the test is the pressure ratio, π, which determines the exit condition of the jet. It is defined as the ratio of the nozzle exit pressure for isentropic exit condition, $(P_e)_{isen}$, to the actual pressure maintained at the nozzle exit during the test, $(P_e)_{actual}$, i.e.

$$\pi \equiv \frac{(P_e)_{isent.}}{(P_e)_{actual}}$$

As mentioned in section 2.1, P_{e1} was taken to be $(P_e)_{actual}$ in our experiment. Thus, $\pi = 1$ corresponds to the case of an isentropic jet, whereas $\pi > 1$ and $\pi < 1$ correspond to underexpanded jet and overexpanded jet, respectively.

In the present experiment, surface pressure measurements were taken for all three types of the impinging jet. Detailed results will be presented only for the case of a nearly isentropic jet in this paper, as the theoretical analysis of the problem was made only for this case. A brief discussion on the results of impingement of a non-isentropic jet will also be given.

Nozzle No. 1 (designed Mach number = 1.75) was used in the first test series. The value of Δ_1 was first set to be 5.08 cm (2 in.) for which extensive surface pressure data were taken. The nozzle block was then lifted to give a value of Δ_1 = 6.35 cm (2½ in.), and some pressure data were recorded. In this series of experiment, it was relatively easy to adjust the stagnation pressure, P_0, and the exit pressure, P_{e1}, independently to yield the desired values for π.

In the experiment with nozzle No. 2 (designed Mach number = 2.75), two series of tests were run. In the first series, some good schlieren photographs were obtained but, unfortunately, no surface pressure data were recorded due to a mechanical failure. Only the readings of P_0 and P_{e1} (and also P_{e2}) were available, and the photographs were used to provide the data of shock shape and location. A second series had to be run using the same nozzle to obtain the surface pressure distribution. Although both photographic data and pressure data were obtained in the second series, the quality of the photographs was not sufficiently good to allow for a quantitative analysis. It was then decided to present the photographic data of the first series and the surface pressure data of the second series in this paper. Since both series were run with the same nozzle, the photographic data of the first series should correspond to the jet Mach number determined by the pitot survey of the second series.

It is noted here that in the course of the experiment with the second nozzle, difficulty was encountered in obtaining the correct exit pressure, P_{e1} (and P_{e2}), for an isentropic jet (π = 1) at a given P_0 when the nozzle-to-plate distance, Δ_1, was smaller than 4.445 cm (1 3/4 in.). It was not possible to bring the P_{e1} reading down to the desired value for a fixed P_0 setting. For example, in the first test series when Δ_1 was set at 3.175 cm (1¼ in.) and P_0 at 1598 mmHg, the lowest P_{e1} we could get was 128 mmHg, (P_{e2} = 17 mmHg) corresponding to $\pi \approx 0.48$, even when a more powerful vacuum pump was turned on; P_{e1} seemed to be controlled by P_0 and could no longer be adjusted independently. At a larger separation distance of Δ_2 = 4.445 cm, it was again possible to adjust the values of P_0 and P_{e1} independently to give any desired values of π, including the case of special interest, i.e. $\pi \approx 1$. Since the impinging jet was supersonic, and the test plate and the nozzle exit was separated by a visible plate shock, the apparent influence of the plate on the (upstream) condition at the nozzle exit was not expected from a theoretical standpoint. However, since the flow field was semi-confined (as opposed to infinite) in the experiment because of the presence of the side plates, the added mass from the air jet to the confined space was likely to build up the pressure near the nozzle exit. Increasing Δ_1 implies an increase in the flow field dimension, and should therefore alleviate the difficulty.

The surface pressure measurements associated with the second nozzle were made with Δ_1 = 4.445 cm (1 3/4 in.) and Δ_1 = 5.08 cm (2 in.).

All the pressure data were recorded on tape using the existing data acquisition system. The recording rate was 8 samples per second. The pressure transducers were calibrated using a mercury manometer with photo-electric detector equipment to set the pressures. At least five pressures were set for each pressure calibration. A least-square-fit was then applied to the data, and a linear calibration curve was obtained for all cases. Tare values were taken before and after each run to account for any transducer shifts.

3. EXPERIMENTAL RESULTS.

3.1 NOZZLE NO. 1

3.1.1 Free Jet Pitot Survey. Four runs were made to survey the jet at two different stagnation pressure settings, P_0, and two different distances from the nozzle exit, Δ_2, using the pitot rake described in section 2.1. The test matrix is shown in the following table.

Table 1. Pitot Survey of Free Jet - Nozzle No. 1

Run No.	P_o (psia)	P_e (psia)	Δ_2 (in)	(M_j)Ave.
13	9.26	1.64	1	1.85
15	6.09	1.10	1	1.83
17	6.13	1.09	1/8	1.84
19	9.70	1.74	1/8	1.85

During these free jet survey runs, the back pressure inside the test chamber was set at approximately the value corresponding to the isentropic exit pressure for the design Mach number of 1.75.

The pitot pressure variations measured in Runs 19 and 15 are shown in Figs. 6 and 7, respectively. Here, variations of the total pressure in both the width direction and the depth direction are shown. The Mach number variation can easily be deduced from the pitot pressure distribution by means of the tables of Ref. (11) assuming that the total pressure upstream of the normal shock of the pitot tube is the same as the stagnation pressure, p_o. The Mach number variations corresponding to Figs. 6 and 7 are shown in Figs. 8 and 9, respectively. In addition, the free jet Mach number distributions corresponding to Runs 17 and 13 are also obtained, and shown in Figs. 10 and 11.

Schlieren photographs of the pitot survey were taken during each run, and representative photographs corresponding to Runs 13, 15, 17 and 19 are reproduced and shown in Figs. 12-15, respectively.

From the results of the survey, a reasonable assessment of the quality of the jet produced by the simple wedge nozzle can be made. As shown in Fig. 6 the total pressure measured by the middle three pitot probes (i.e. pitot Nos. 2, 3 and 4) was uniform to within 5% across the most part of the nozzle width, except near the edges ($\tilde{x} \approx \pm 1$) where some three-dimensional effects were expected. The variation of the total pressure in the depth direction was also limited to about 5% with the maximum variation occurring near the symmetry plane ($\tilde{x} = 0$). The corresponding Mach number variation (Fig. 8) was found roughly the same as the total pressure variation. The Mach number variation measured near the exit plane but at a lower p_o, i.e., Run 17 was in very close agreement with that of Run 19, (see Fig. 10). The average free jet Mach number, M_j, for nozzle No. 1 was thus determined to be 1.85. However it should be borne in mind that the local values of M_j near the exit plane actually varied from 1.82 to 1.92, excluding the values near the edges of the nozzle width where the rapid expansion around the corner apparently resulted in much higher Mach numbers.

11. Ames Research Staff, "Equations, Tables, and Charts for Compressible Flow," NACA Report 1135, 1953.

In a distance of 1 in. downstream of the nozzle exit, the free jet Mach number stayed practically the same, as a comparison between Figs. 8, 10 and Figs. 9, 11 suggests. We also note that the nozzle boundary layer apparently had very little effect on the jet, as the Mach number distribution near the nozzle exit was essentially the same for the two runs with different stagnation pressures (therefore difference Reynolds numbers) based on a comparison between Figs. 8 and 10.

A mild drop in M_j in the vicinity of the symmetry plane (Fig. 8) is perhaps attributable to the oblique shocks originated inside the nozzle, which are faintly visible as a small triangle near the center of the nozzle exit in Figs. 12-15. However, the shocks if indeed existed, seemed too weak to warrant any concern. Note also that the hump flattens out when the pitot measurements were taken outside the small triangular region, as shown in Fig. 11.

3.1.2 <u>Surface Pressure Measurements: $\pi \approx 1$</u>. Fig. 16 summarizes the surface pressure data obtained in the test with Nozzle No. 1 for $\pi \approx 1$. The surface pressure was measured by five pressure taps, P_1 through P_5, along the depth of the nozzle. Characteristically, the readings of the three middle taps, P_2, P_3 and P_4 agreed to within about 3% in the region of interest, $-1 \leq \tilde{x} \leq 1$, and the readings of P_1 and P_5 generally differed by 6∿10% from the three middle ones in this region. This suggests that some three-dimensional effects were still present despite the use of the side plates. Therefore, it was decided to disregard the readings of P_1 and P_5, and use the average readings of P_2, P_3 and P_4 for the surface pressure data. This was the procedure used in the data analysis for both nozzles.

It should be noted here that if the readings of the two end pitot probes were also disregarded in evaluating the average jet Mach number in consistence with the procedure used in reducing surface pressure data, the value of M_j would be about 1.82, and the values for π under the listed test conditions would be very close to one. It is therefore felt that the results in Fig. 16 correspond to a nearly isentropic jet.

The pressure data of the three different runs with Δ_1 = 5.08 cm are seen to agree very closely, and the expected symmetry in the data with respect to the nozzle symmetry plane is clearly visible. Therefore, the good quality of the experimental results and their high reproducibility seem assured. The data with Δ_1 = 6.35 cm are also included in Fig. 16 to indicate the effect of Δ_1 on the surface pressure distribution. Note that in the ideal case of a uniform, isentropic, inviscid jet as assumed in the theory, Δ_1, should have no effect on the flow. However, in the experiment, the effect seemed to exist as the data showed a distinct, though slight, deviation from those of the other three runs. The effect of Δ_1 on surface pressure apparently becomes more pronounced for an underexpanded jet ($\pi > 1$) as will be discussed later.

We note here that in the course of this series of experiment, the second static pressure probe near the nozzle exit was not installed and therefore readings of P_{e2} were not available.

3.1.3 <u>Plate-Shock Measurements</u>. Schlieren photographs were taken of the impingement flow which showed the position and the shape of the impingement shock wave, referred to here as the plate shock. The photographs of Run 23 and 37 show the shock wave clearly, and were used to measure the shock shape and shock position relative to the plate. These two photographs are reproduced in Fig. 17 (Run 23) and Fig. 18 (Run 37). The shock location was measured from these photographs, and the results are shown in Fig. 19 where Δ_s is the vertical distance of the shock measured from the plate surface. The results of the two runs appear to be less consistent than the results of surface pressure for the corresponding runs.

3.1.4 Surface Pressure Measurements: $\pi > 1$. Two runs (No. 41 and No. 63) were made with the back pressure maintained at a substantially lower value than the corresponding value for isentropic expansion so that the exit jet was in an underexpanded condition. The degree of expansion was chosen to be roughly the same ($\pi \approx 3.9$ based on $M_j = 1.85$) whereas the values of Δ_1 were different (5.08 cm for Run 41 and 6.35 cm for Run 63). The effect of Δ_1 on the surface pressure can thus be determined. The results are shown in Fig. 20. It is clear that the plate-to-nozzle distance has a considerable influence on surface pressure, as opposed to the case of a nearly isentropic jet (Fig. 16). The effect appears particularly pronounced in the region near the stagnation point.

A plausible explanation of this result can perhaps be given in terms of the interaction of the expansion waves emanating from the nozzle edges due to the severe underexpansion of the jet. At a larger value of Δ_1 (Run 63), the plate shock is expected to be farther away from the nozzle exit plane, allowing the expansion waves from the two edges to interact near the symmetry plane upstream of the plate-shock. The interaction results in an increased jet Mach number and hence a stronger shock. As a consequence, the normalized surface pressure in the region near the stagnation point is lower than that for a smaller Δ_1 (Run 41). This finding is in accordance with that of Gummer and Hunt[12] in their study of the underexpanded axisymmetric jet impingement problem.

The surface pressure results corresponding to a slightly underexpanded impinging jet ($\pi \approx 1.3$) at two values of Δ_1 are shown in Fig. 21. In this case of minor underexpansion, the interaction between the expansion waves mentioned above is apparently too weak to change the flow field structure, and the normalized surface pressure near the stagnation point is practically the same for the two values of Δ_1. On the other hand, the viscous effects here apparently dominated the inviscid effects of wave interaction. In Run 59 where Δ_1 = 2 1/2 in., the jet traveled a longer distance upstream of the shock than the jet in Run 44 (Δ_1 = 2 in.) and the viscous effects appeared to have decreased its effective Mach number more, resulting in a slightly weaker shock (and thus slightly higher normalized surface pressure readings). However, it must be noted that a quantitative assessment of these effects is not possible with the presently available data.

3.1.5 Surface Pressure Measurements: $\pi < 1$. In this series of measurements, the case of the impingement of an overexpanded jet was also studied in which the jet exit pressure was maintained at a value higher than that required for isentropic exit condition. Here, a system of complicated shock waves was expected near the nozzle exit, and the associated impingement flow becomes extremely complex. The results of surface pressure measurement of one run at $\pi \approx 0.46$ are shown in

12. Gummer, J. H. and Hunt, B. L., "The Impingement of Non-Uniform, Axisymmetric, Supersonic Jets on a Perpendicular Flat Plate," Israel Journal of Technology, Vol. 12, 1974, pp. 221-235.

Fig. 22. While results are not extensive enough to show the effects of various parameters, the figure does suggest that the Mach number of the impinging jet was somewhat lower than that of the case where $\pi \geq 1$, because the surface pressure at the stagnation point in this case was the highest among all ranges of π studied. The lower value of the jet Mach number is, of course, attributable to the presence of various shock waves upstream of the plate shock. Perhaps coincidentally, the "effective" jet Mach number in this case based on the stagnation pressure on the plate was roughly the same as the design Mach number of the jet, 1.85.

3.2 NOZZLE NO. 2

3.2.1 Free Jet Pitot Survey. As in the test series of Nozzle No. 1, four runs were made to survey the free jet using the pitot rake described in section 2.1. The test matrix is shown in the following table.

Table 2. Pitot Survey of Free Jet - Nozzle No. 2

Run No.	P_o (psia)	T_o (°R)	P_e (psia)	Δ_2 (in.)	$(M_j)_{Ave.}$
5	20.2	537	0.722	1/8	2.78
6	15.11	547	0.535	1/8	2.77
9	20.1	540	0.725	1	2.87
10	14.98	552	0.554	1	2.87

Pitot results for Run 5 and Run 9 are shown in Fig. 23 and Fig. 24, respectively, and the corresponding Mach number distributions are deduced using the tables of Ref. 11, as in Section 3.1.1. The Mach number variations for the four runs are shown in Figs. 25-28. Generally speaking, the degree of uniformity of the free jet is roughly the same as that of the Nozzle No. 1 jet. Disregarding the readings of the two end probes (i.e., No. 1 and No. 5) as in the case of Nozzle No. 1, the Mach number variation across the nozzle width near the exit plane (Figs. 25 and 26) was about 3% or less for $0.8 < |\tilde{x}| < 1$. Again the characteristic drop of M_j away from $\tilde{x} = 0$ as discussed in Section 3.1.1 is visible, suggesting the possible existence of weak oblique shocks originated inside the wedge nozzle. We note that in Figs. 25 and 26, and also in Figs. 24, 27 and 28, the readings of the pitot probes No. 2 and No. 4 are not shown, because they are very close to those of the center probe, No. 3. This implies that the uniformity of the jet in the nozzle depth direction was also very good. It should be noted here that the jet appeared to have gone through a noticeable expansion in a distance of 1 in., as the average jet Mach number changed from 2.77 to 2.87 between a distance of 1/8 in. and 1 in. from the exit plane (see Table 2). This percentage increase in M_j, though still within the percentage variation in the jet width and depth directions, was not observed in the free jet of Nozzle No. 1. It was perhaps due to the larger wedge angle of this nozzle ($\theta_w = 5°34'$ compared to 2°13' of Nozzle No. 1).

3.2.2 Surface Pressure Measurements: $\pi \sim 1$. Fig. 33 shows the results of the surface pressure measurements for a nearly isentropic jet. Three runs were made at different stagnation pressures and a fixed plate-to-nozzle distance,

Δ_1 = 4.445 cm (1 3/4 in.). As in the case of nozzle No. 1, the readings of the two end pressure taps P_1 and P_5 were discarded because of their excessive deviation from the readings of the three middle taps. The deviation seemed considerably larger in this series of test (lower than the middle readings by as much as 25%) than in the series of nozzle No. 1. However, the agreement among P_2, P_3 and P_4 continued to be very good (typically, 3-5%).

The readings of P_0, P_{e1} and P_{e2} all remained practically constant during all runs. However, a considerable difference in the readings of P_{e1} and P_{e2} was always present in each of these runs, indicating the existence of nonuniformity in the ambient conditions.

As can be seen from Fig. 33, the expected symmetry of the surface pressure distribution and the close agreement among the data of the three runs at different stagnation pressures continued to exist in this series of test.

Another set of surface pressure measurements was taken at a larger plate-to-nozzle, Δ_1 = 2 in., but with the jet still at approximately isentropic exit condition. The results are shown in Fig. 34. The effect of Δ_1 on surface pressure distribution at this M_j is similar to the previous series with M_j = 1.85, except that it appears more pronounced at this higher M_j. Here, the stagnation point pressure (non-dimensional) is appreciably lower than that with Δ_1 = 1 3/4 in., suggesting the presence of a continuing expansion of the jet after the nozzle exit. This finding is consistent with the speculation made on the basis of free-jet pitot-survey results in Section 3.2.1.

3.2.3 Plate-Shock Measurements. Schlieren photographs of the impingement flow field were obtained in a separate (first) series of experiment where no surface pressure data were recorded due to a mechanical failure of the data acquisition procedure. Two representative schlieren photographs, Run 135 and Run 145, are reproduced in Figs. 35 and 36, both being at nearly isentropic jet condition ($\pi \approx 1$):

Run 135: P_0 = 21.8 psia, P_{e1} = 0.81 psia, P_{e2} = 0.67 psia, Δ_1 = 1 3/4 in.

Run 145: P_0 = 21.1 psia, P_{e1} = 0.77 psia, P_{e2} = 0.62 psia, Δ_1 = 1 3/4 in.

We note that although schlieren pictures were also taken of the second series of experiment with Nozzle No. 2, those pictures were not of good enough quality for use in quantitative analysis of the shock waves. The shock measurements for the Nozzle No. 2 experiment were thus entirely based on the pictures of the first series, i.e., Run 135 and Run 145.

The result of the shock measurements is shown in Fig. 37. Again, we see that the agreement of the shock wave measurements between the two runs is not as good as the surface pressure results. The maximum discrepancy was found to be in the vicinity of the symmetry plane, $\tilde{x} = 0$.

3.2.4 Pitot Survey of the Impinging Jet. The properties of the impinging jet in the presence of the test flat plate and the two side plates during the measurement of surface pressure distribution might be different from those measured in the open configuration of a freely expanding jet where the test plate and the side plates were removed. The difference was suspected when the surface pressure results of both nozzles were analyzed, as the stagnation pressure on the plate surface indicated a Mach number considerably different from that of the corresponding free jet. It was therefore decided to conduct a pitot survey of the impinging jet in the impingement configuration.

A single-tube pitot apparatus was used in this experiment, and a view of the arrangement is included in Fig. 4. The tube was fastened on a flat plate which was in turn clamped onto the test plate during this series of the measurement. The axial traverse mechanism thus provided the controlled movement to the tube as it traversed the nozzle width. The distance between the surface of the new plate and the nozzle exit plane was set at Δ_1 = 1 3/4 in. The pitot tube was first set at a distance 1/8 in. downstream of the nozzle exit (Δ_2 = 1/8 in.). It was then cut from the tip after each run to provide the surveys at different values of Δ_2, while the values of P_o and P_e were maintained at approximately the same for all runs in this series. The experiment was designed to provide qualitative information only, and the measuring device was not nearly as precise as that used in the previous measurements. We note here that the plate shock, in the absence of the single pitot tube, was expected to be at a distance of about 1 in. from the plate at the center line $\tilde{x} = 1$, according to the plate shock measurements of Section 3.2.3. This means that for $\Delta_2 < 3/4$ in. in this series of experiments, the measurement should indicate a uniform jet under ideal conditions.

Results of the survey are shown in Figs. 38a - 42 for Δ_2 = 1/8 in., 15/32 in., 3/4 in., 15/16 in. and 1 7/16 in., respectively, with the corresponding schlieren photographs shown in Figs. 38b - 41b (no schlieren picture was taken of the last experiment with Δ_2 = 1 7/16 in.).

At Δ_2 = 1/8 in. (Fig. 38a), the impinging jet appeared to have roughly the free jet Mach number, i.e., $M_j = 2.77$ near $\tilde{x} = 0$, because the pitot readings were about the same as those of Run 5 and Run 6 of the free-jet pitot surveys. However, it is important to point out that unlike the case of a free jet, this value of M_j prevailed only in $|\tilde{x}| < 0.3$, outside which M_j appeared to have decreased rather substantially. Similar observations can be made from the results in Fig. 39a, (Δ_2 = 15/32 in.) which shows the situation further downstream of the exit. Here the region of uniform flow (near the center) is even narrower. As Δ_2 increases further (beyond 3/4 in.), the plate shock (in the absence of the pitot tube) would appear upstream of the pitot tube, and the interpretation of the pitot results becomes very difficult.

The above discussion of the pitot results is, at best, qualitative, and it is obviously based on the tacit assumption that the existence of the pitot tube in the flow field would not cause any noticeable change in the basic structure of the original impingement flow. The assumption becomes increasingly questionable when the pitot tube is imbedded in the impingement flow field, i.e. downstream of the plate shock.

4. DISCUSSION AND CONCLUSION

The measured surface pressure distribution and shock wave patterns of the impingement flow field associated with a nearly isentropic jet are all compared with the theoretical calculations[6] in Figs. 16, 19, 33 and 37.

In the comparison of the surface pressure results (Figs. 16 and 33), it is clear that the agreement is rather unsatisfactory if the theoretical results are based on the average Mach number of the free jet, $M_j = 1.85$ and $M_j = 2.77$, respectively, determined from the pitot surveys of the free jets. In particular, the measured surface pressures at the stagnation point, $x = 0$, do not correspond to the total pressure behind the normal shock at the respective free jet Mach numbers.

4.1 CORRECTION FOR EXPANSION OF JET AFTER EXIT. To account for this discrepancy, a simple analysis was first carried out to determine the "corrected" jet Mach number which takes into account the "radial" expansion of the jet after the exit plane. The analysis was based on a source flow model for inviscid air. The results are shown in Figs. 43 and 44 for Nozzle No. 1 and 2 respectively. The corrected Mach number, M_{jc}, plotted as a function of the distance from the exit plane, Δ, nondimensionalized by the half nozzle exit width, R.

In Nozzle No. 1 experiments with $\Delta_1 = 2$ in., the plate shock was approximately located at $\Delta_s = 1\ 1/2$ in. (see Fig. 19), which means $\Delta \approx 1/2$ in., as $\Delta/R \approx 2/3$. The corrected jet Mach number from Fig. 43 is about 1.87. The correction based on the inviscid source flow model is therefore seen to be not nearly enough to account for the discrepancy between theory and experiment. In the case of nozzle No. 2, with $\Delta_1 = 1\ 3/4$ in., the plate shock was approximately at $\Delta_s = 1$ in. (Fig. 37) which gives $\Delta \approx 3/4$ in., or $\Delta/R \approx 1$. M_{jc} in this case would be 2.86 which again fails to bring better agreement between theory and experiment.

4.2 "EFFECTIVE" JET MACH NUMBER. The difficulty is thus believed to be due to the complicated conditions under which the experiment was conducted, as opposed to the idealized conditions assumed in the theory. It is almost impossible to account for these complications in the experiments, and the introduction of an "effective" Mach number becomes necessary.

$(M_j)_{eff}$ is based on the measured surface pressure at the stagnation point, assuming isentropic flow between the plate and the downstream side of the shock caused by the plate. In fact, Gummer and Hunt(7) based the determination of their jet Mach number on such a pressure measurement in their axisymmetric jet impingement experiment, in the absence of a pitot survey of the free jet. The "effective" jet Mach number was found to be 2.10 in the experiment with the first nozzle and 2.60 in the experiment with the second nozzle. The theoretical surface pressure distributions based on $(M_j)_{eff}$ show reasonably good agreement with the measured distributions, especially near the stagnation point where the most severe heating is expected to take place.

In view of the uncertainties and nonuniformities existing in the ambient conditions of the experiment, notably the difficulty in maintaining a uniform back pressure in the semi-confined configuration used in the surface pressure measurement, it is difficult to expect that the impinging jet had a constant and uniform Mach number equal to that of the freely expanding jet. Other complications such as viscous effects which could become more pronounced in a confined space than in an open space could also contribute to the deviation of the Mach number of the jet from its free expansion value. Therefore the use of $(M_j)_{eff}$ in lieu of M_j in the comparison between theory and experiment does not seem unjustified. Note that $(M_j)_{eff}$ differs from M_j only by about 7% in the Mach 2.77 experiment, although the difference is in the reversed direction relative to that in the Mach 1.85 experiment.

4.3 SHOCK PATTERNS. The comparison of the shock location is shown in Figs. 19 and 37. Here the experimental data are not as consistent as the surface pressure data, and a considerable data scatter can be seen. The scatter reflects, among other things, the optical difficulty in photographing a flow field of a depth of 5.74 cm (the width of the test plate). The shock trace as shown in the schlieren photographs can, at best, be taken as the projection of the shock envelope averaged over the field depth.

The measured shock height is greater than the theoretical predictions based on the free jet Mach number, and the trend persists in the experiments with both nozzles. The use of the effective Mach number would improve the agreement for the Mach 2.77 case, but further deteriorate the agreement for the Mach 1.85 case. In light of the large scatter among the experimental data themselves, the comparison between theory and experiment on the shock shapes and locations must be viewed as inconclusive at present. It provides insufficient grounds either to affirm or to negate the concept of effective jet Mach number.

4.4 CONCLUSION. In conclusion, we enumerate the following observations based on the present study: (1) the simple wedge nozzles appear adequate for providing two-dimensional free jets of good quality; (2) the two-dimensionality of the plate pressure distribution in the jet-impingement experiment was achieved in the center portion of the plate in the present semi-confined configuration; (3) the semi-confined configuration apparently caused the Mach number of the impinging jet to deviate from its value based on the free expansion condition, and the "effective" jet Mach number of the impinging jet could be determined from the surface pressure at the stagnation point; (4) the simple approximate theory seems adequate to predict the pressure distribution on the plate surface; and (5) the considerable scatter in the measured shock shape and location makes it difficult to draw any definitive conclusions from the comparison between theory and experiment regarding the accuracy of the theory in predicting the shocks.

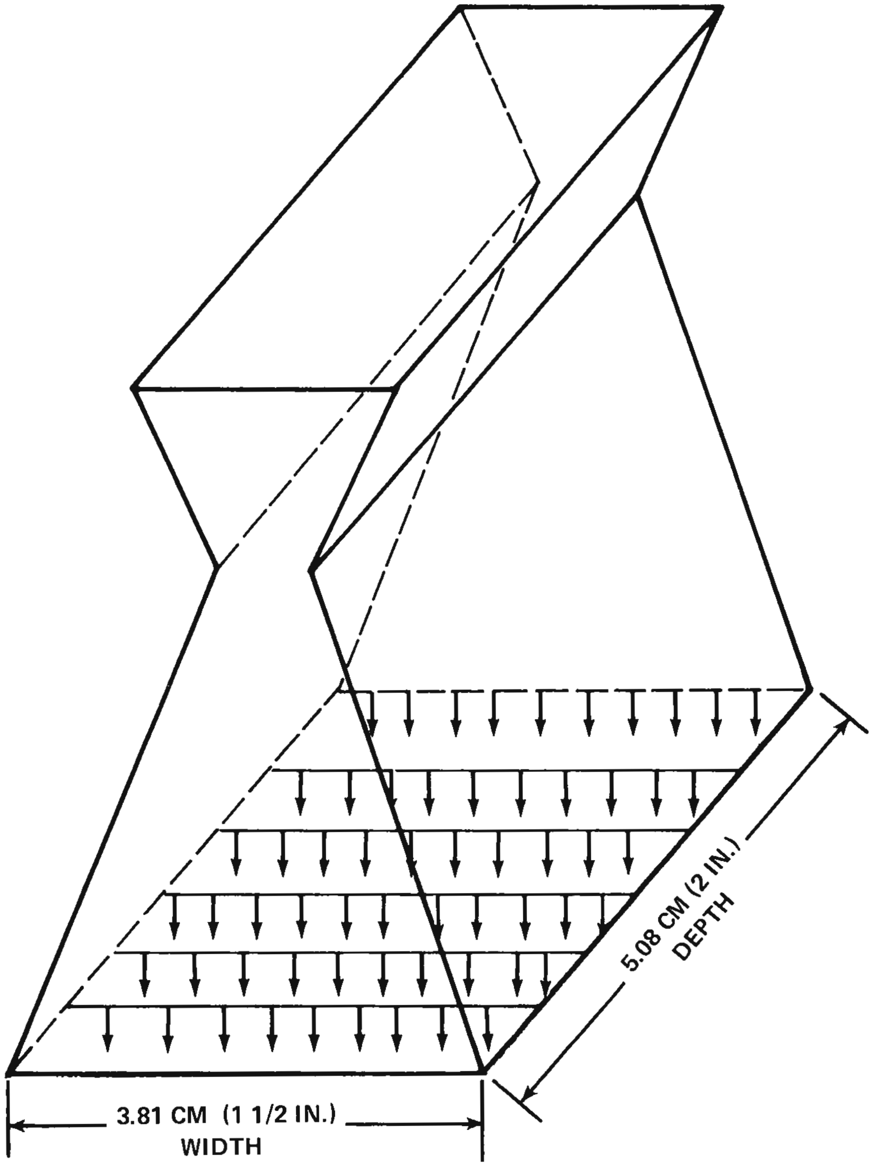

FIGURE 1 SKETCH OF WEDGE NOZZLES

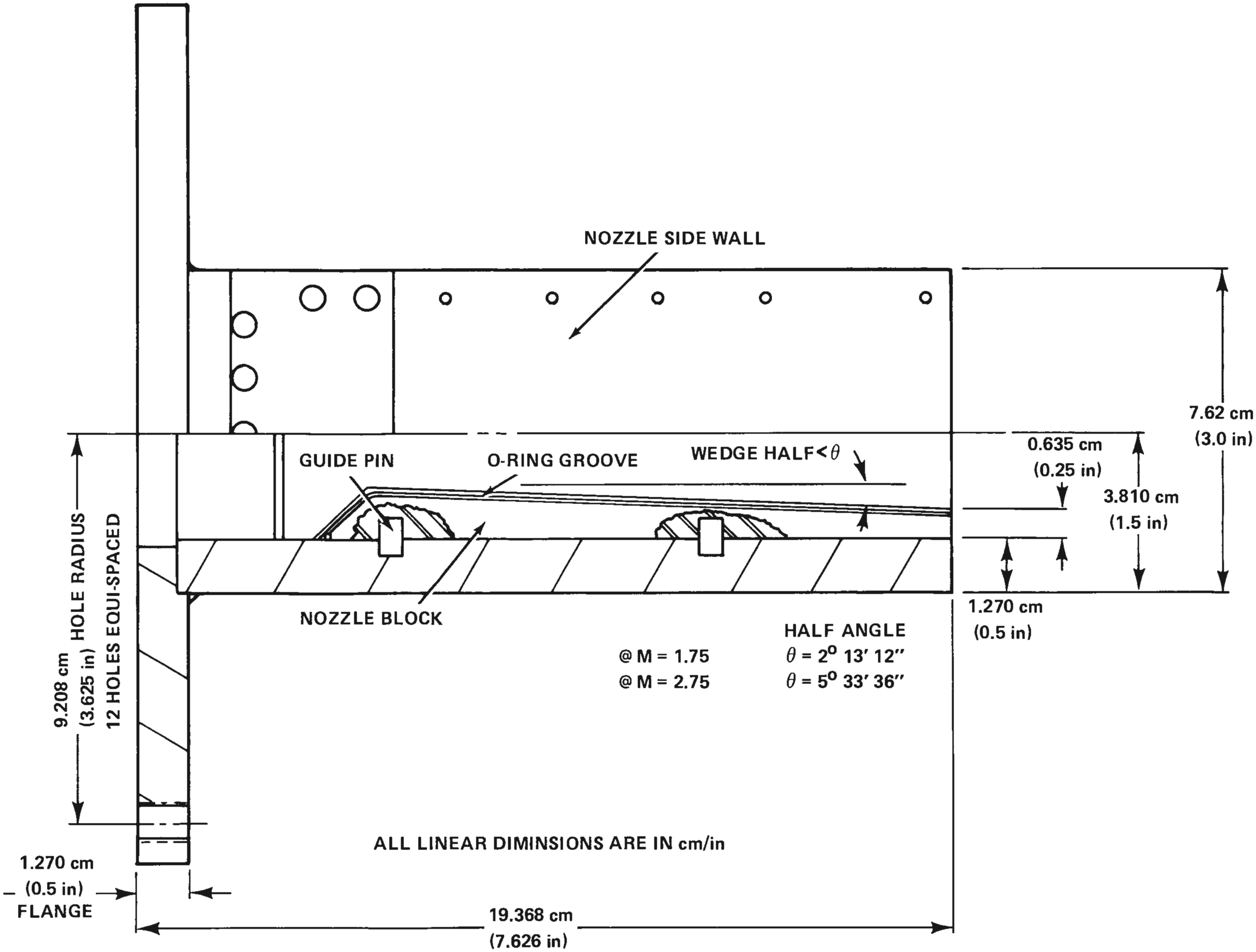

FIGURE 2 SKETCH OF NOZZLE BLOCK HOLDER SHOWING THE HALF-SECTIONED SIDE VIEW OF THE M = 1.75 NOZZLE BLOCK

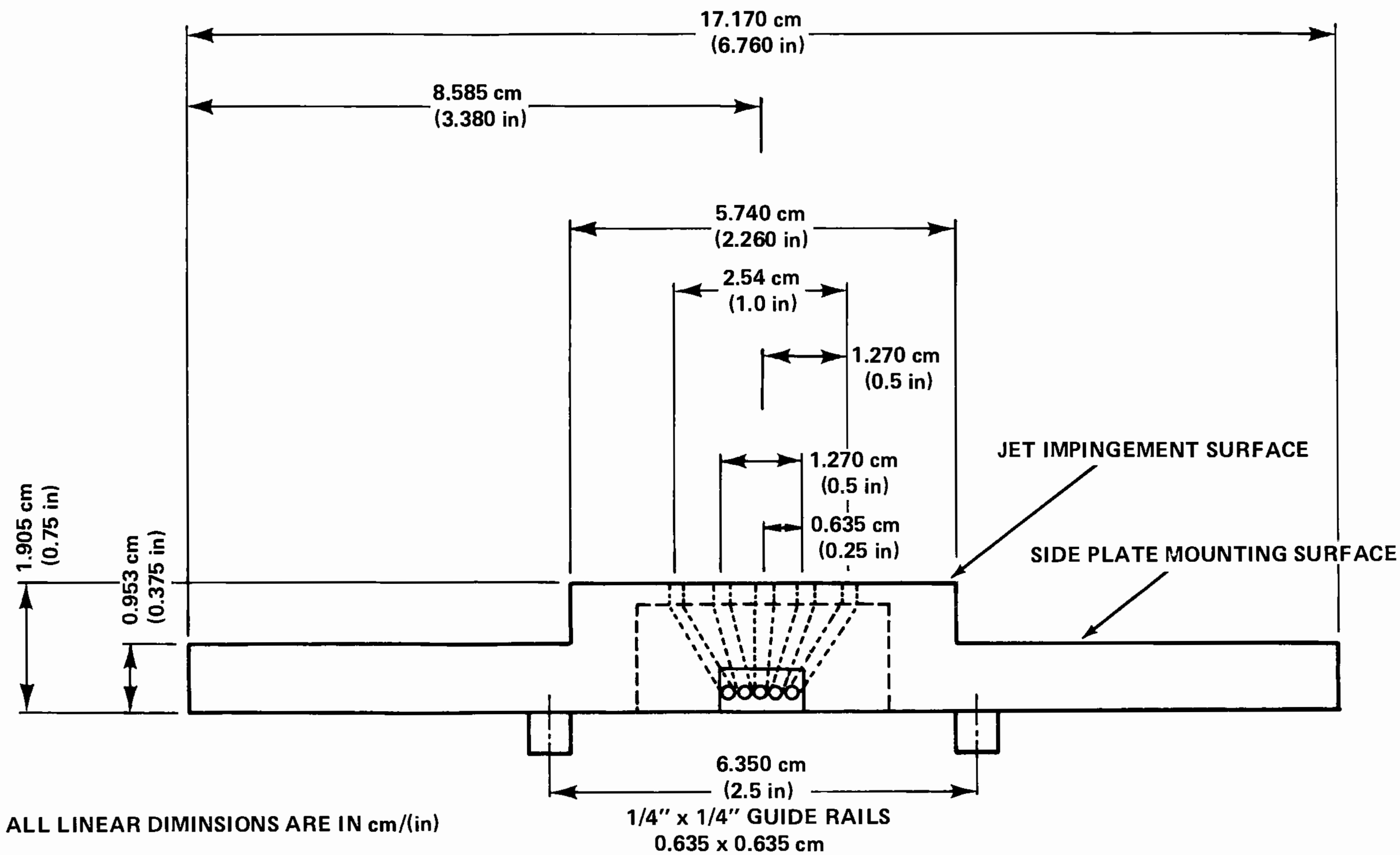

FIGURE 3 END VIEW OF SLIDING FLAT PLATE (WITHOUT SIDE PLATES) SHOWING STATIC SURFACE PRESSURE TAPS(0.0625 OD STAINLESS STEEL TUBING).

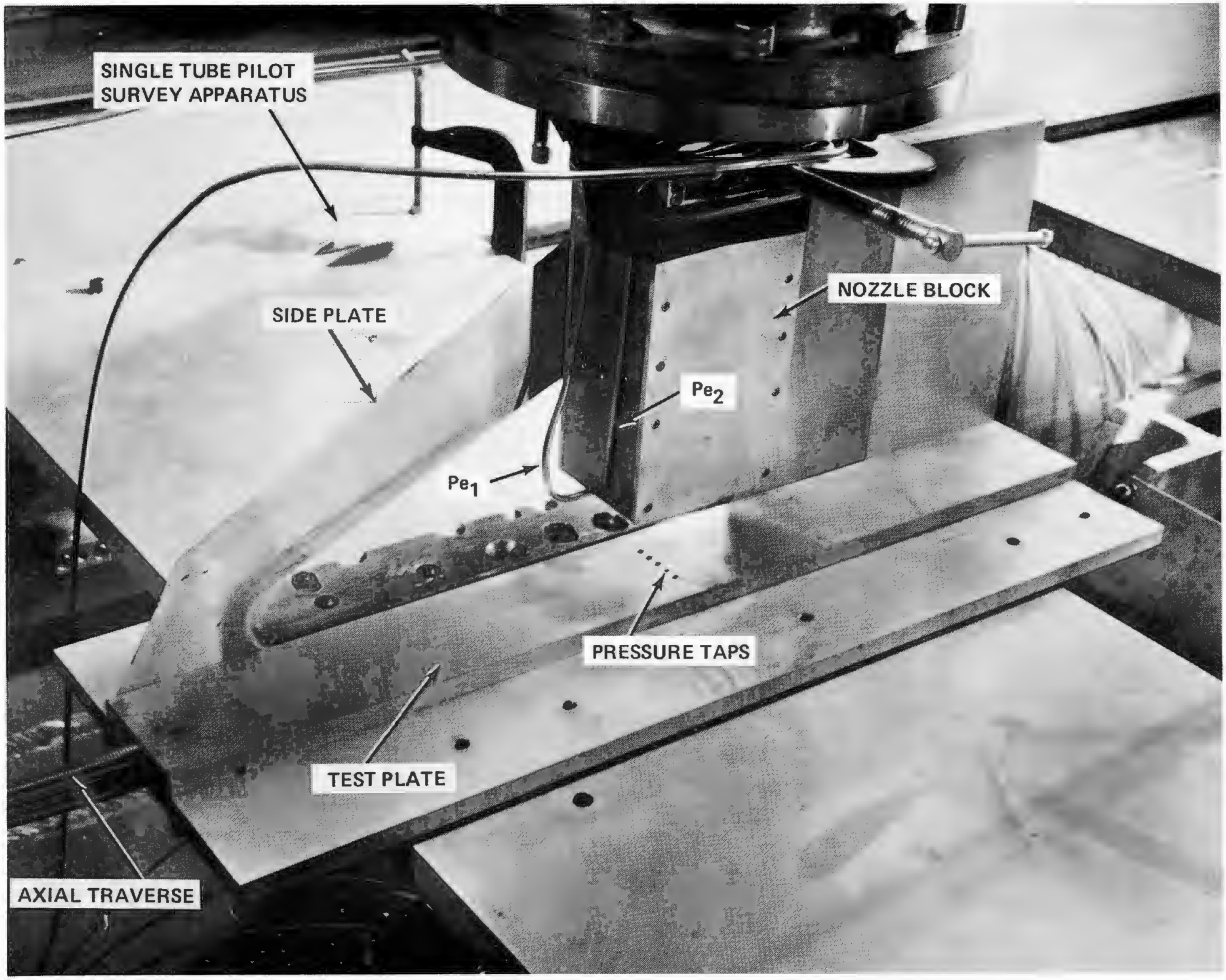

FIGURE 4 a EXPERIMENTAL SETUP

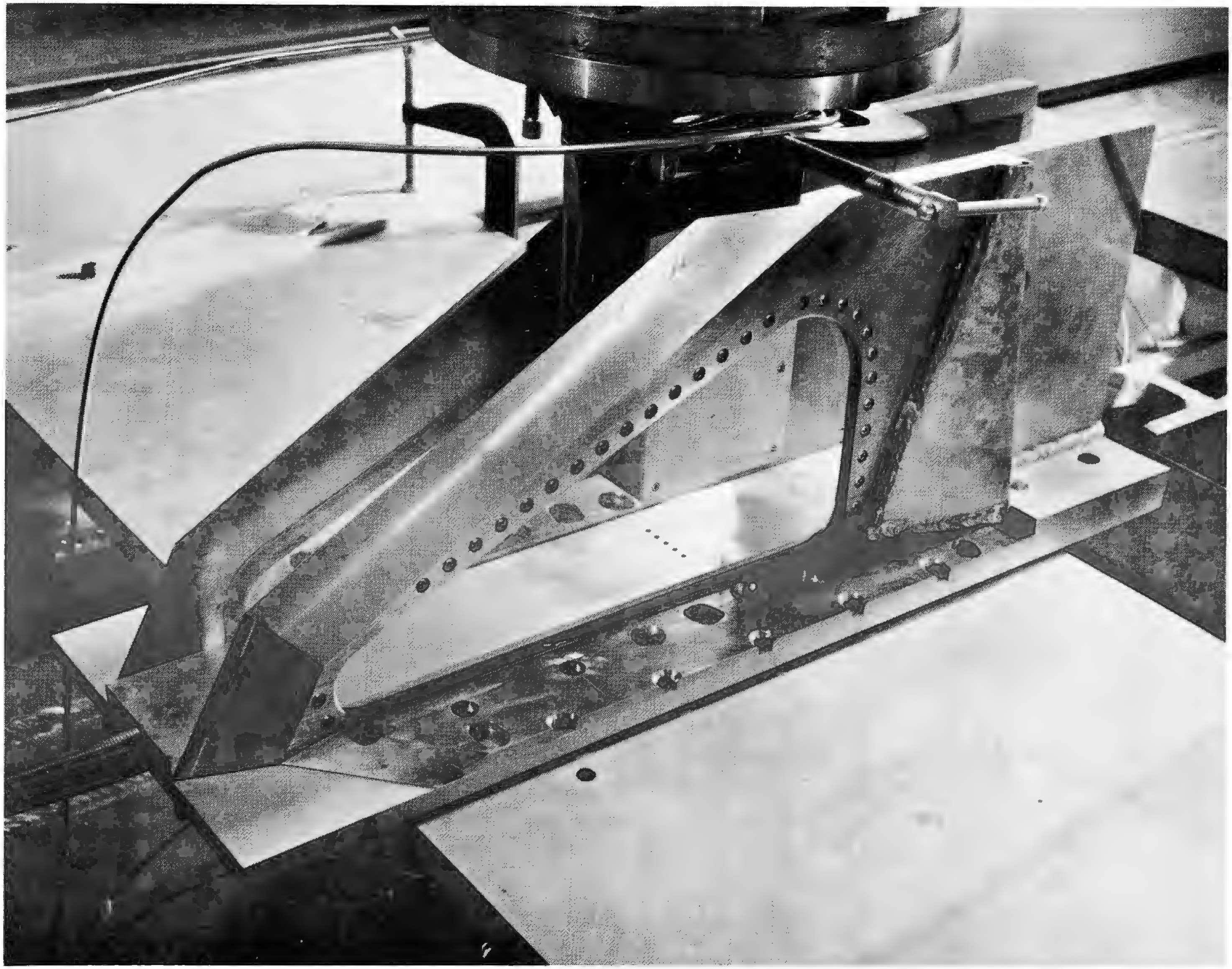

FIGURE 4b THE NOZZLE-PLATE ASSEMBLY FOR IMPINGEMENT FLOW STUDY

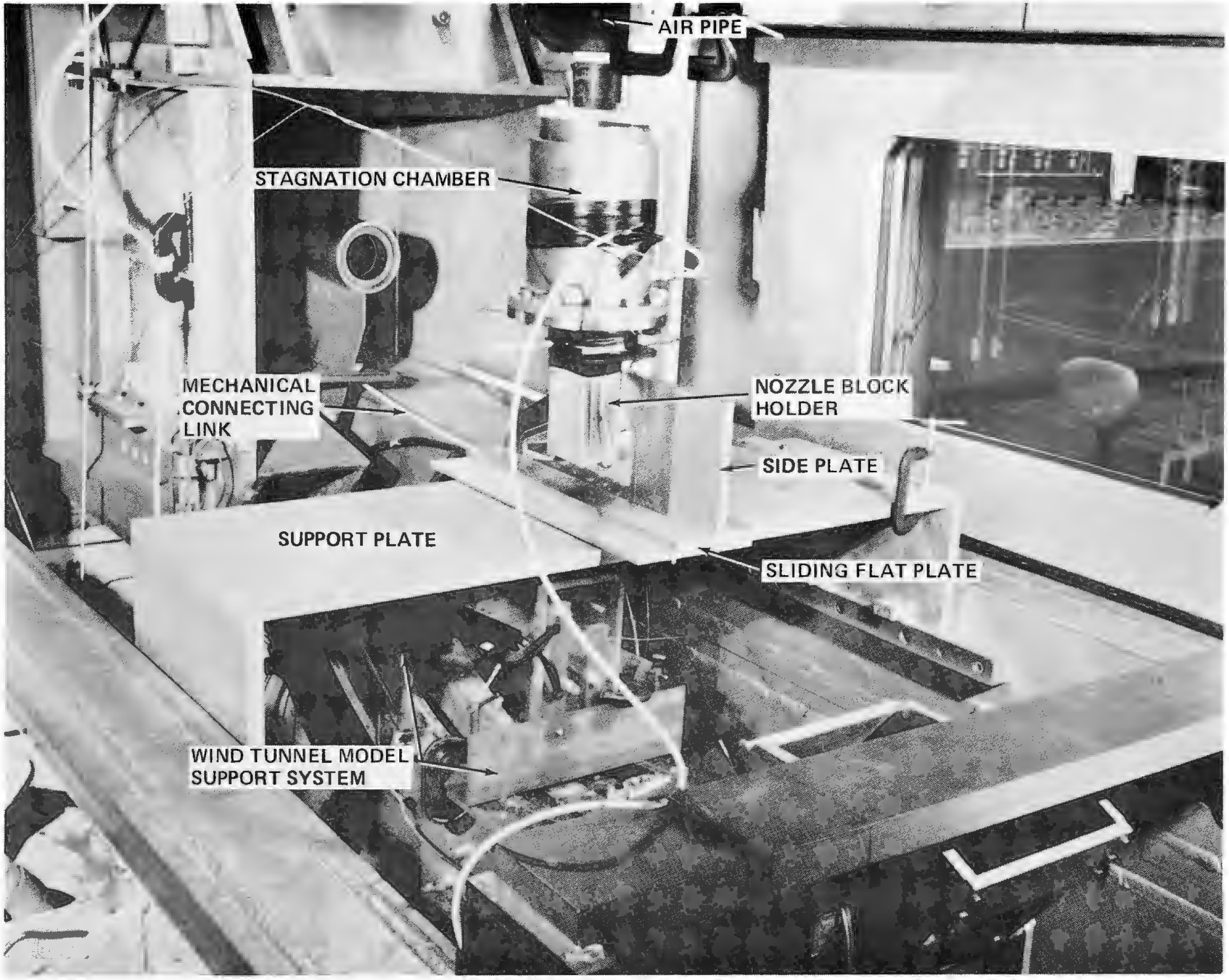

FIGURE 5 OVERVIEW OF THE JET IMPINGEMENT APPARATUS (LEFT SIDE PLATE REMOVED)

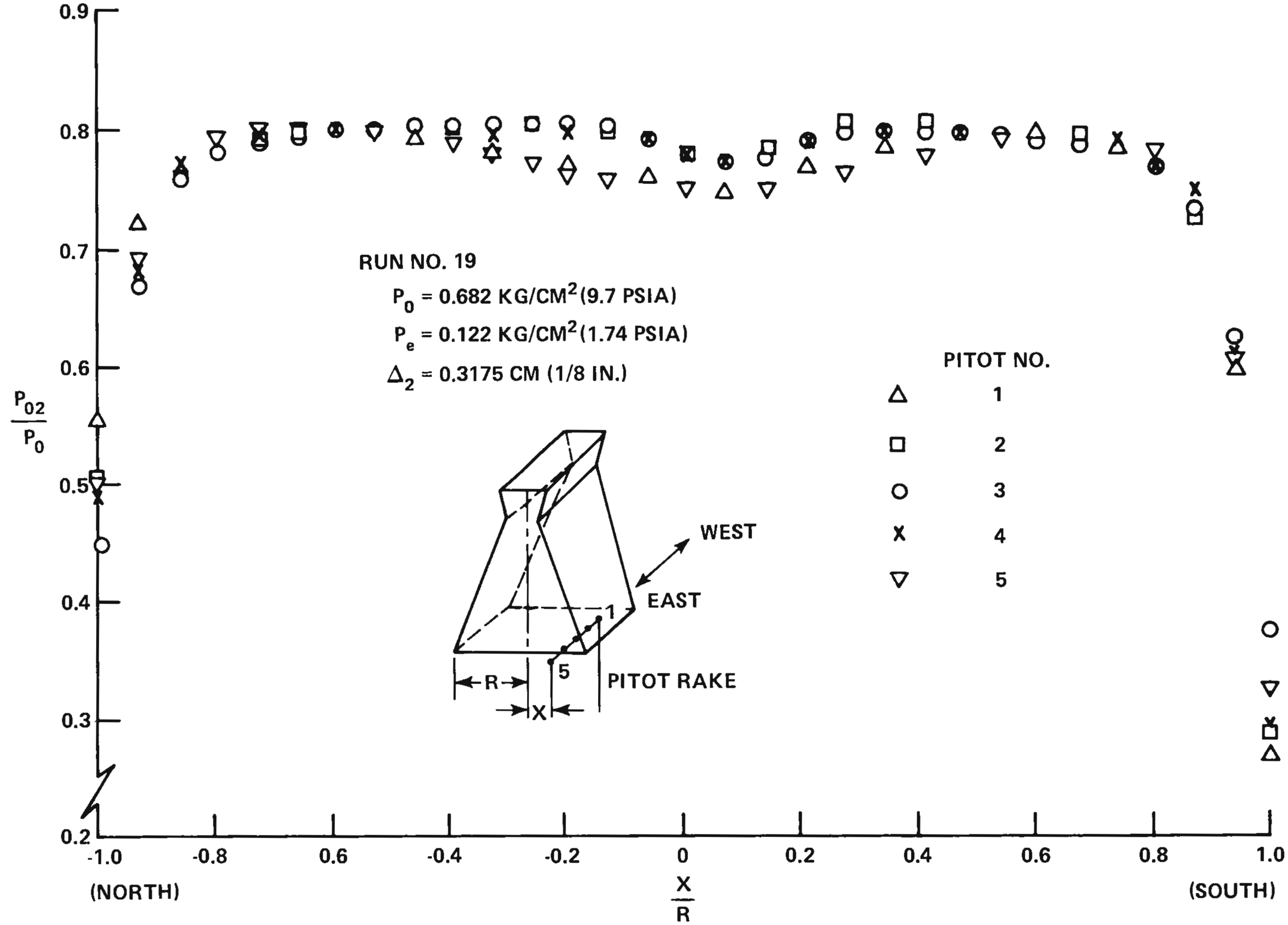

FIGURE 6 PITOT SURVEY – NOZZLE NO. 1

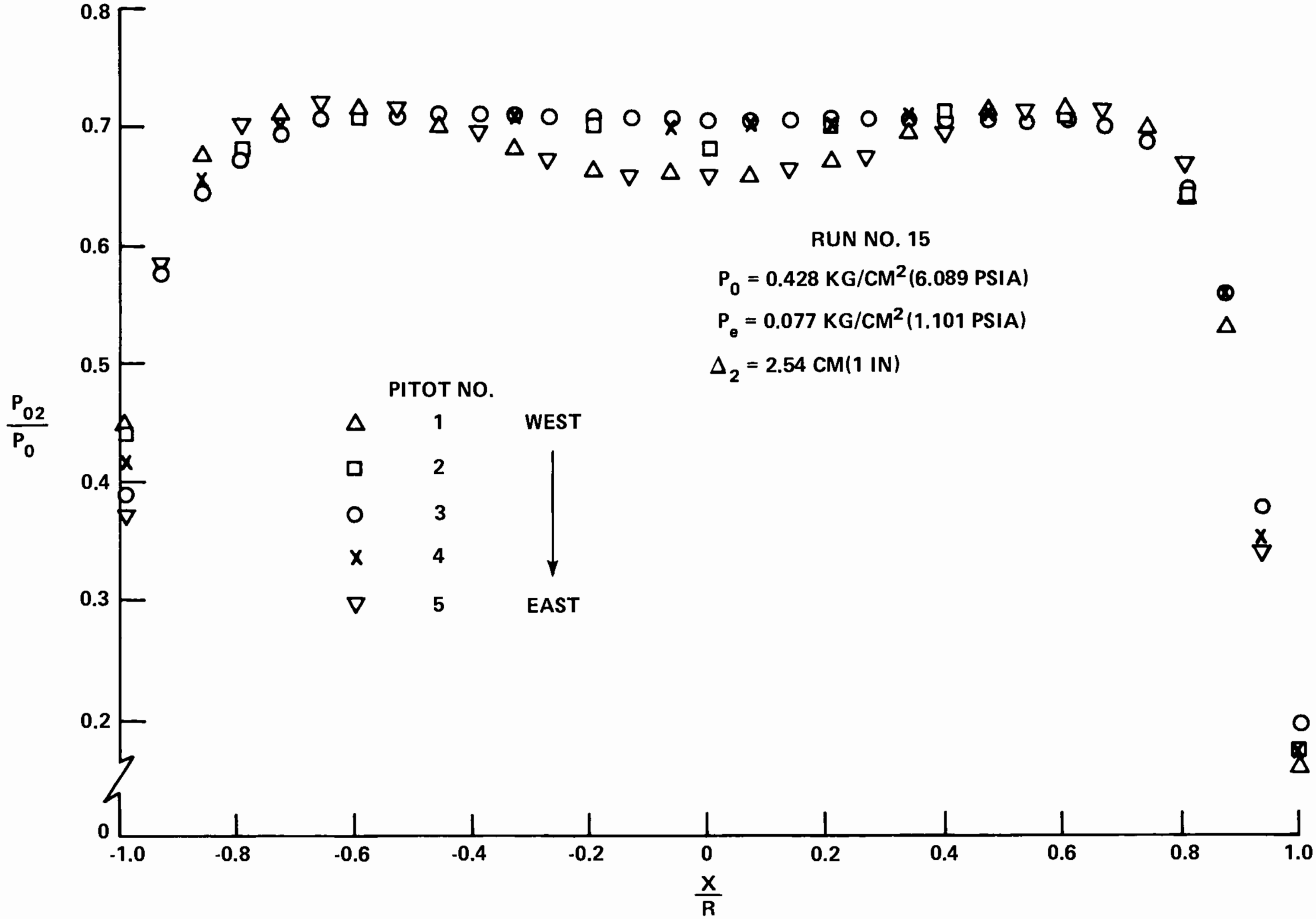

FIGURE 7 PITOT SURVEY – NOZZLE NO. 1

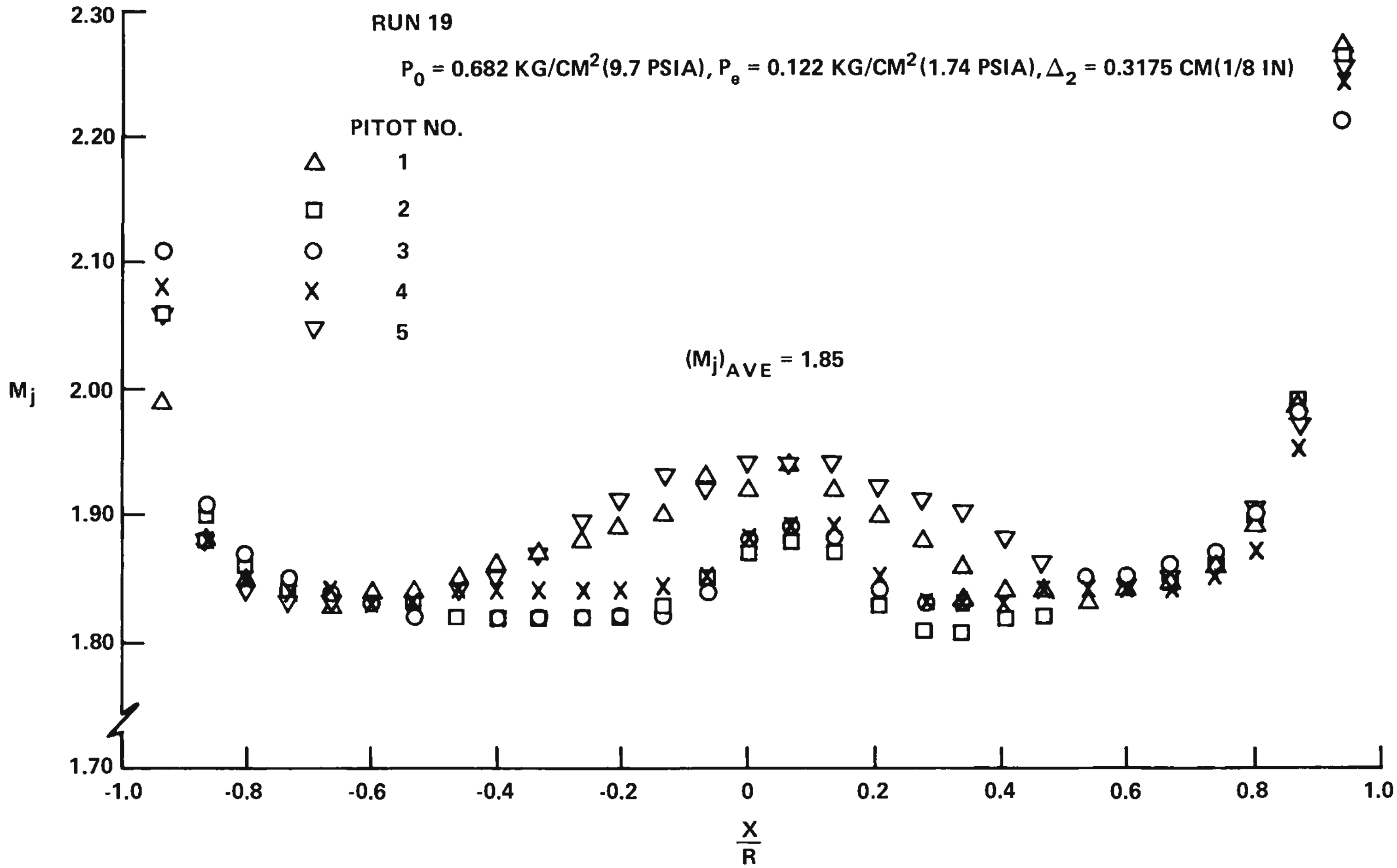

FIGURE 8 FREE JET MACH NO. – NOZZLE NO. 1 (PITOT SURVEY)

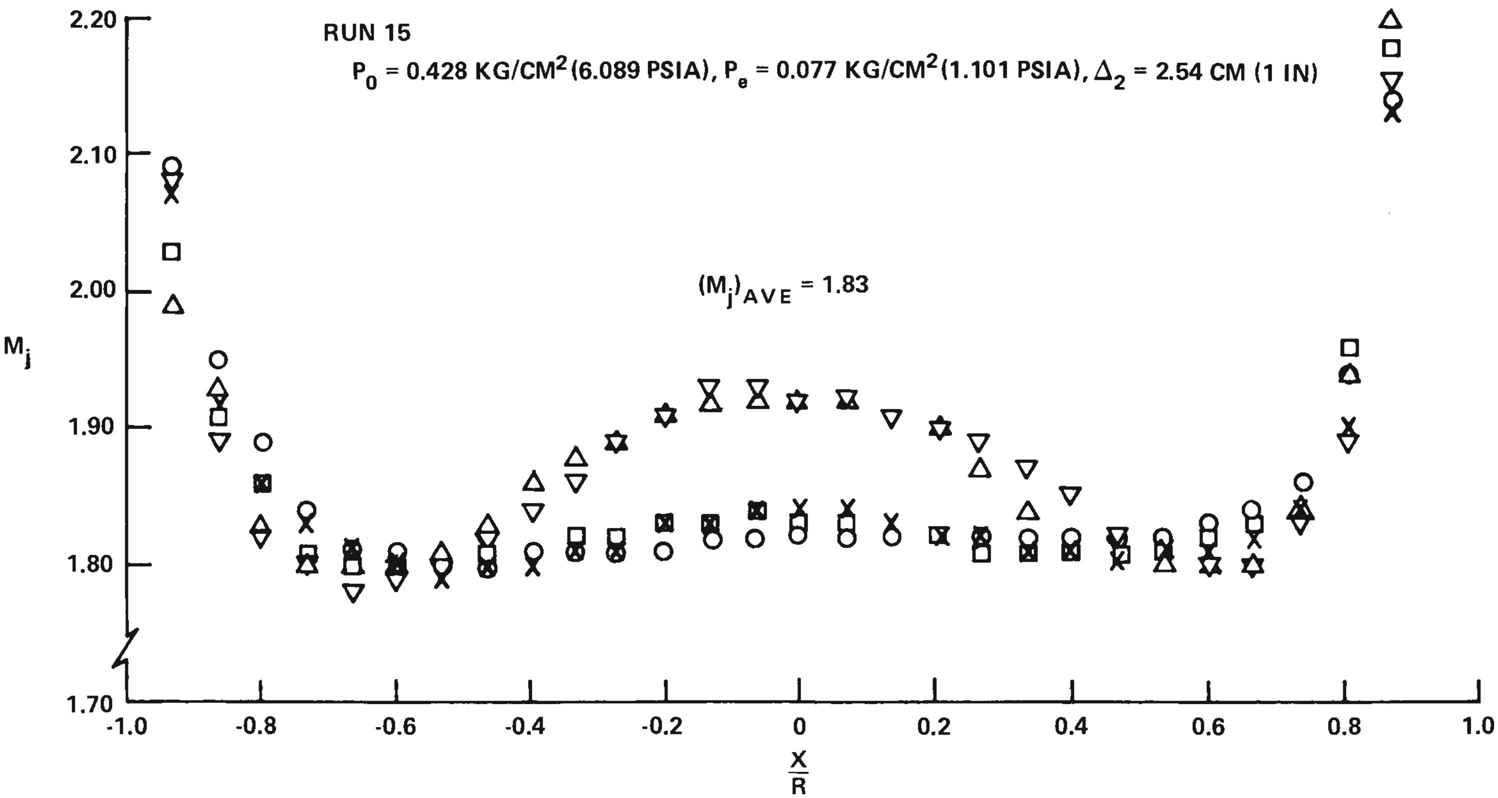

FIGURE 9 FREE JET MACH NO. – NOZZLE NO. 1 (PITOT SURVEY)

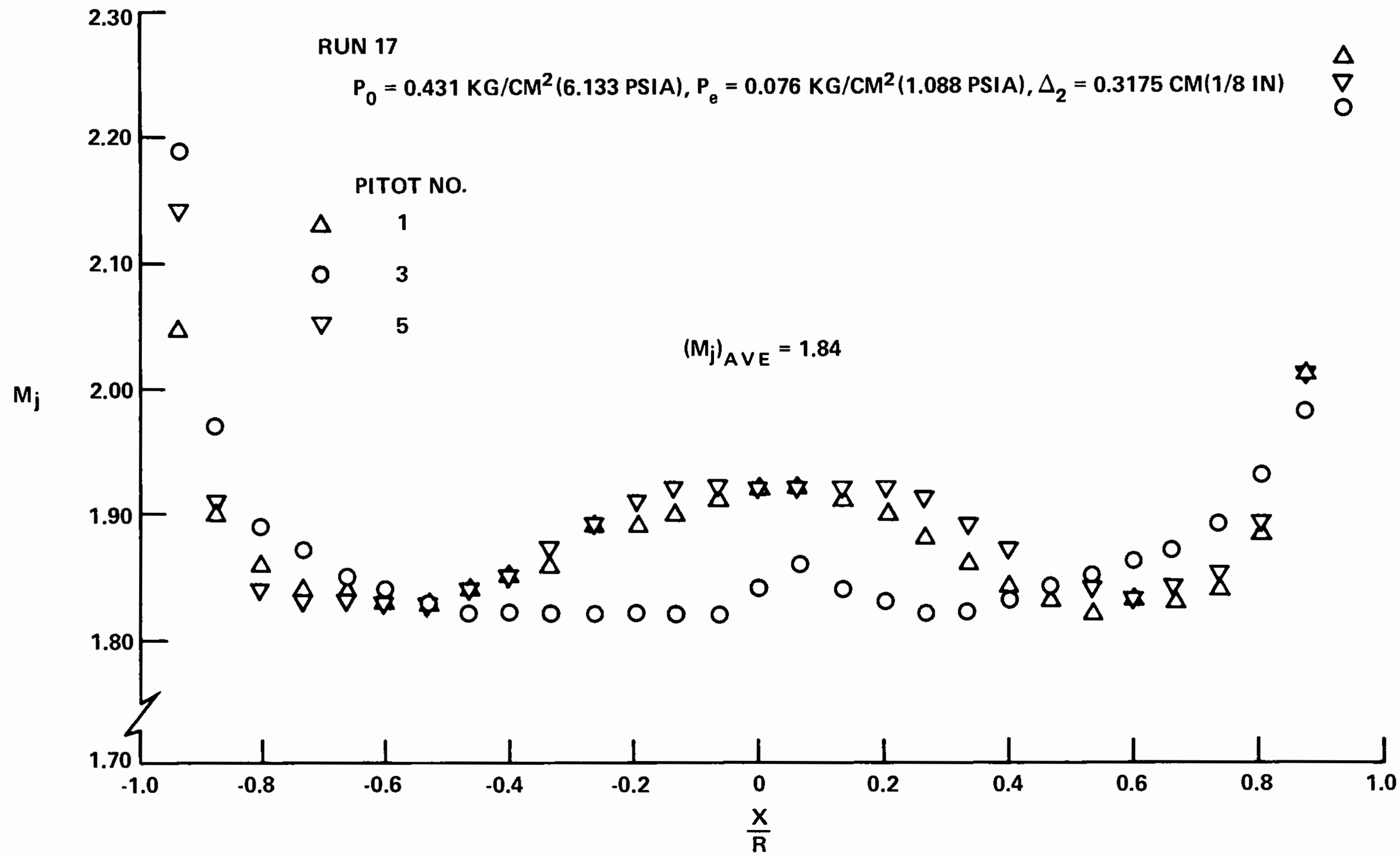

FIGURE 10 FREE JET MACH NO. – NOZZLE NO. 1 (PITOT SURVEY)

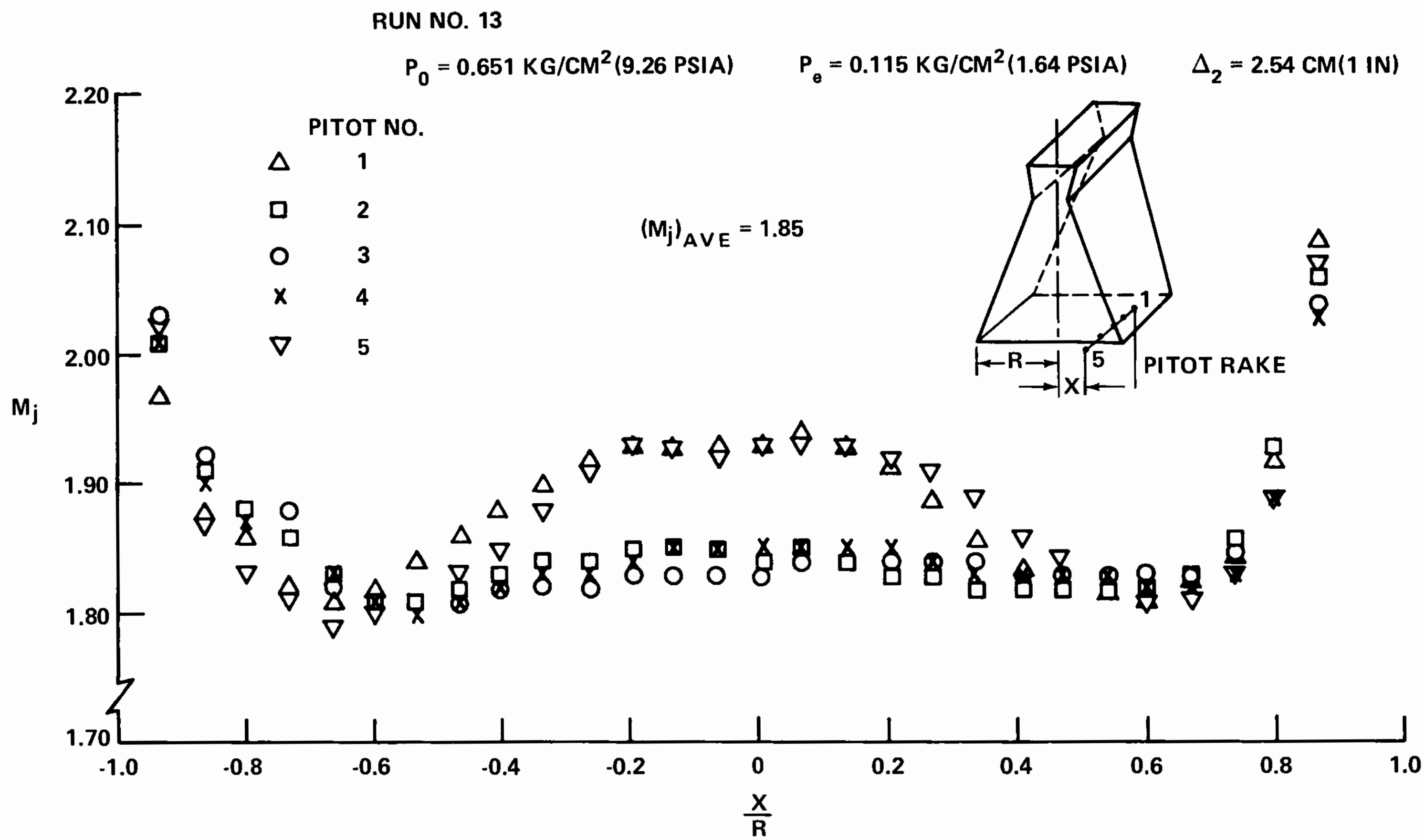

FIGURE 11 FREE JET MACH NO. – NOZZLE NO. 1 (PITOT SURVEY)

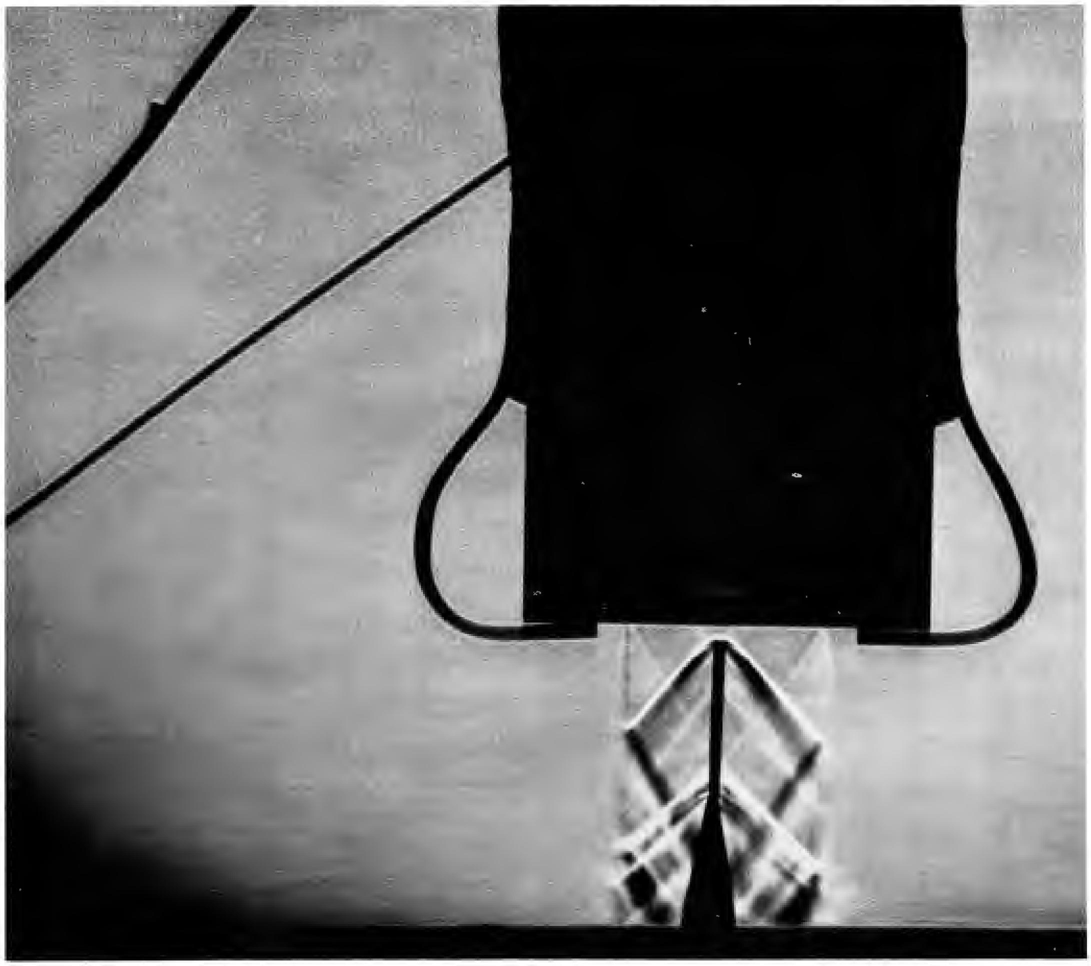

FIGURE 12 SCHLIEREN PHOTOGRAPH OF PITOT SURVEY: NOZZLE NO. 1 (RUN 19)

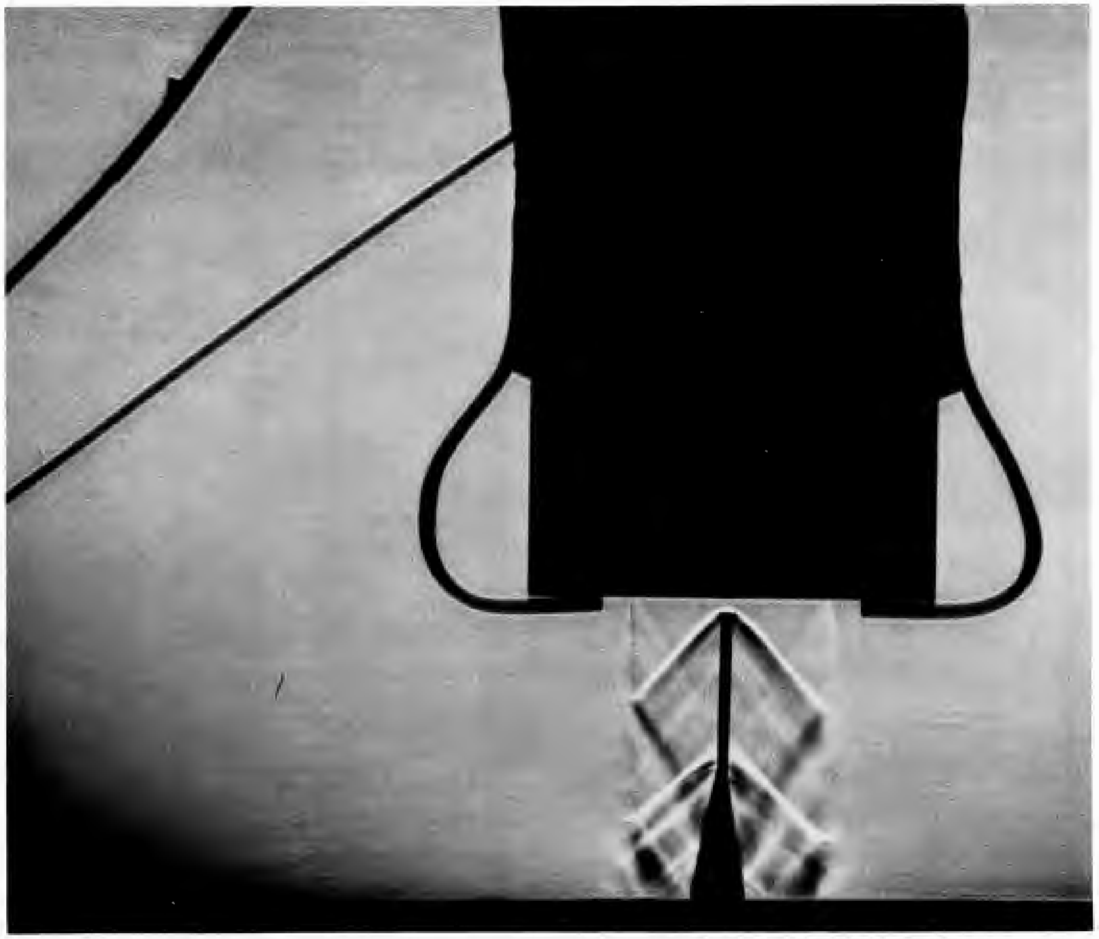

FIGURE 13 SCHLIEREN PHOTOGRAPH OF PITOT SURVEY: NOZZLE NO. 1 (RUN 17)

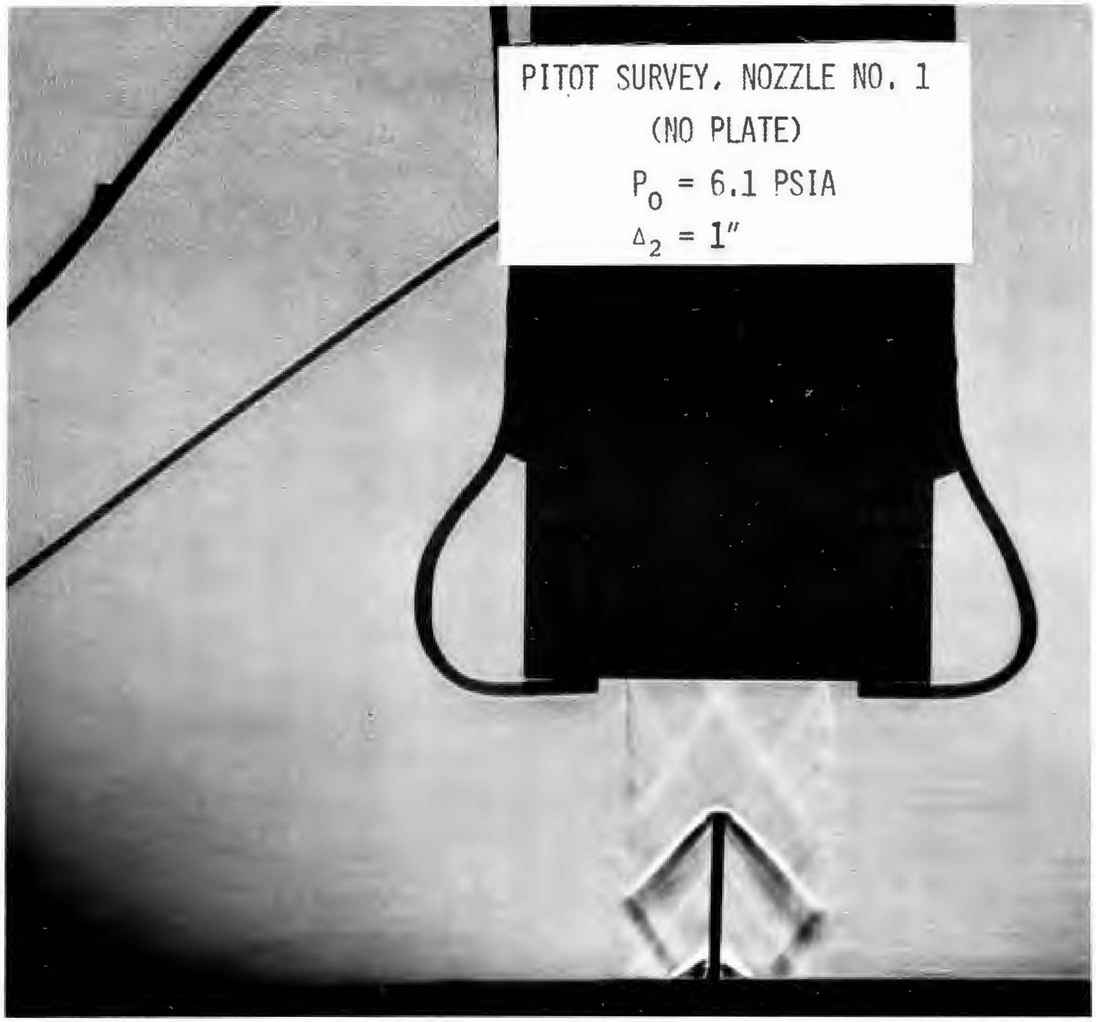

FIGURE 14 SCHLIEREN PHOTOGRAPH OF PITOT SURVEY: NOZZLE NO. 1 (RUN 15)

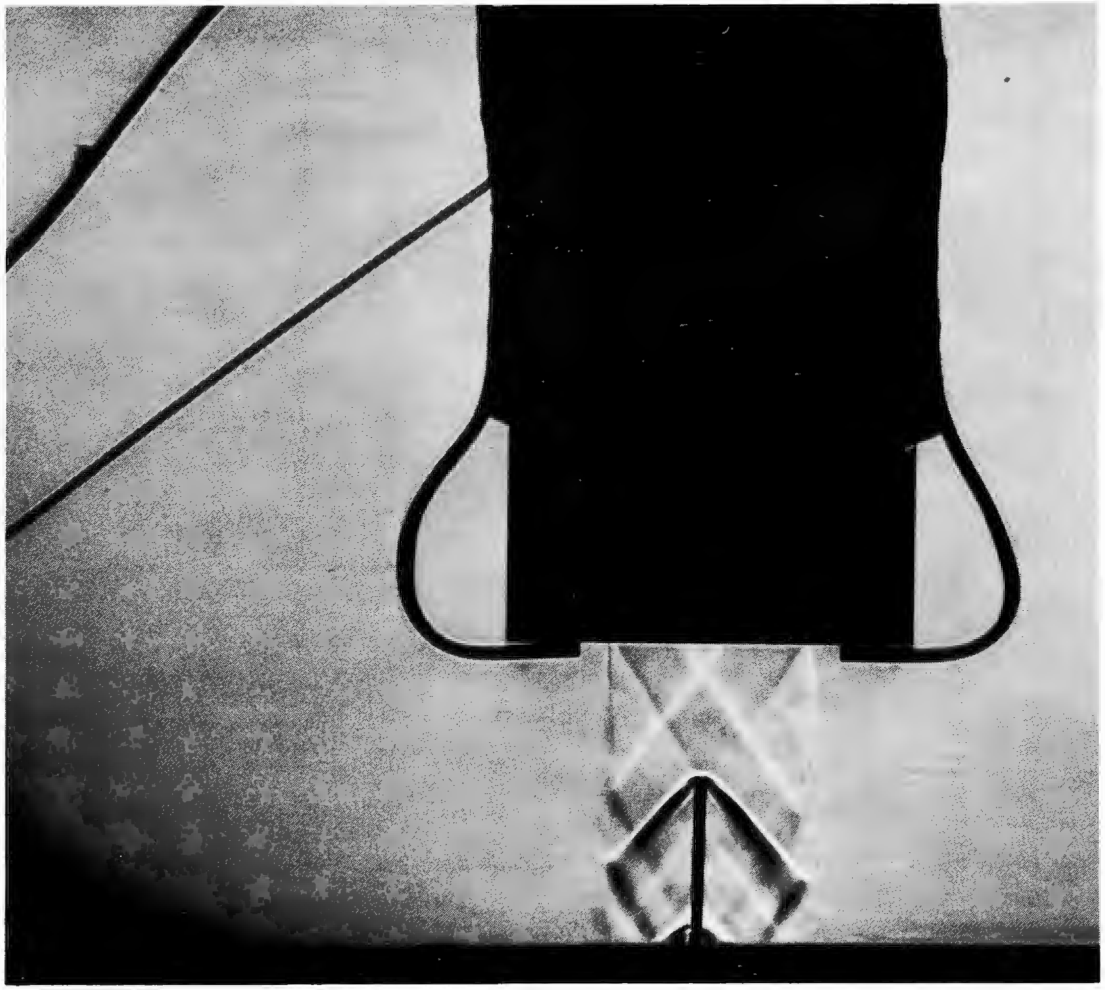

FIGURE 15 SCHLIEREN PHOTOGRAPH OF PITOT SURVEY: NOZZLE NO. 1 (RUN 13)

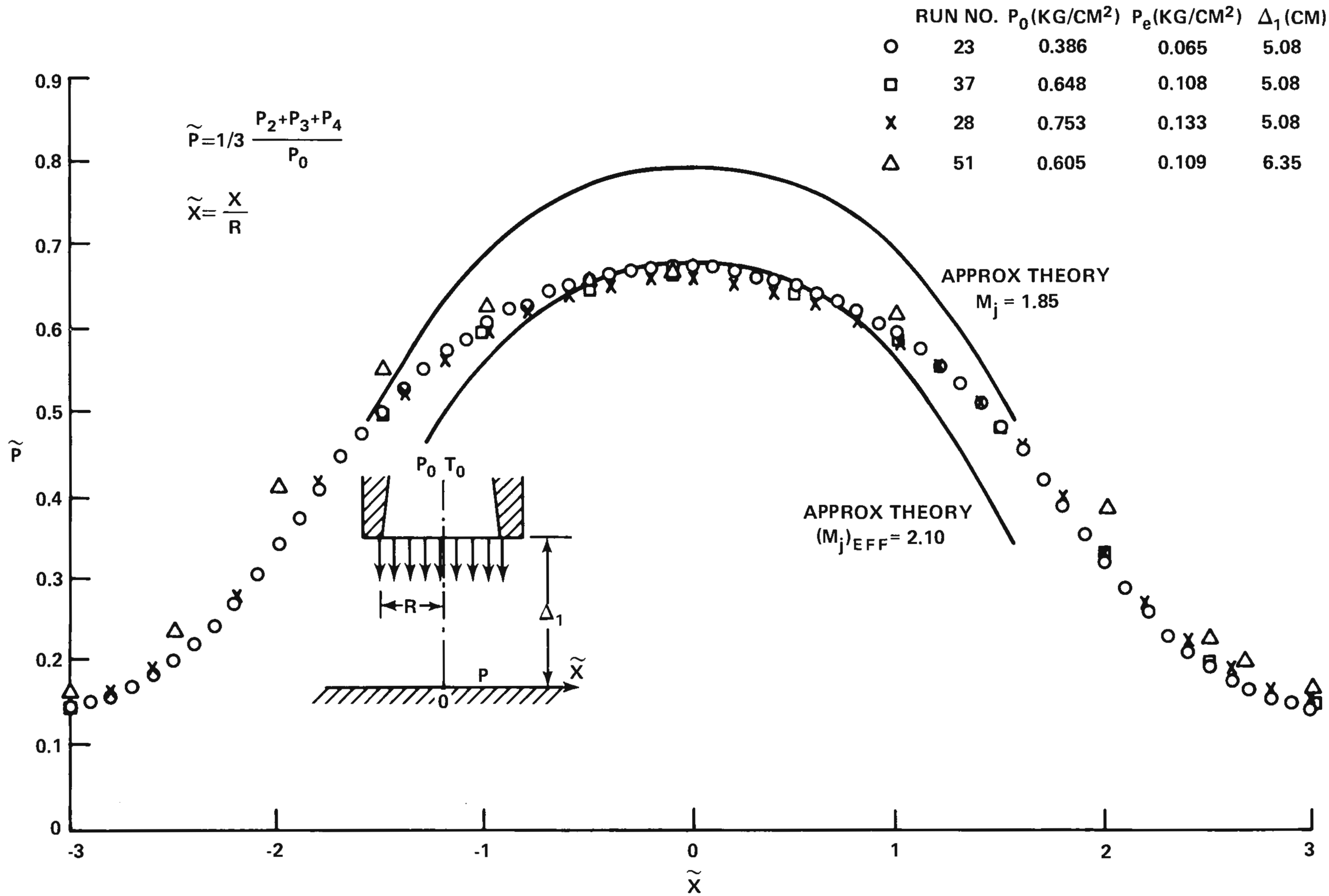

FIGURE 16 SURFACE PRESSURE RESULTS: NOZZLE NO. 1 (NEARLY ISENTROPIC JET)

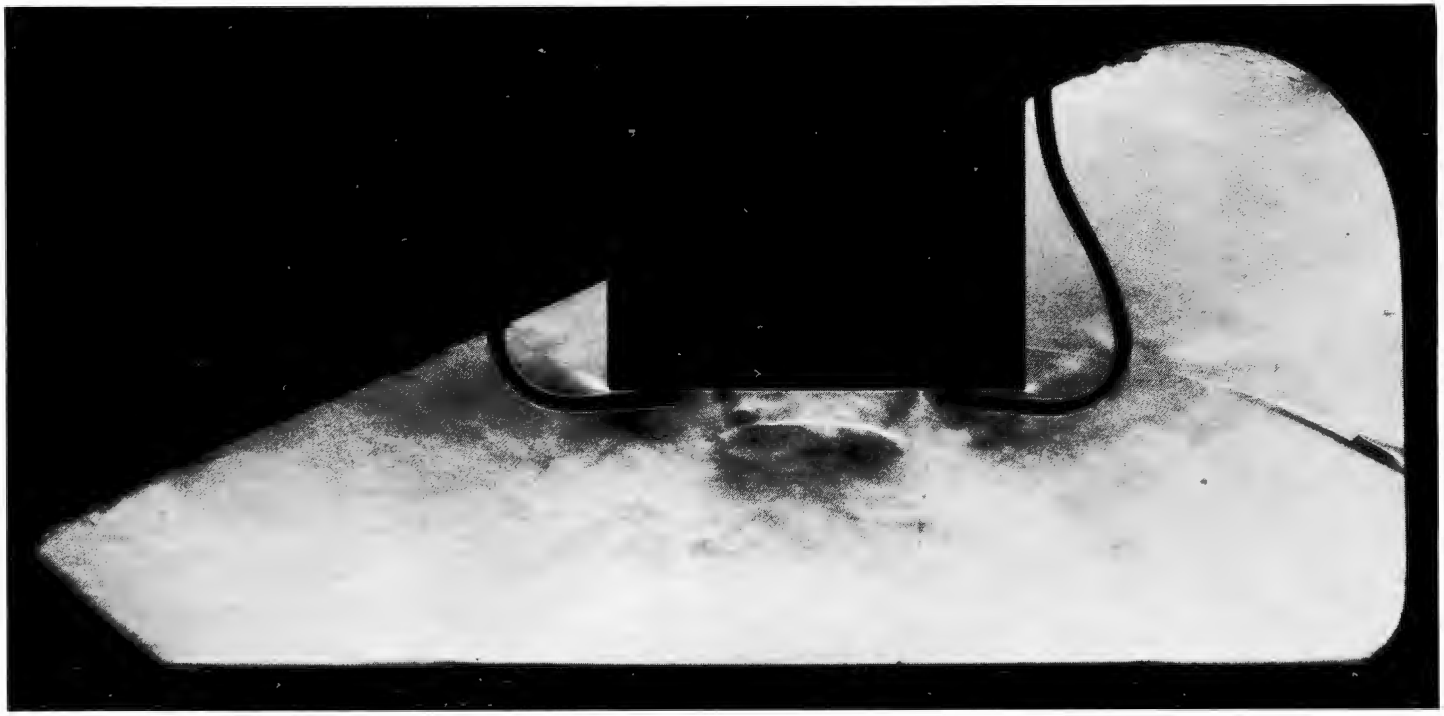

FIGURE 17 SCHLIEREN PHOTOGRAPH OF IMPINGEMENT FLOW: NOZZLE NO. 1 (RUN 23)

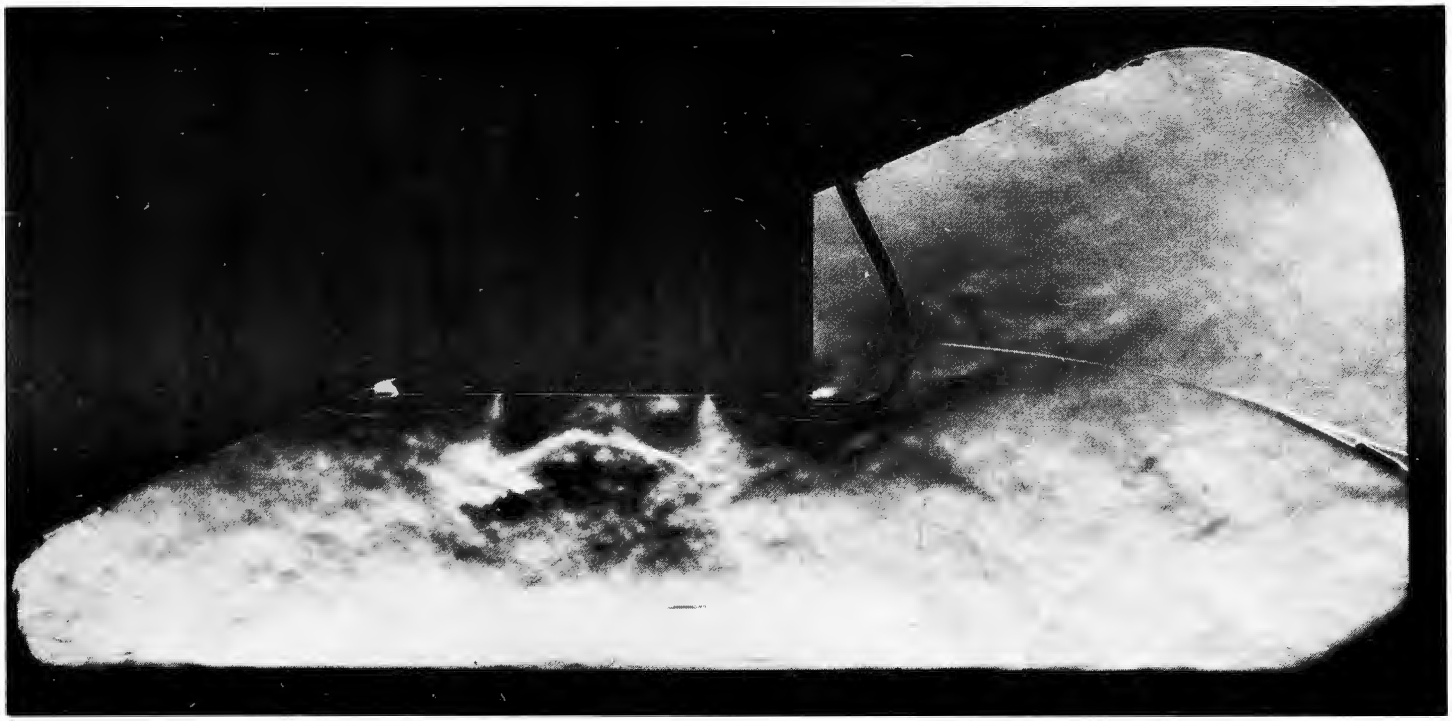

FIGURE 18 SCHLIEREN PHOTOGRAPH OF IMPINGEMENT FLOW: NOZZLE NO. 1 (RUN 37)

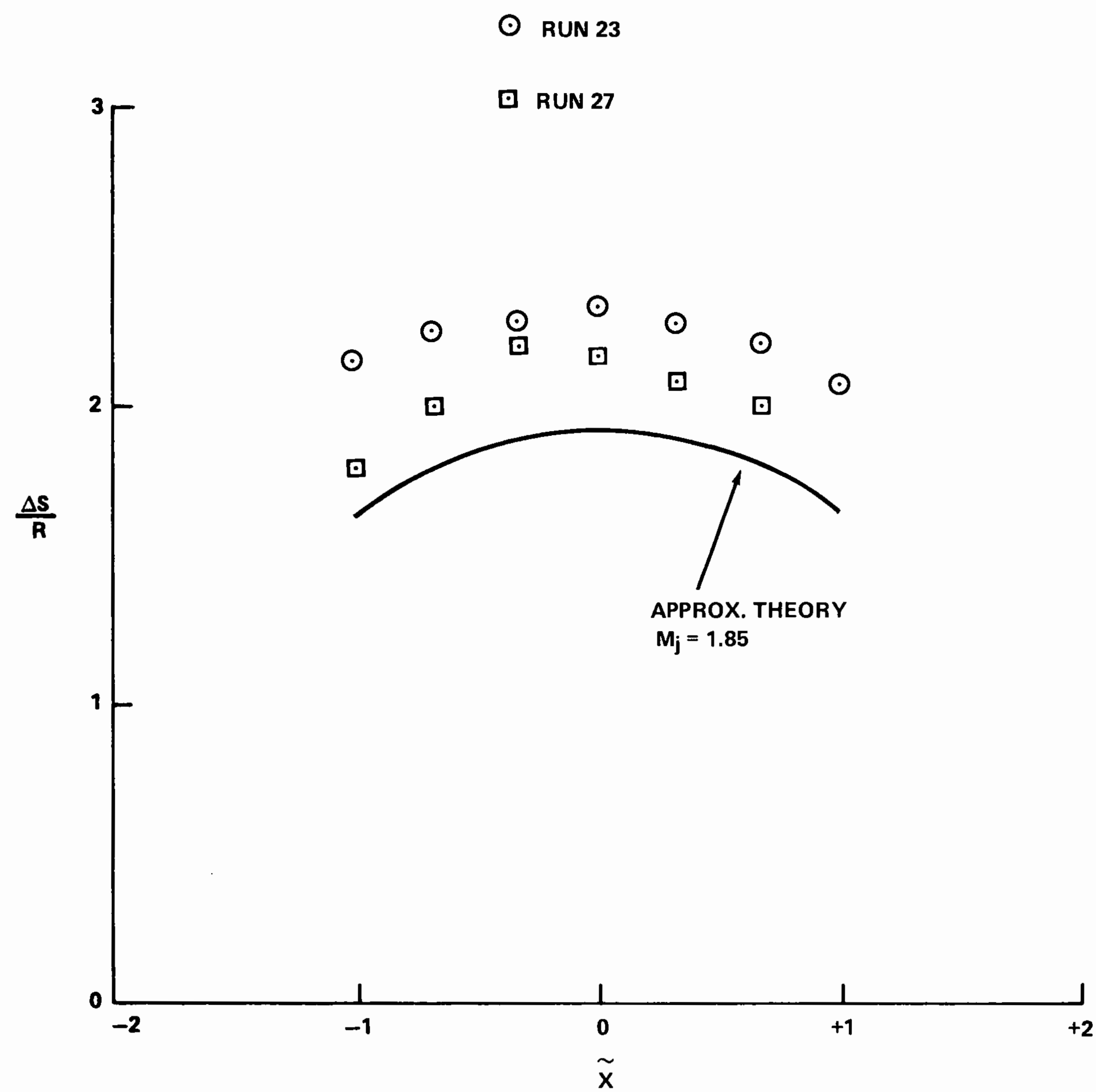

FIGURE 19 SHOCK MEASUREMENTS: NOZZLE NO. 1

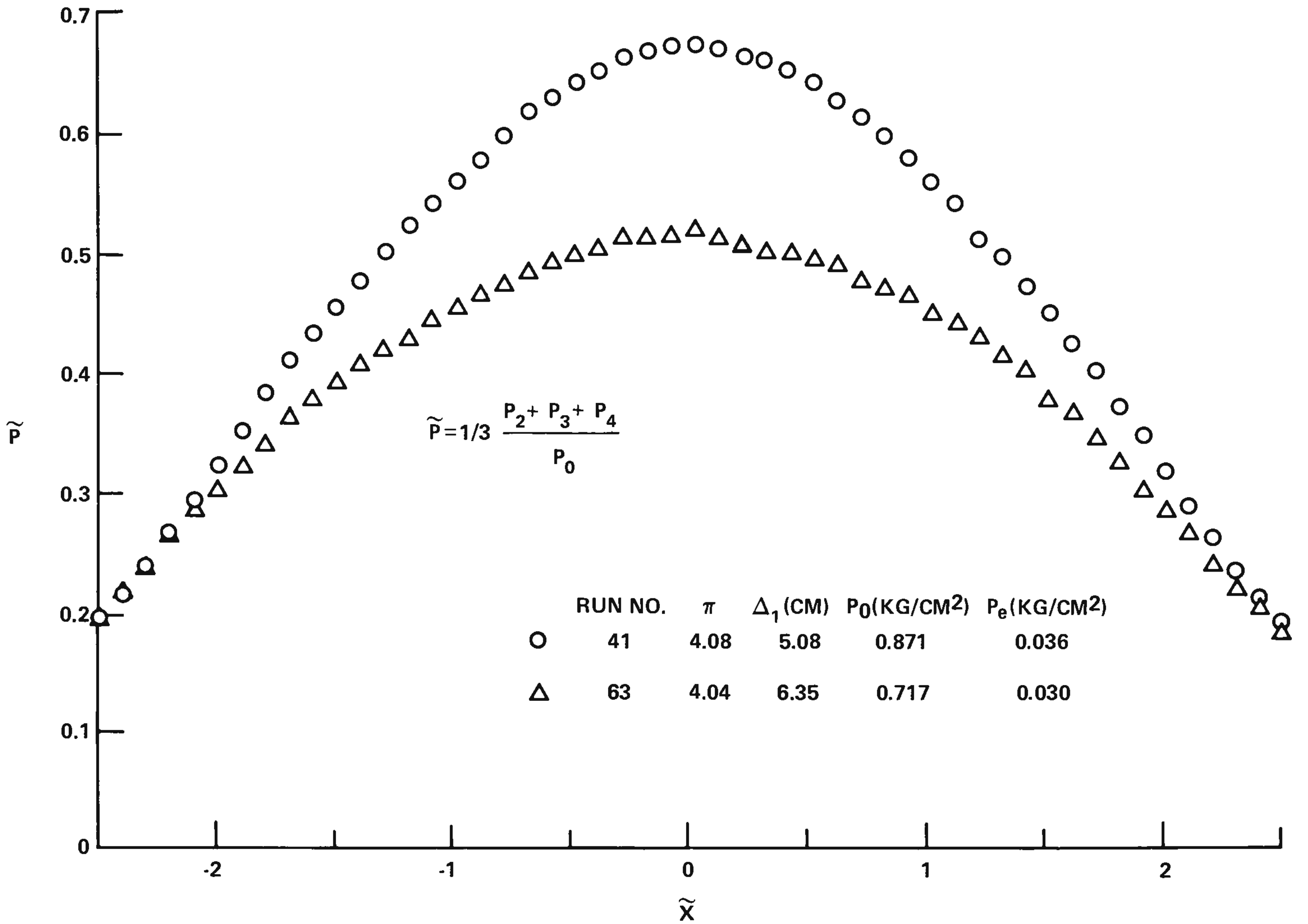

FIGURE 20 EFFECTS OF NOZZLE – PLATE DISTANCE ON SURFACE PRESSURE: UNDEREXPANDED JET (NOZZLE NO. 1)

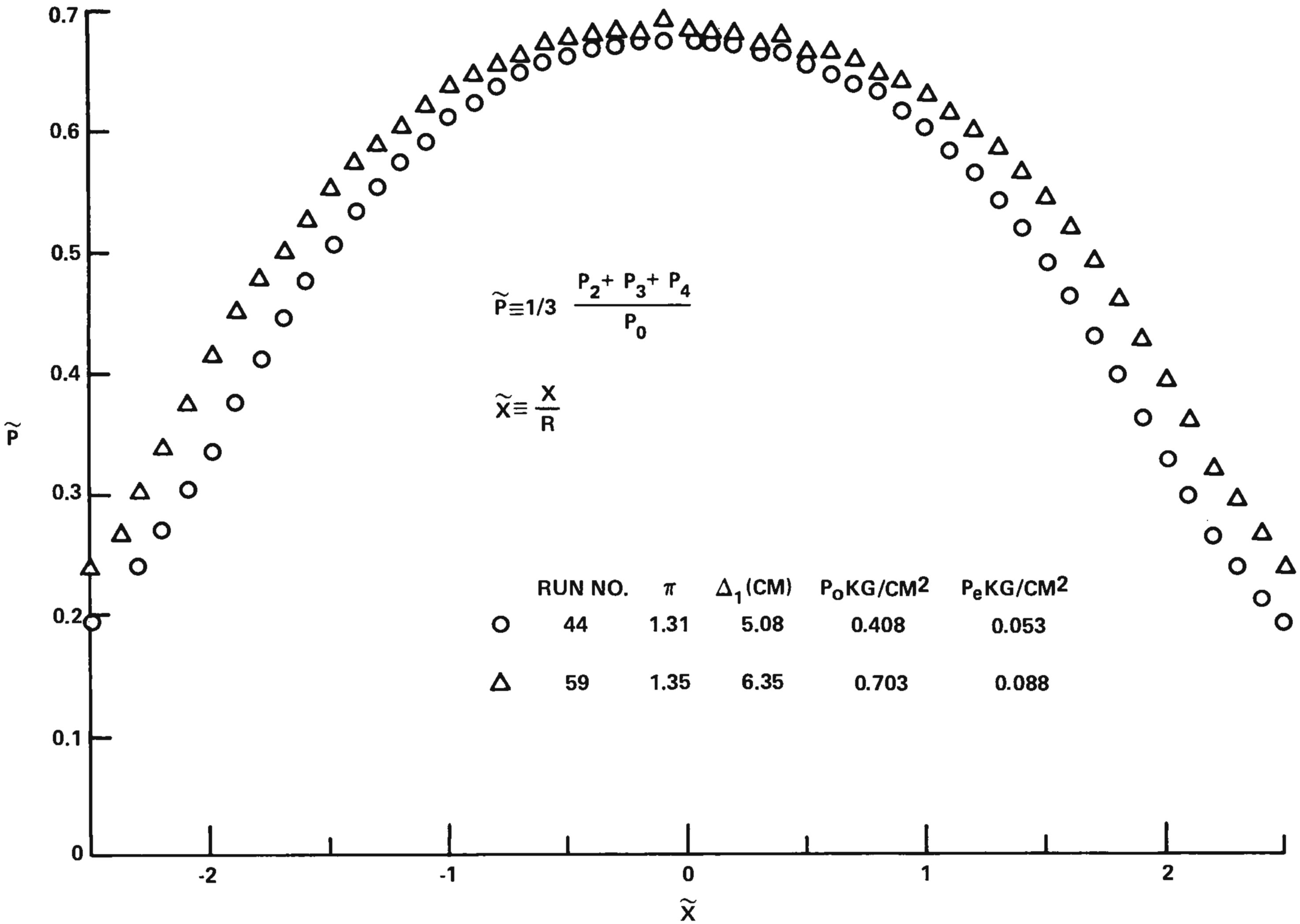

FIGURE 21 EFFECTS OF NOZZLE – PLATE DISTANCE ON SURFACE PRESSURE: UNDEREXPANDED JET (NOZZLE NO. 1)

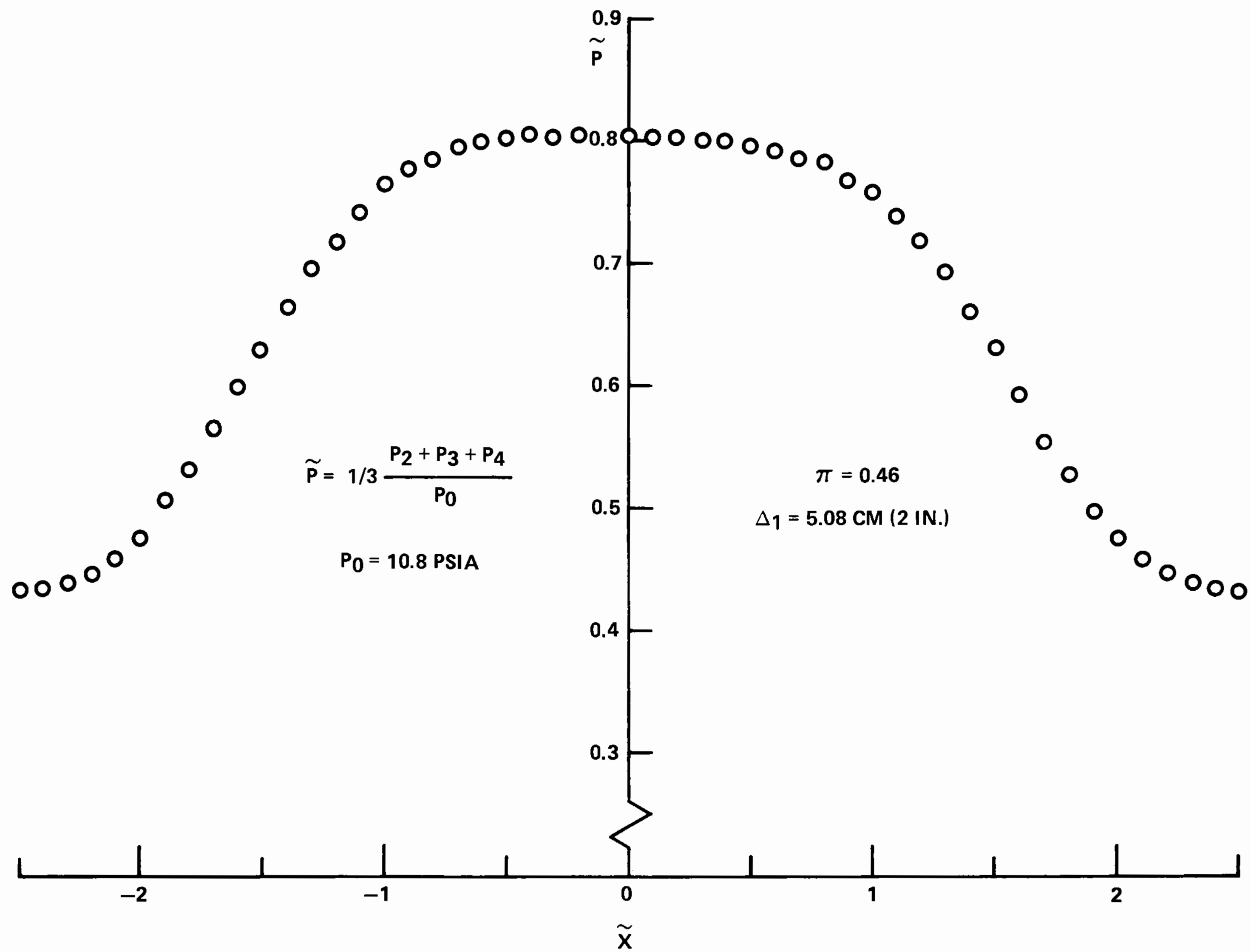

FIGURE 22 SURFACE PRESSURE RESULTS: NOZZLE NO. 1 (OVEREXPANDED JET, π = 0.46)

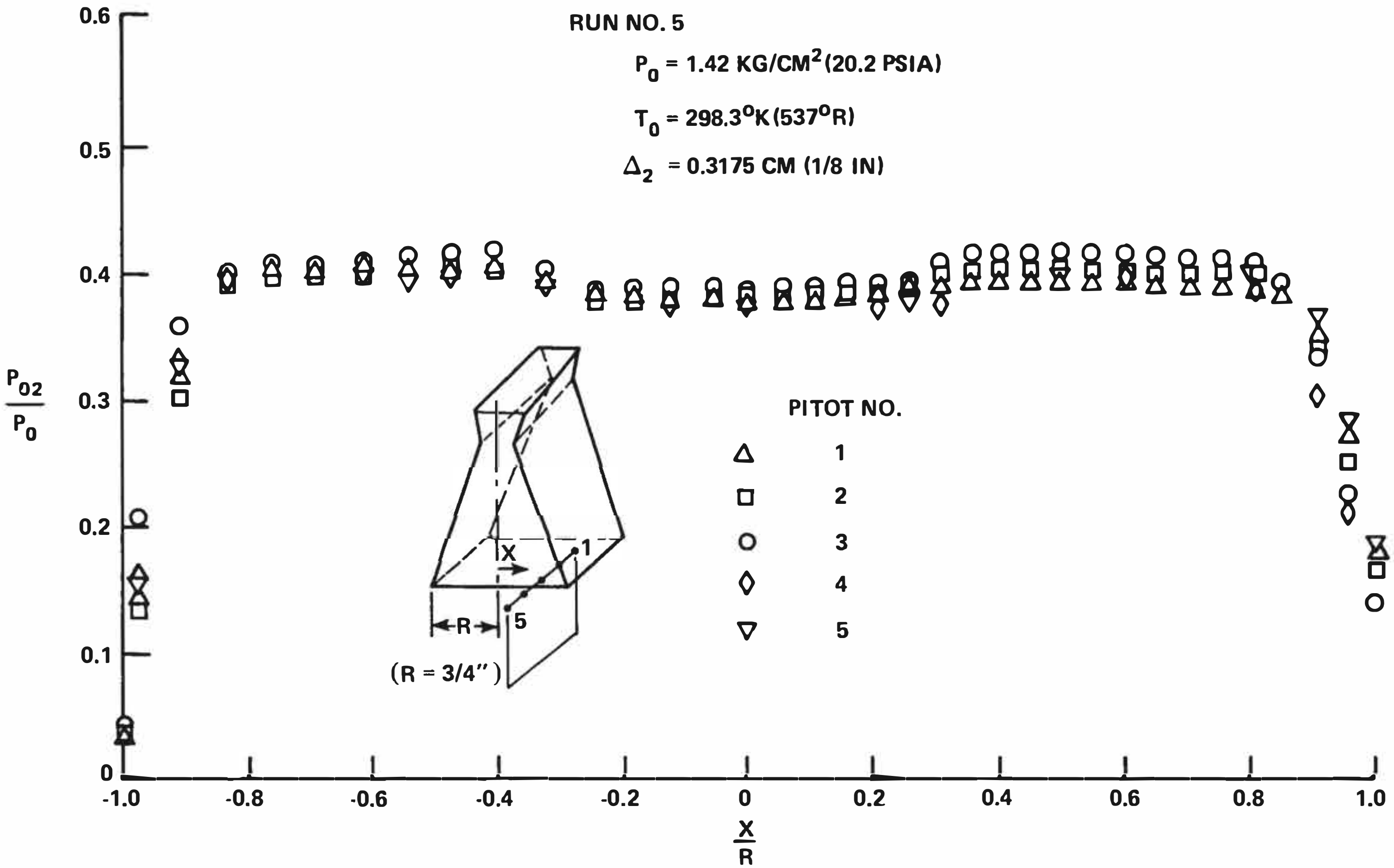

FIGURE 23 PITOT SURVEY – NOZZLE NO. 2

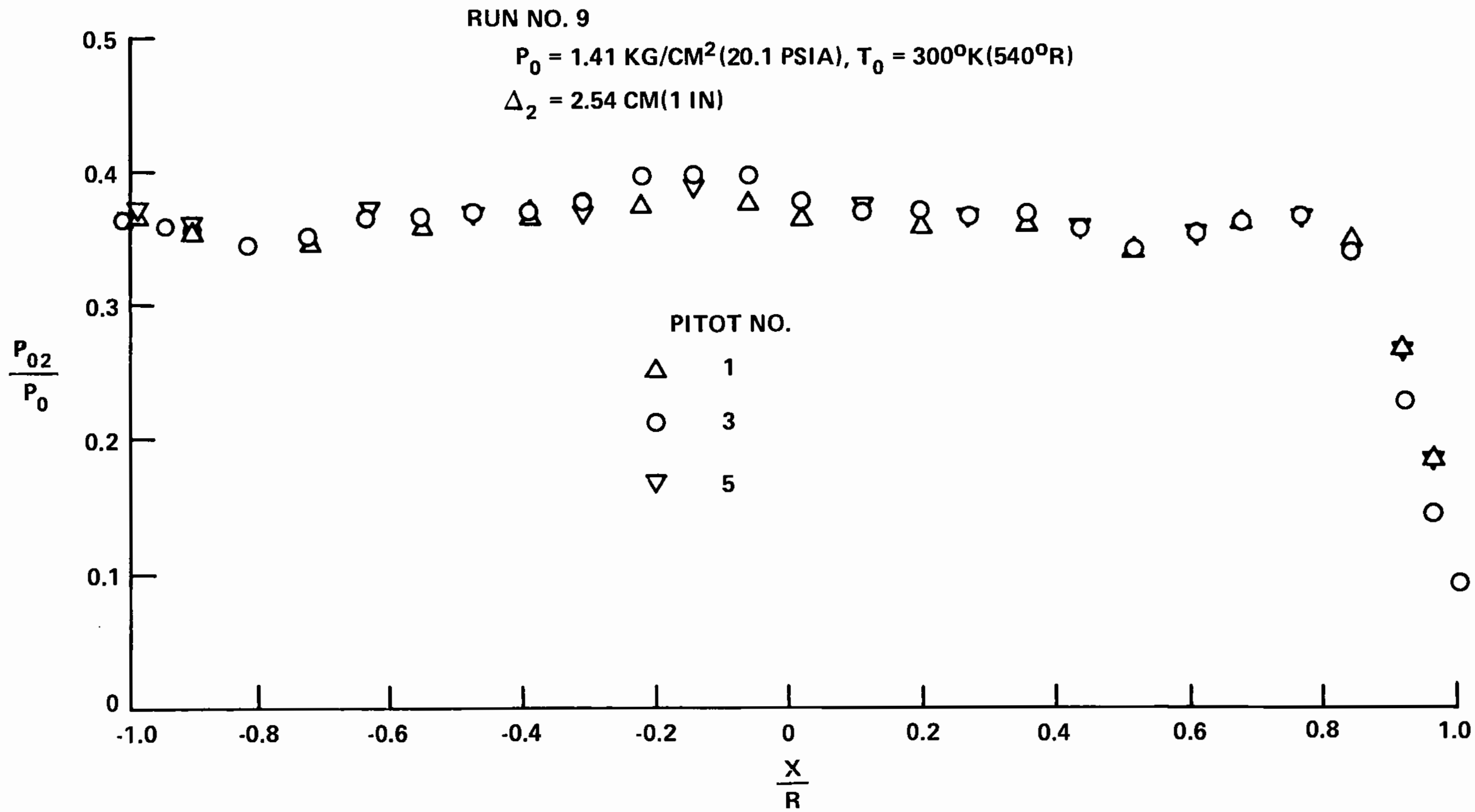

FIGURE 24 PITOT SURVEY – NOZZLE NO. 2

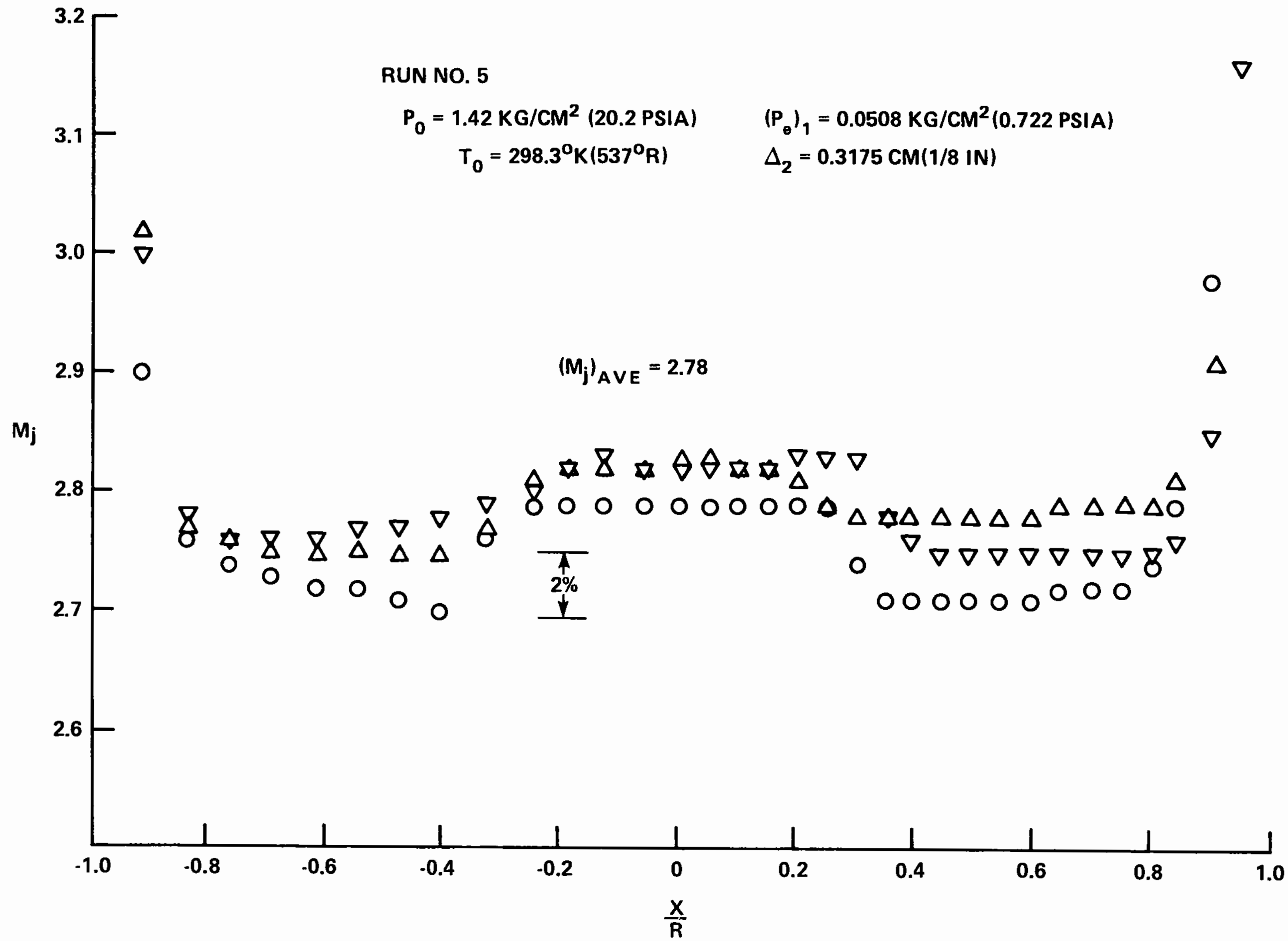

FIGURE 25 FREE JET MACH NO. – NOZZLE NO. 2 (PITOT SURVEY)

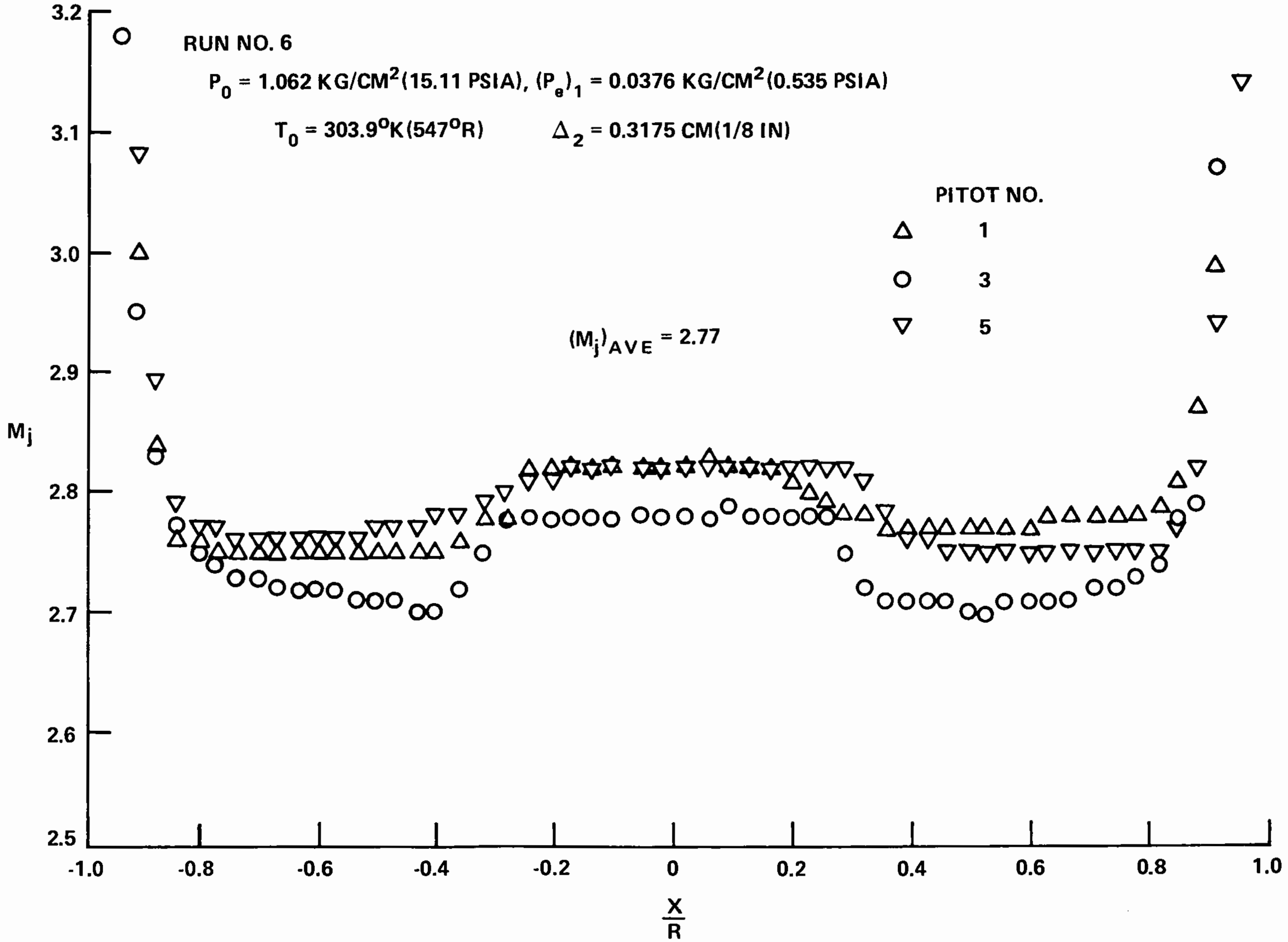

FIGURE 26 FREE JET MACH NO. – NOZZLE NO. 2 (PITOT SURVEY)

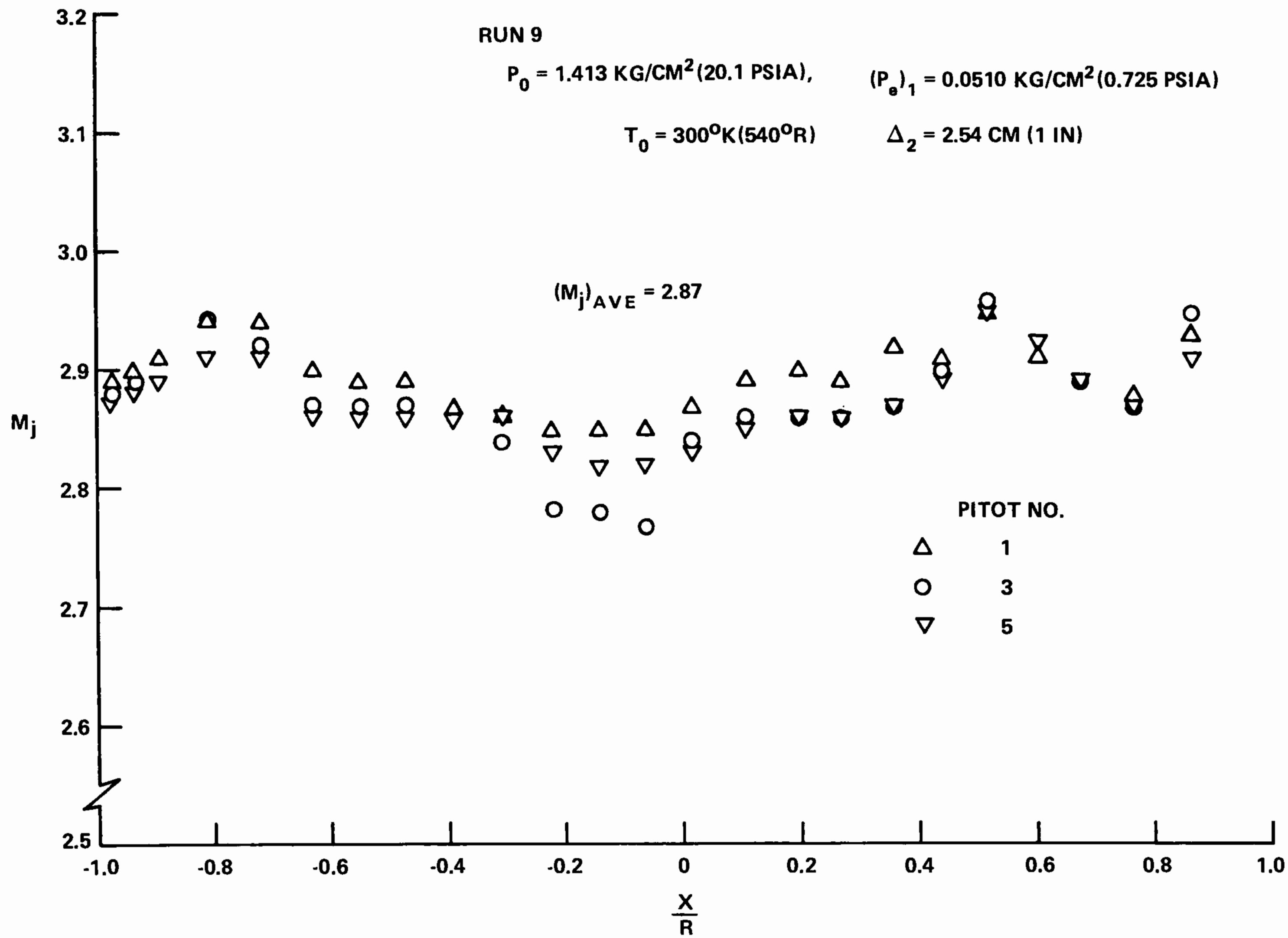

FIGURE 27 FREE JET MACH NO. – NOZZLE NO. 2 (PITOT SURVEY)

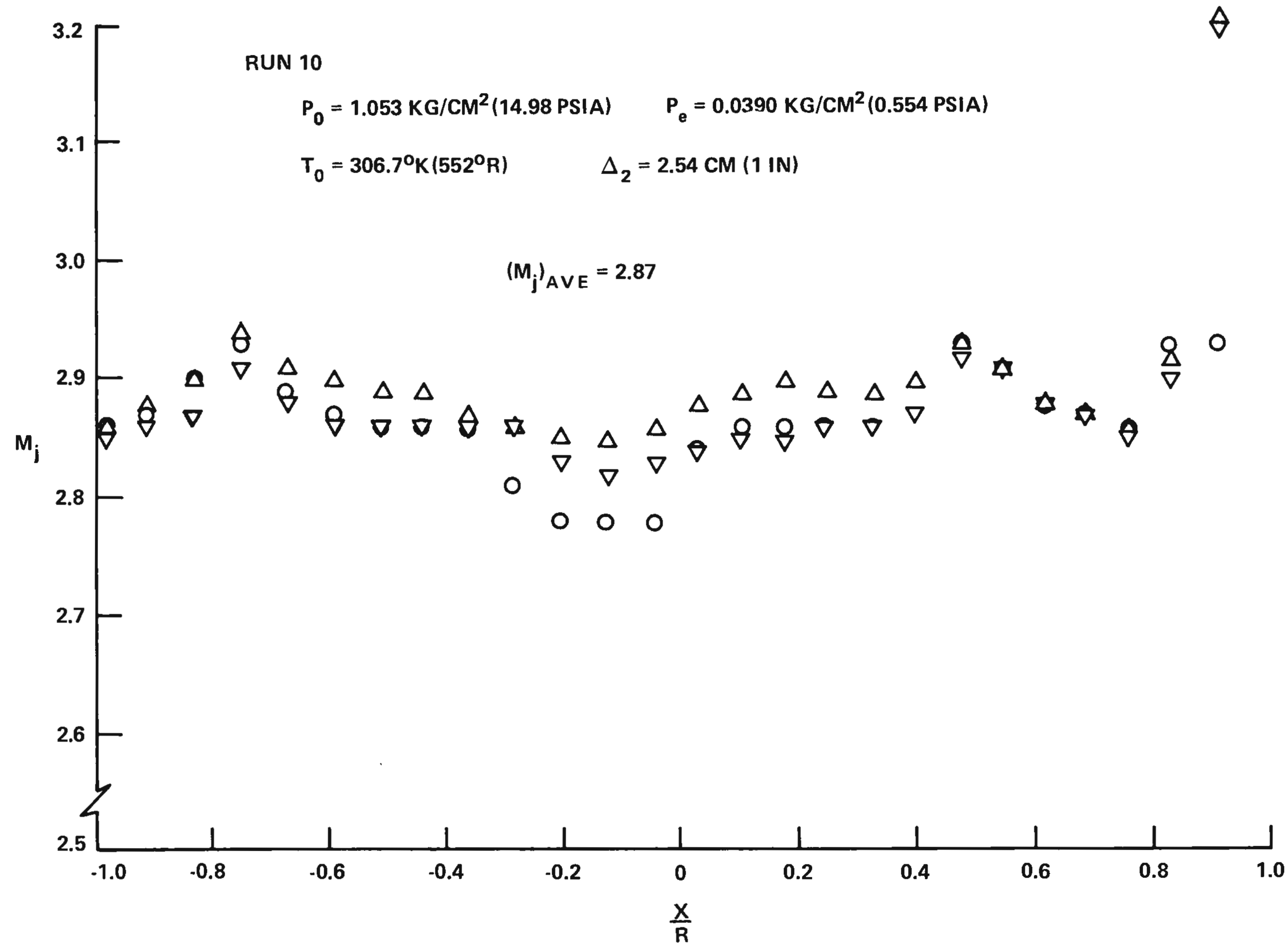

FIGURE 28 FREE JET MACH NO. – NOZZLE NO. 2 (PITOT SURVEY)

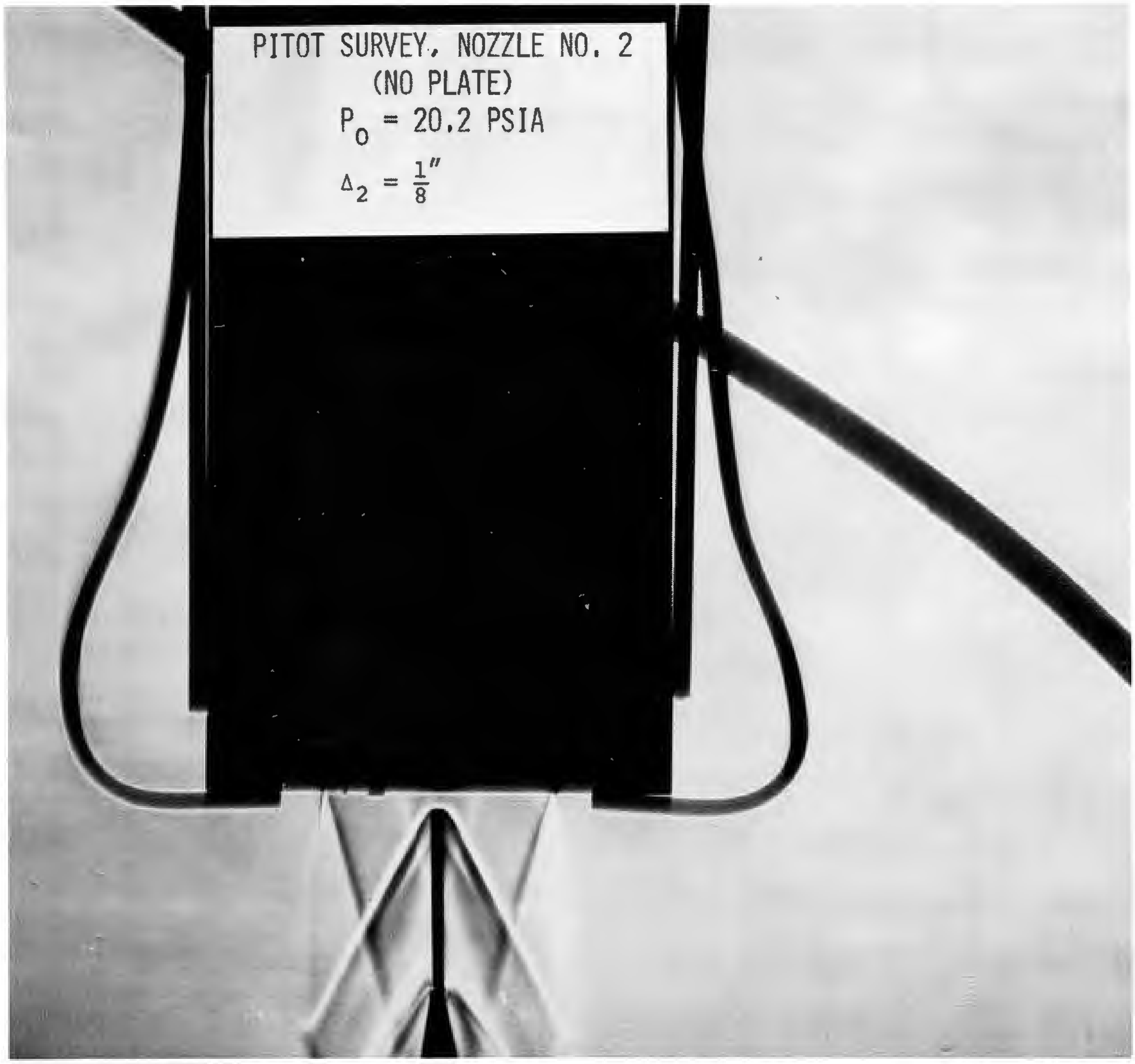

FIGURE 29 SCHLIEREN PHOTOGRAPH OF PITOT SURVEY: NOZZLE NO. 2 (RUN 5)

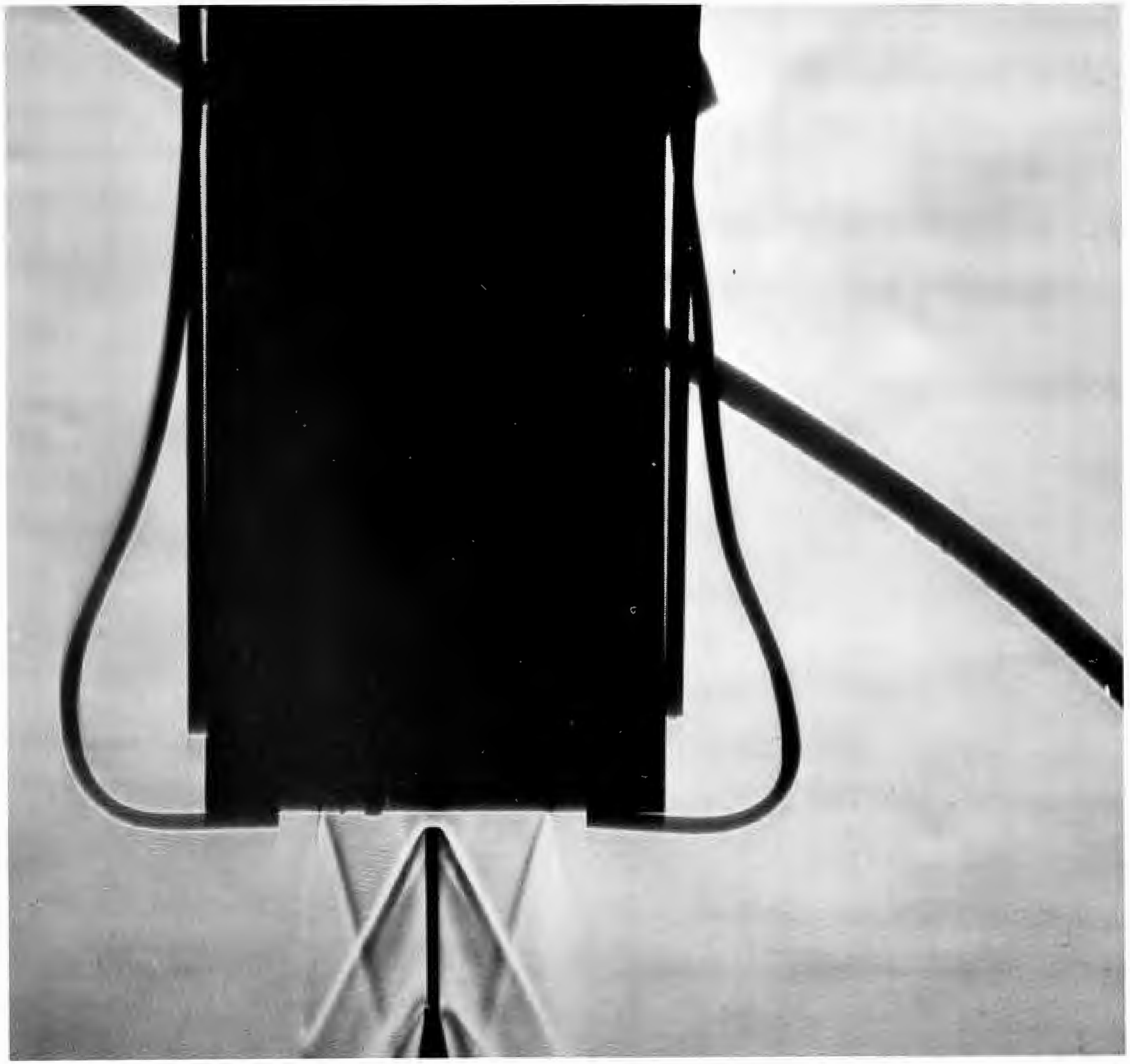

FIGURE 30 SCHLIEREN PHOTOGRAPH OF PITOT SURVEY: NOZZLE NO. 2 (RUN 6)

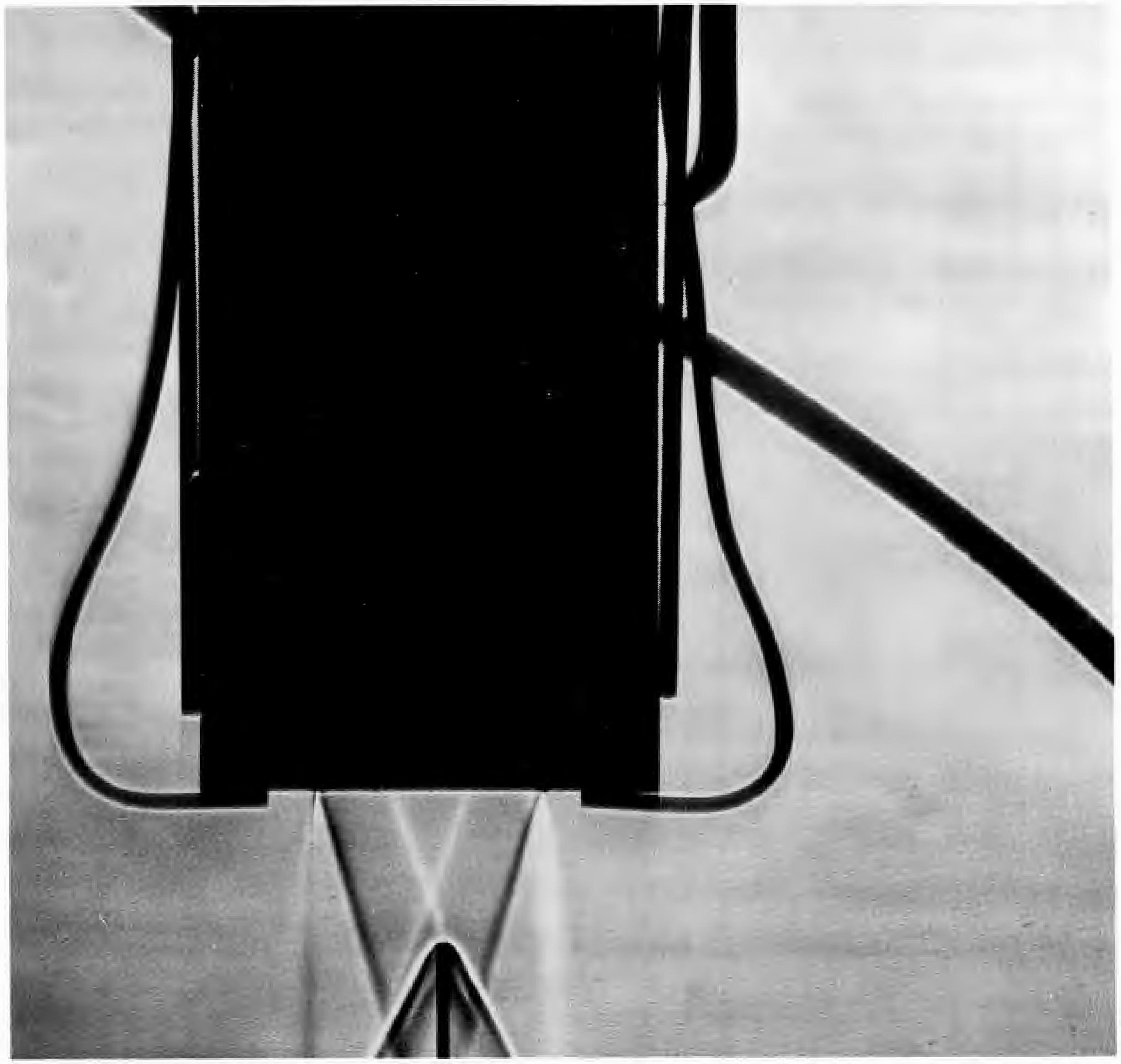

FIGURE 31 SCHLIEREN PHOTOGRAPH OF PITOT SURVEY: NOZZLE NO. 2 (RUN 9)

FIGURE 32 SCHLIEREN PHOTOGRAPH OF PITOT SURVEY: NOZZLE NO. 2 (RUN 10)

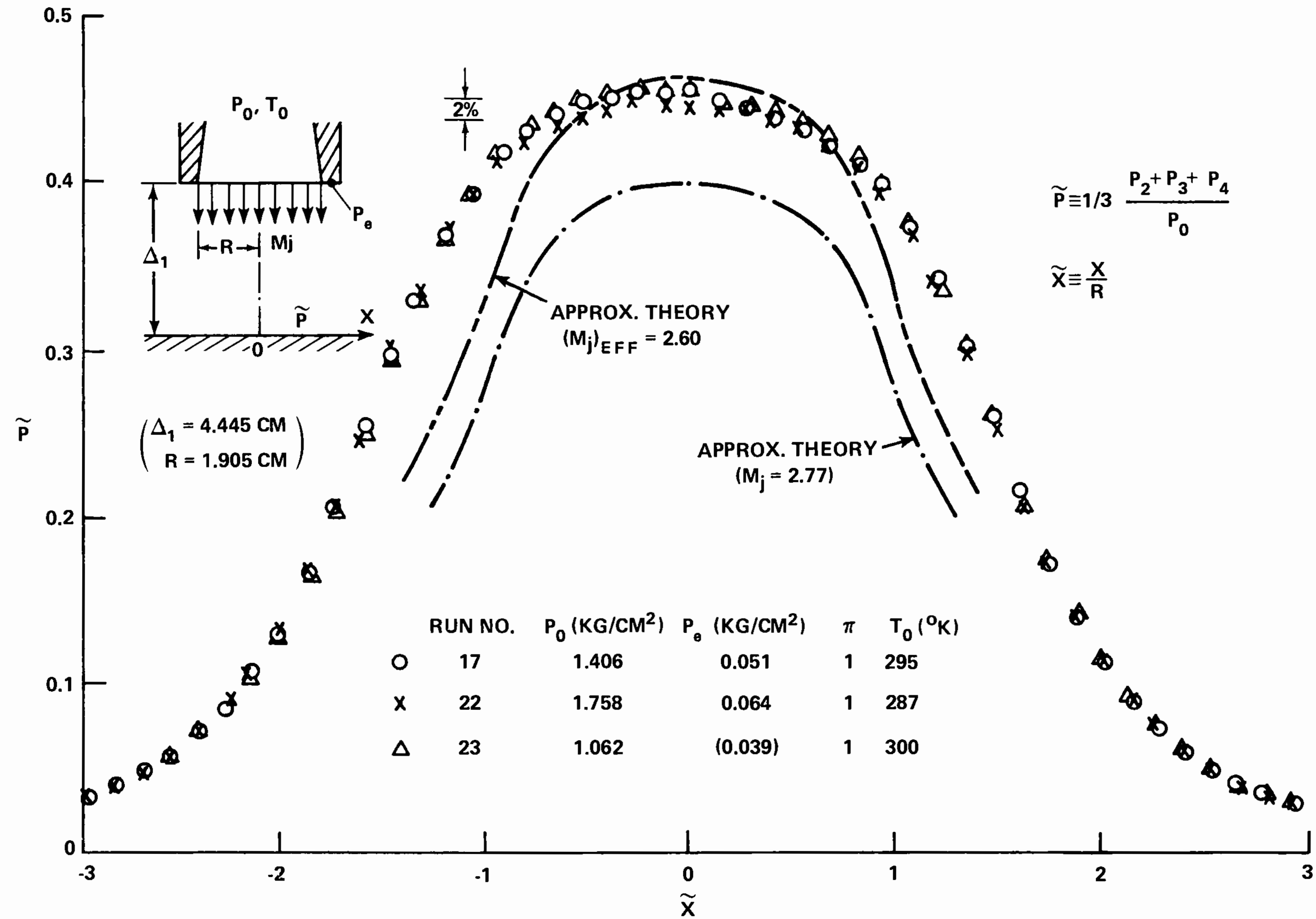

FIGURE 33 SURFACE PRESSURE RESULTS: NOZZLE NO. 2 (NEARLY ISENTROPIC JET)

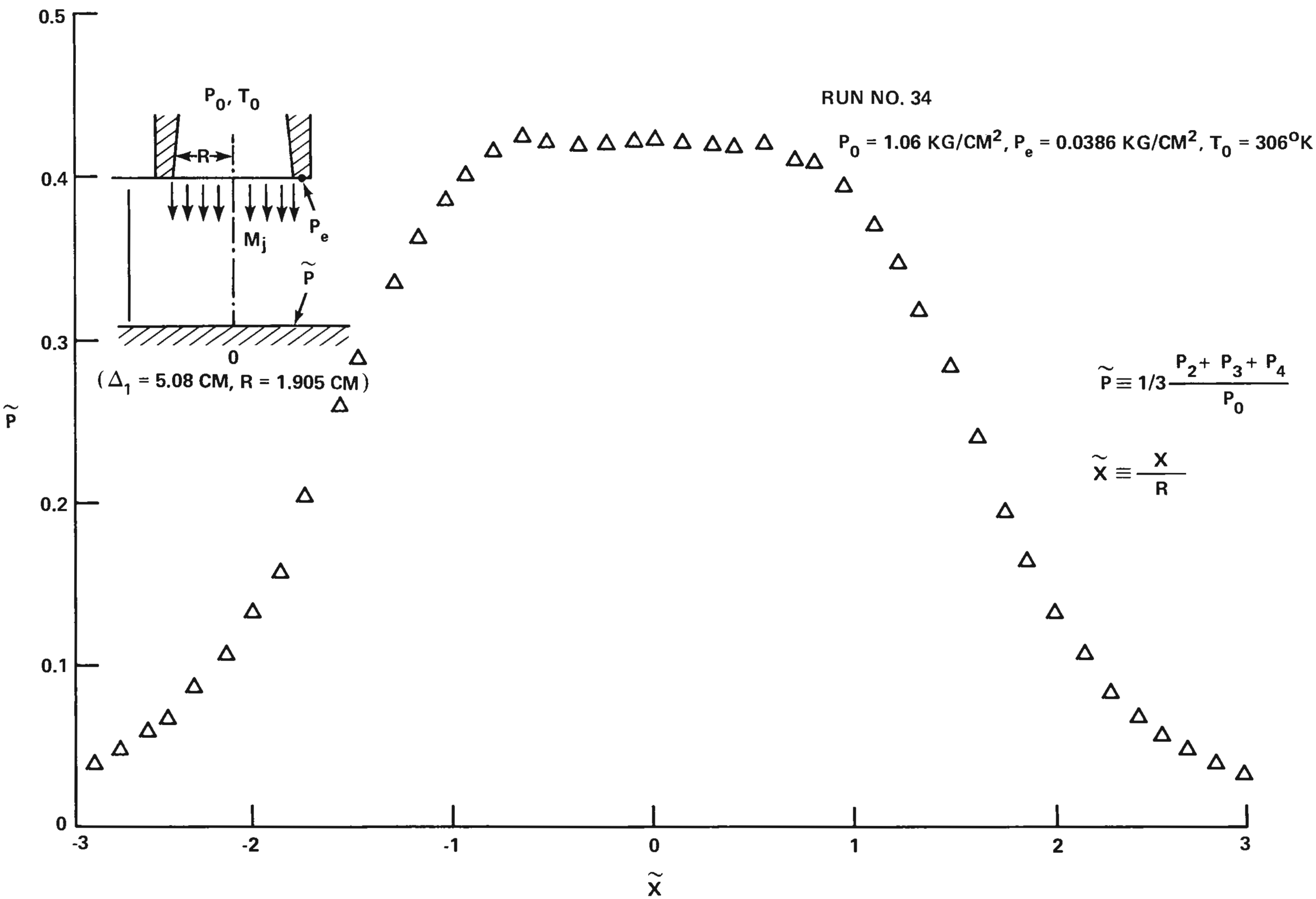

FIGURE 34 SURFACE PRESSURE RESULTS: NOZZLE NO. 2 (NEARLY ISENTROPIC JET)

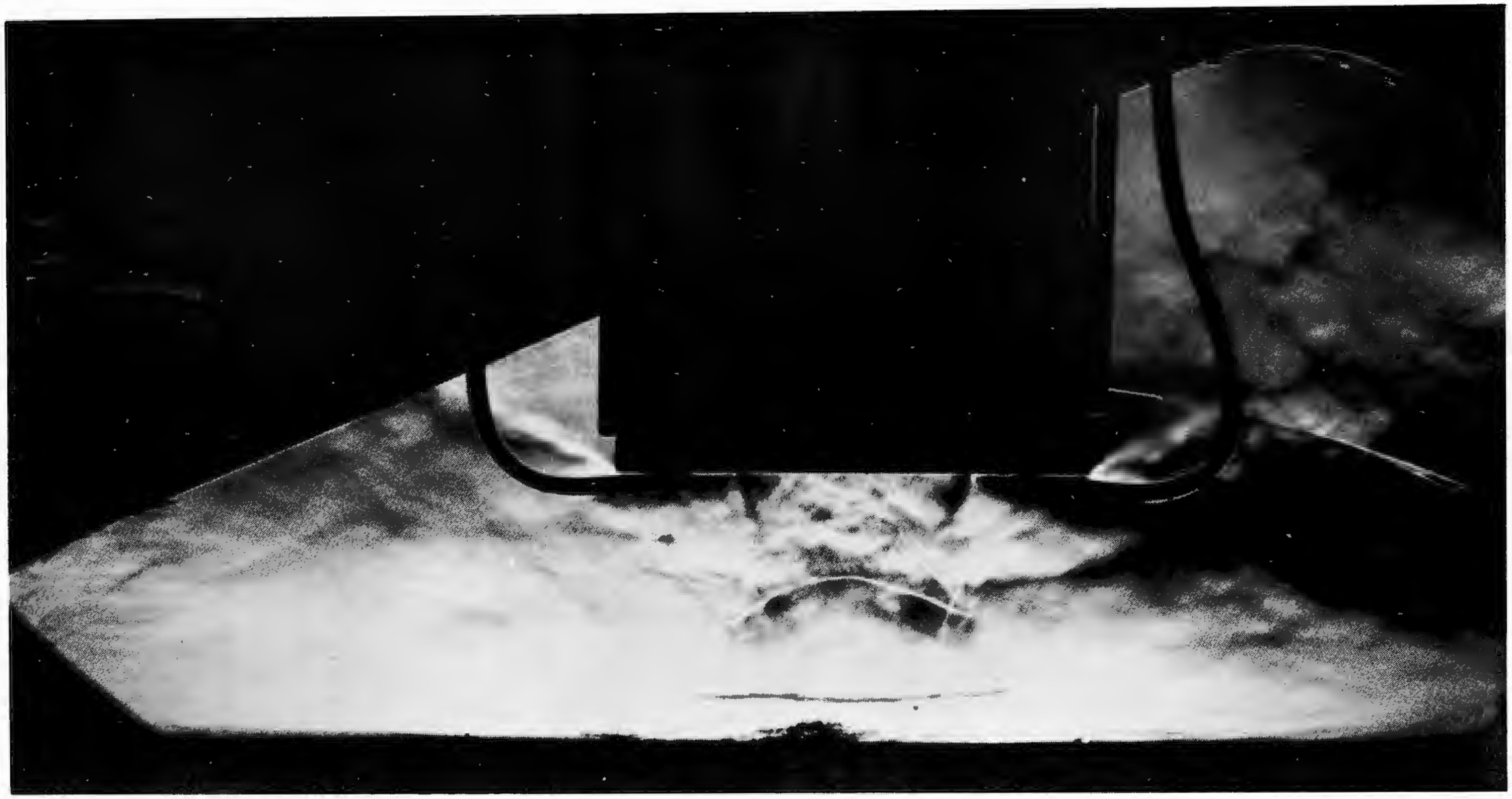

FIGURE 35 SCHLIEREN PHOTOGRAPH OF IMPINGMENT FLOW: NOZZLE NO. 2 (RUN 135)

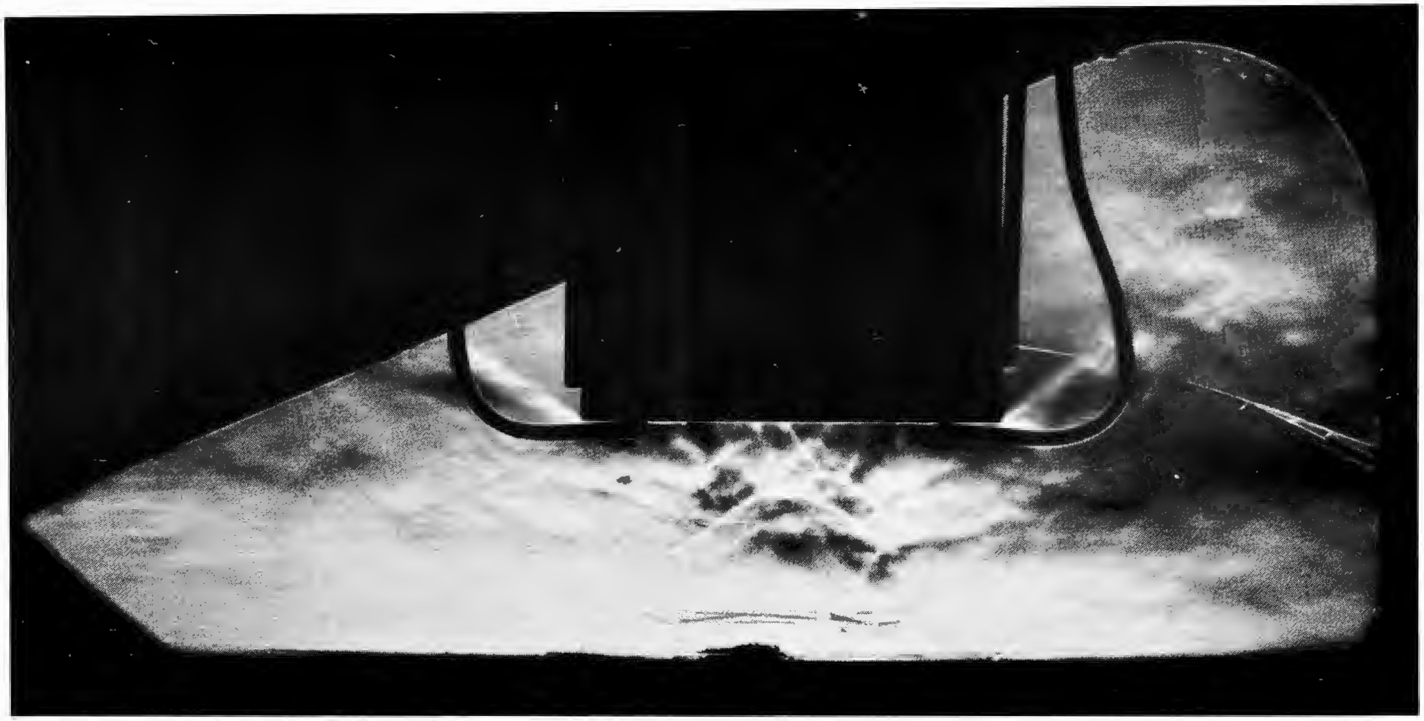

FIGURE 36 SCHLIEREN PHOTOGRAPH OF IMPINGEMENT FLOW: NOZZLE NO. 2 (RUN 145)

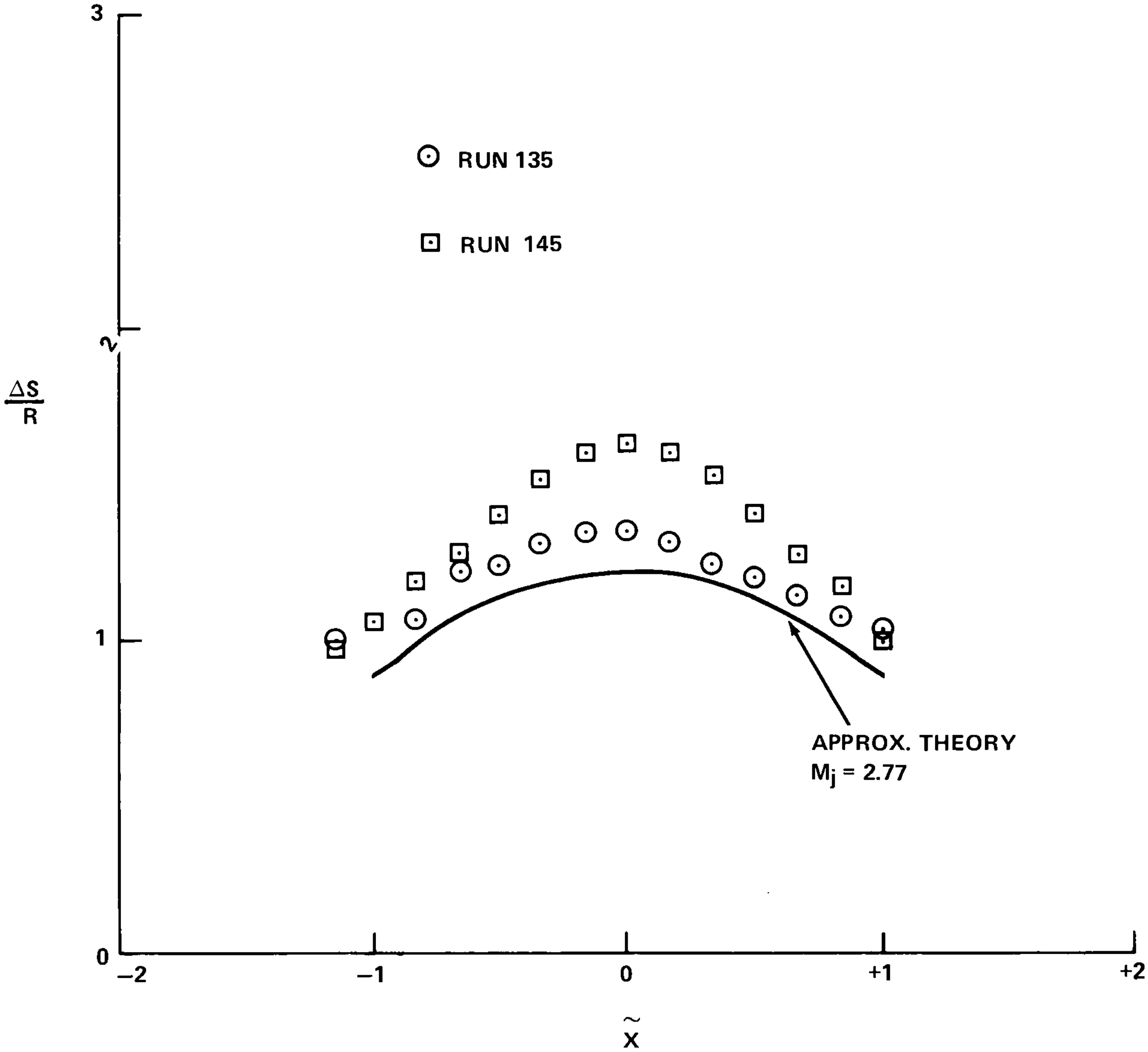

FIGURE 37 SHOCK MEASUREMENTS: NOZZLE NO. 2

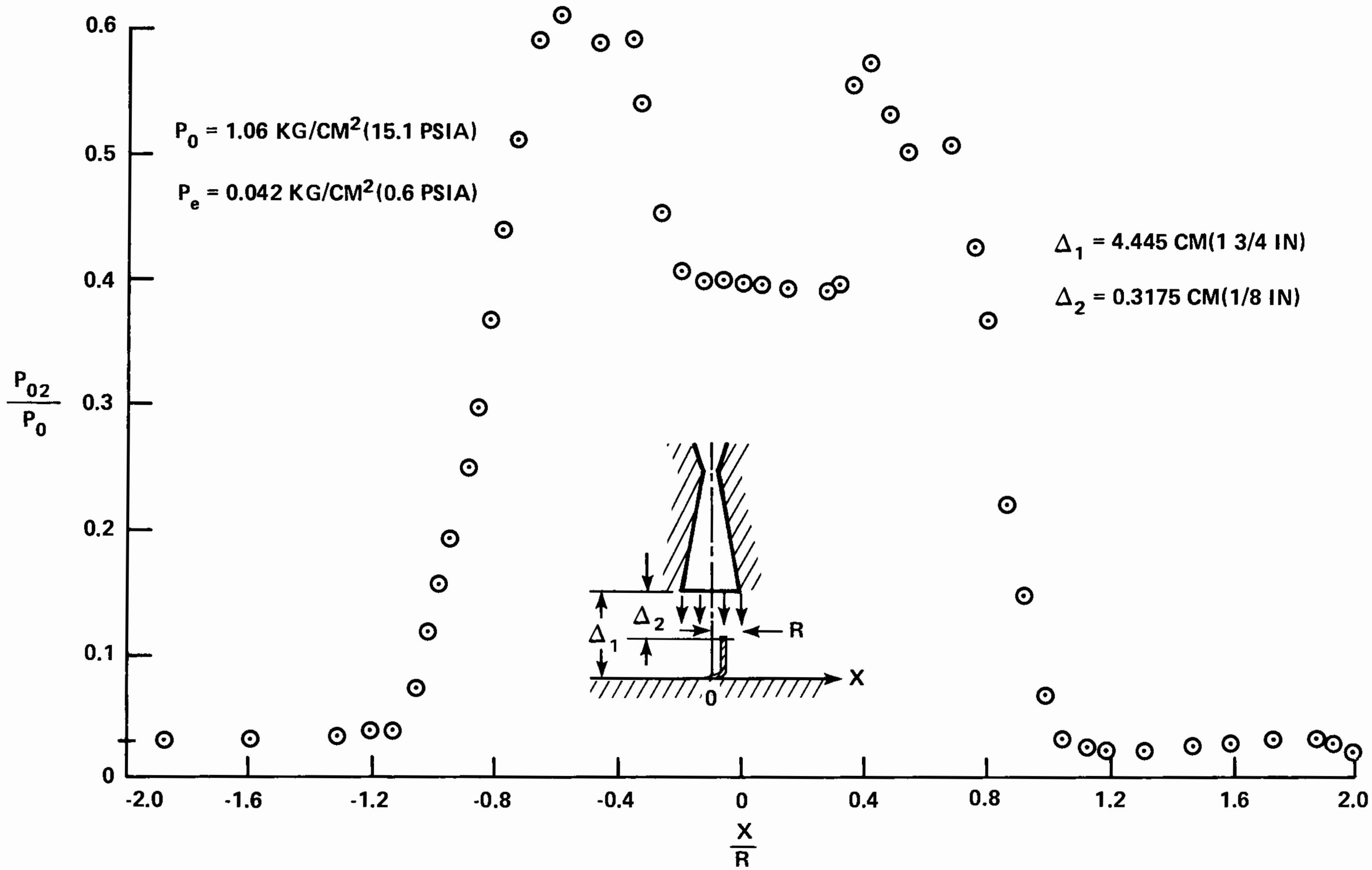

FIGURE 38a. PITOT SURVEY — PITOT-PLATE CONFIGURATION NOZZLE NO. 2 (RUN NO. 40)

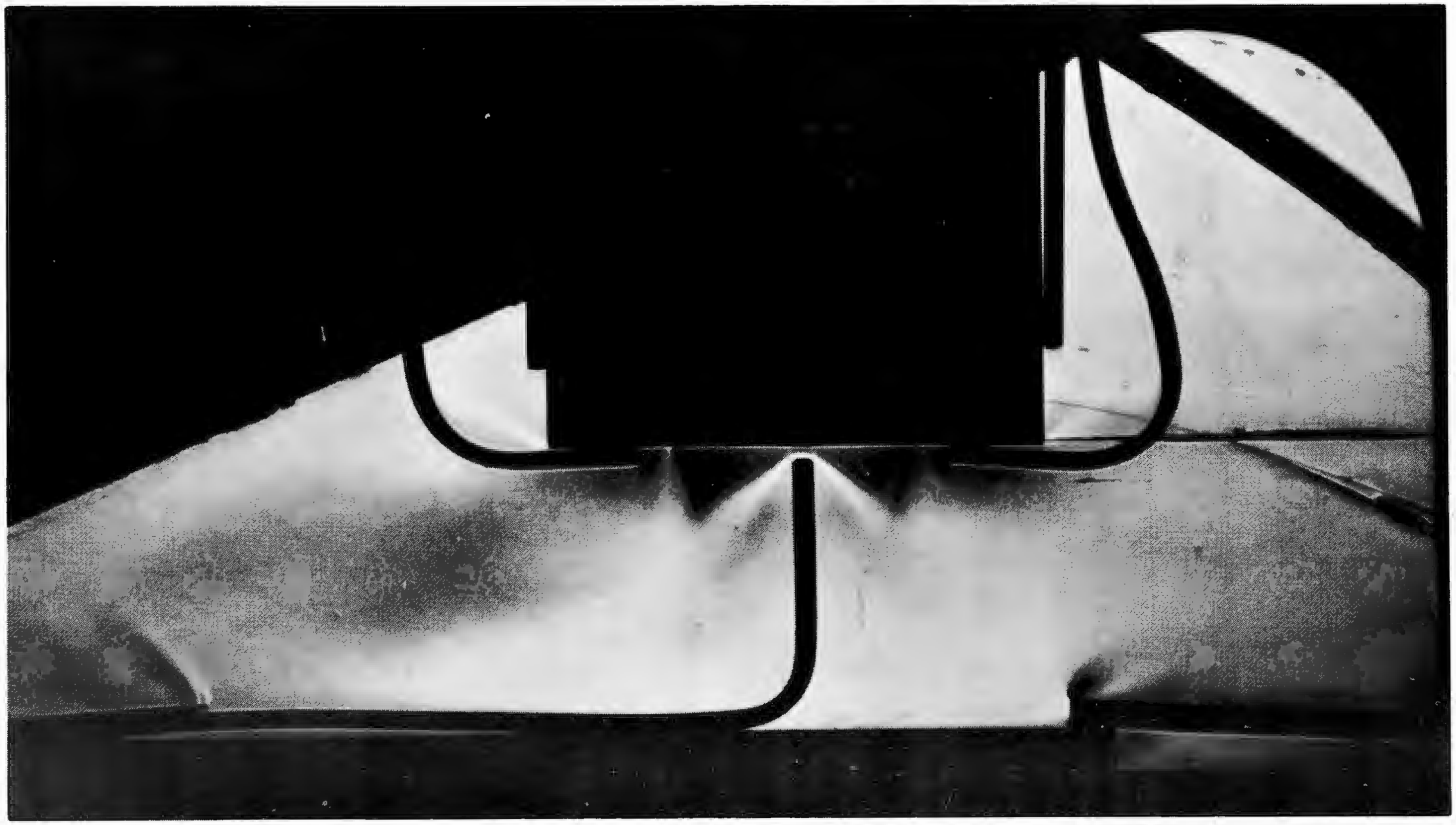

FIGURE 38b SCHLIEREN PHOTOGRAPH OF PITOT SURVEY OF IMPINGING JET: NOZZLE NO. 2 (RUN 40)

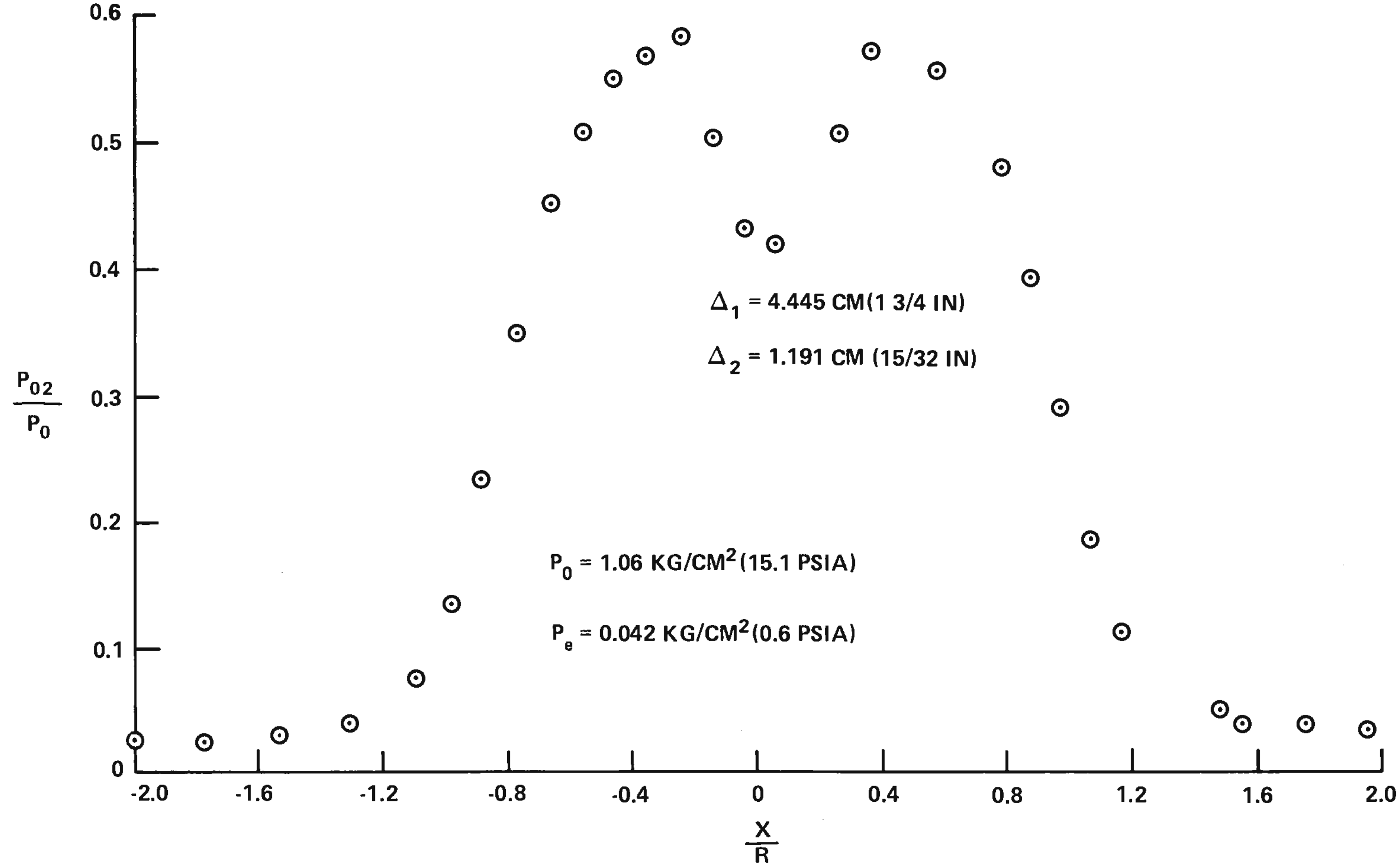

FIGURE 39a. PITOT SURVEY — PITOT-PLATE CONFIGURATION NOZZLE NO. 2 (RUN NO. 42)

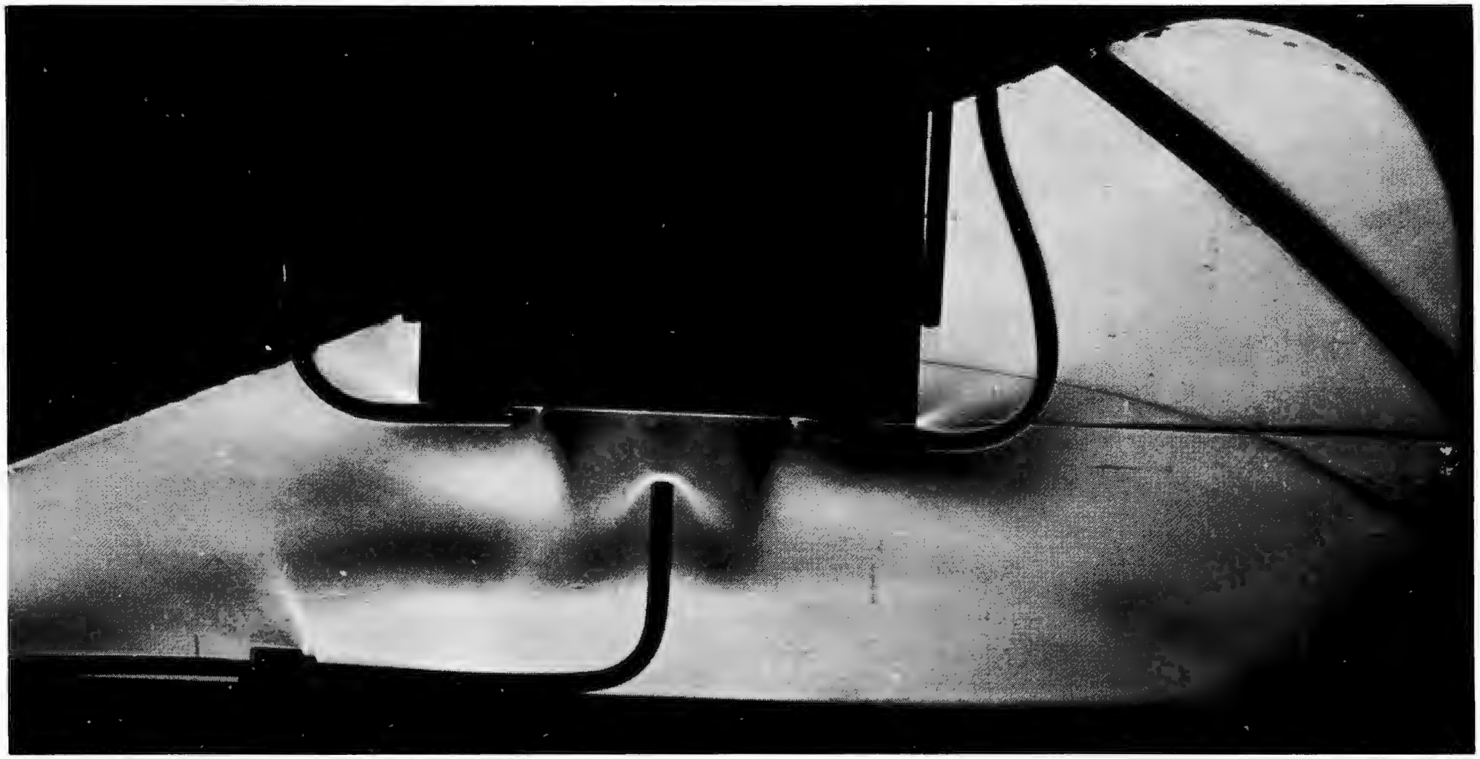

FIGURE 39b SCHLIEREN PHOTOGRAPH OF PITOT SURVEY OF IMPINGING JET: NOZZLE NO. 2 (RUN 42)

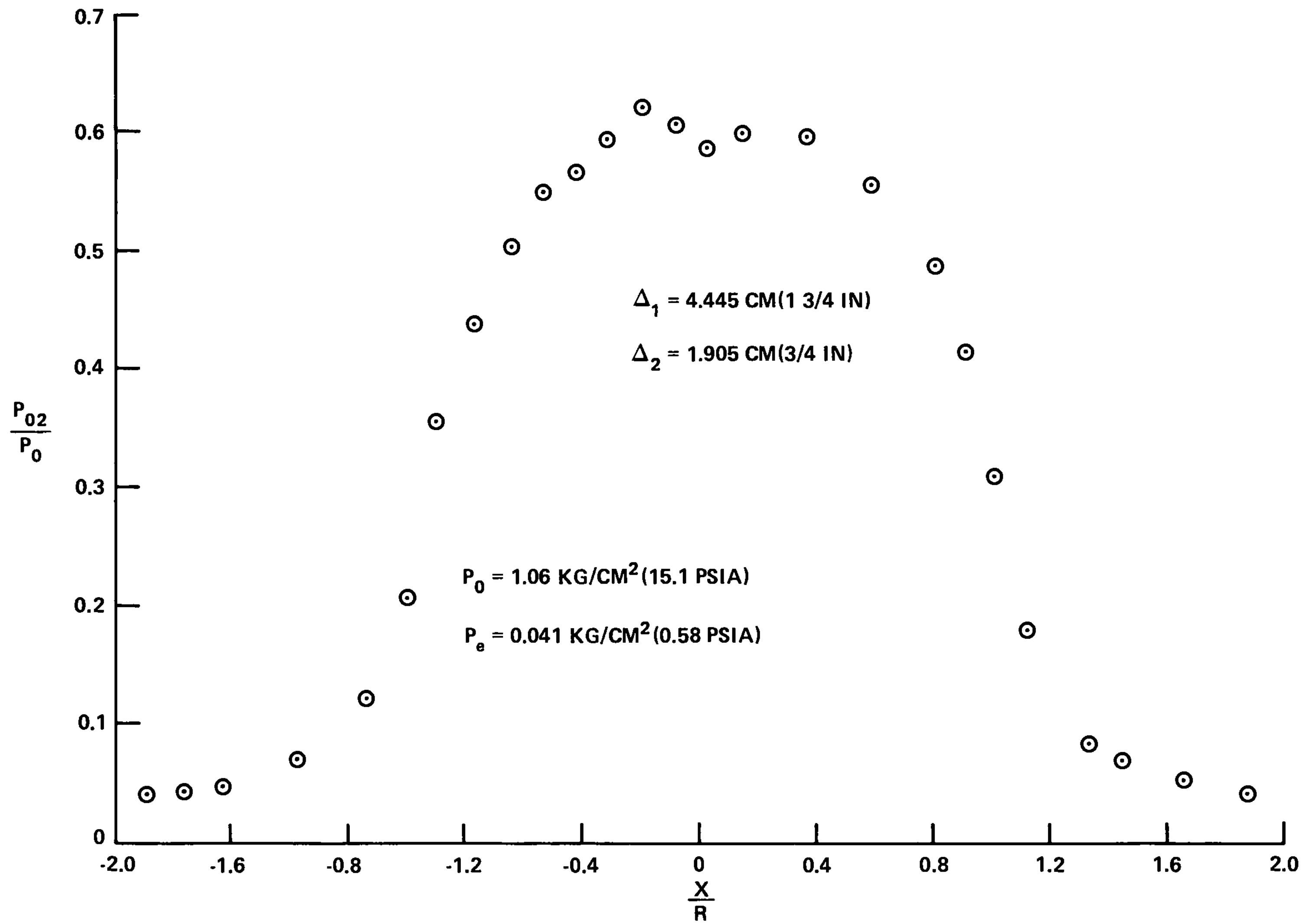

FIGURE 40a. PITOT SURVEY — PITOT-PLATE CONFIGURATION NOZZLE NO. 2 (RUN NO. 43)

FIGURE 40b SCHLIEREN PHOTOGRAPH OF PITOT SURVEY OF IMPINGING JET: NOZZLE NO. 2 (RUN 43)

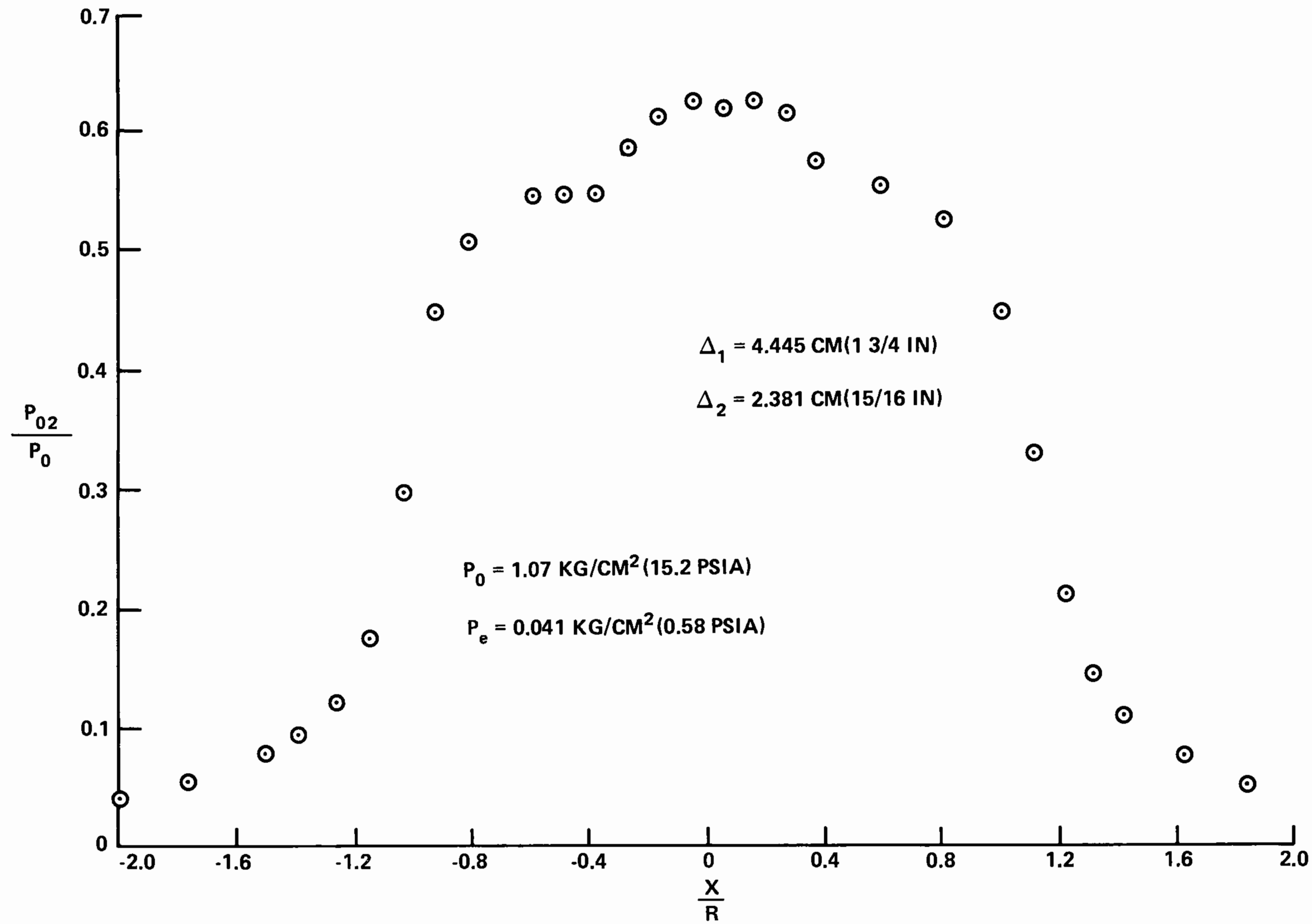

FIGURE 41a. PITOT SURVEY — PITOT -PLATE CONFIGURATION NOZZLE NO. 2 (RUN NO. 44)

FIGURE 41b SCHLIEREN PHOTOGRAPH OF PITOT SURVEY OF IMPINGING JET, NOZZLE NO. 2 (RUN 44)

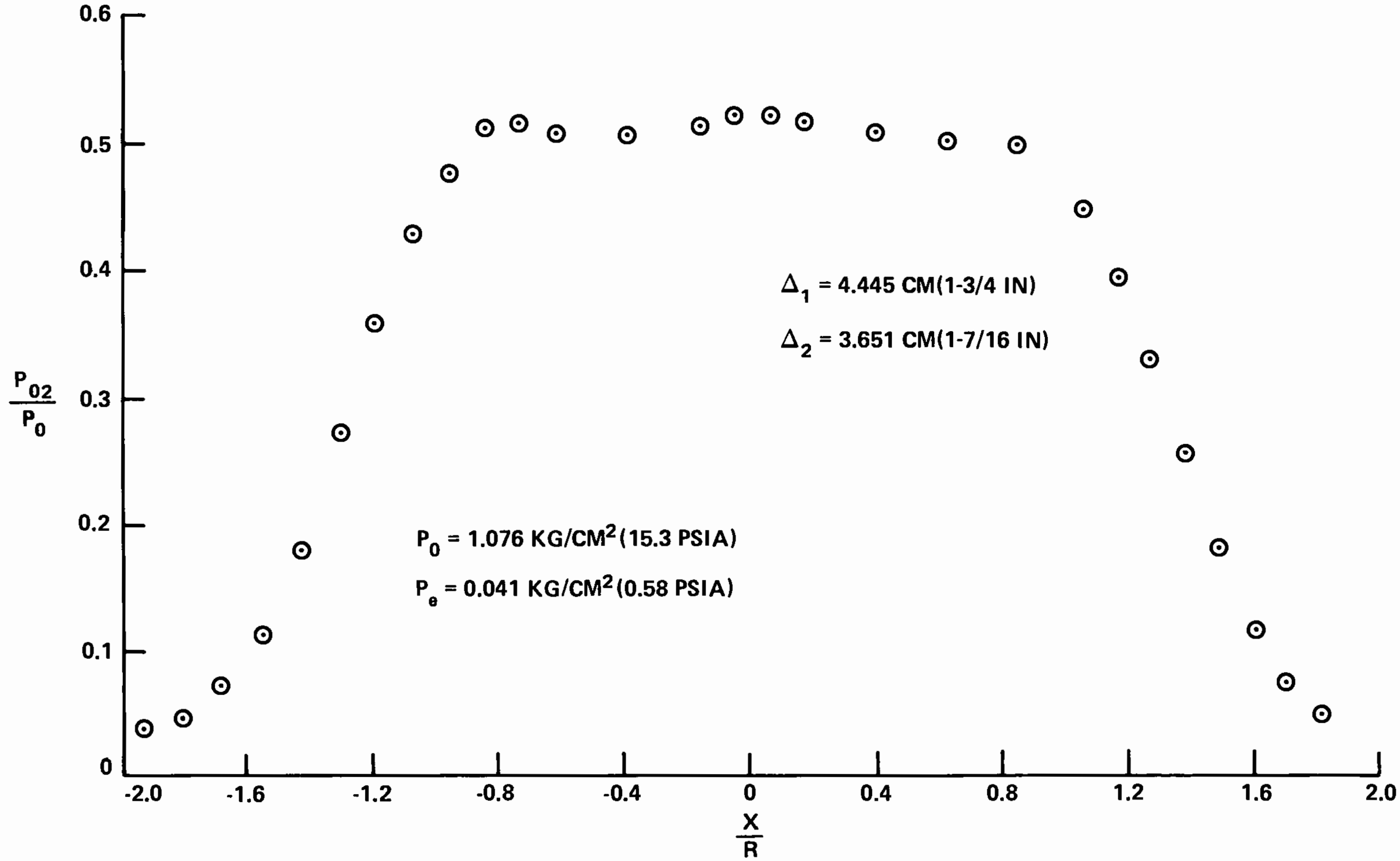

FIGURE 42 PITOT SURVEY – PITOT-PLATE CONFIGURATION – NOZZLE NO. 2 (RUN NO. 45)

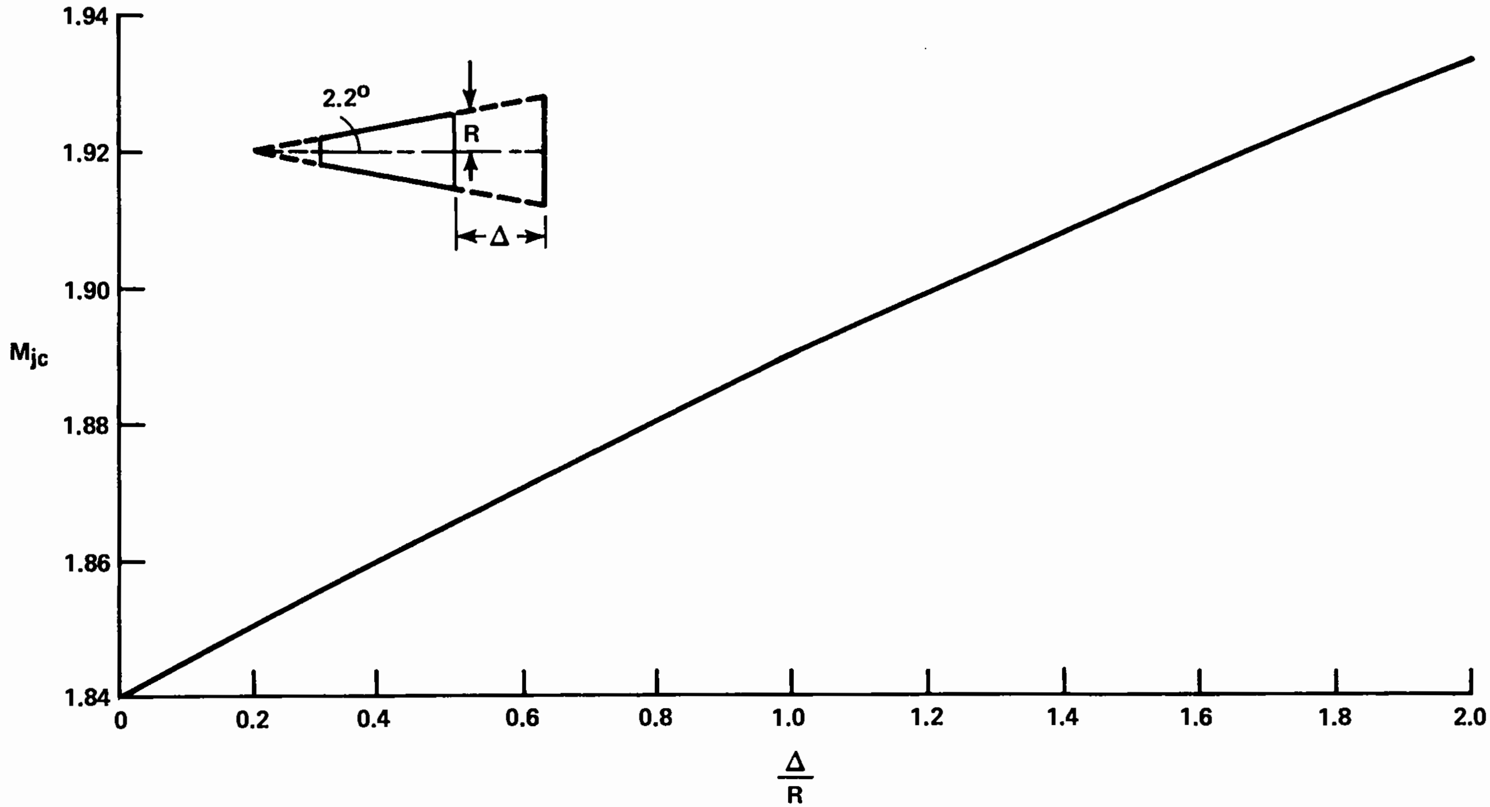

FIGURE 43 MACH NO. CORRECTION – NOZZLE NO. 1

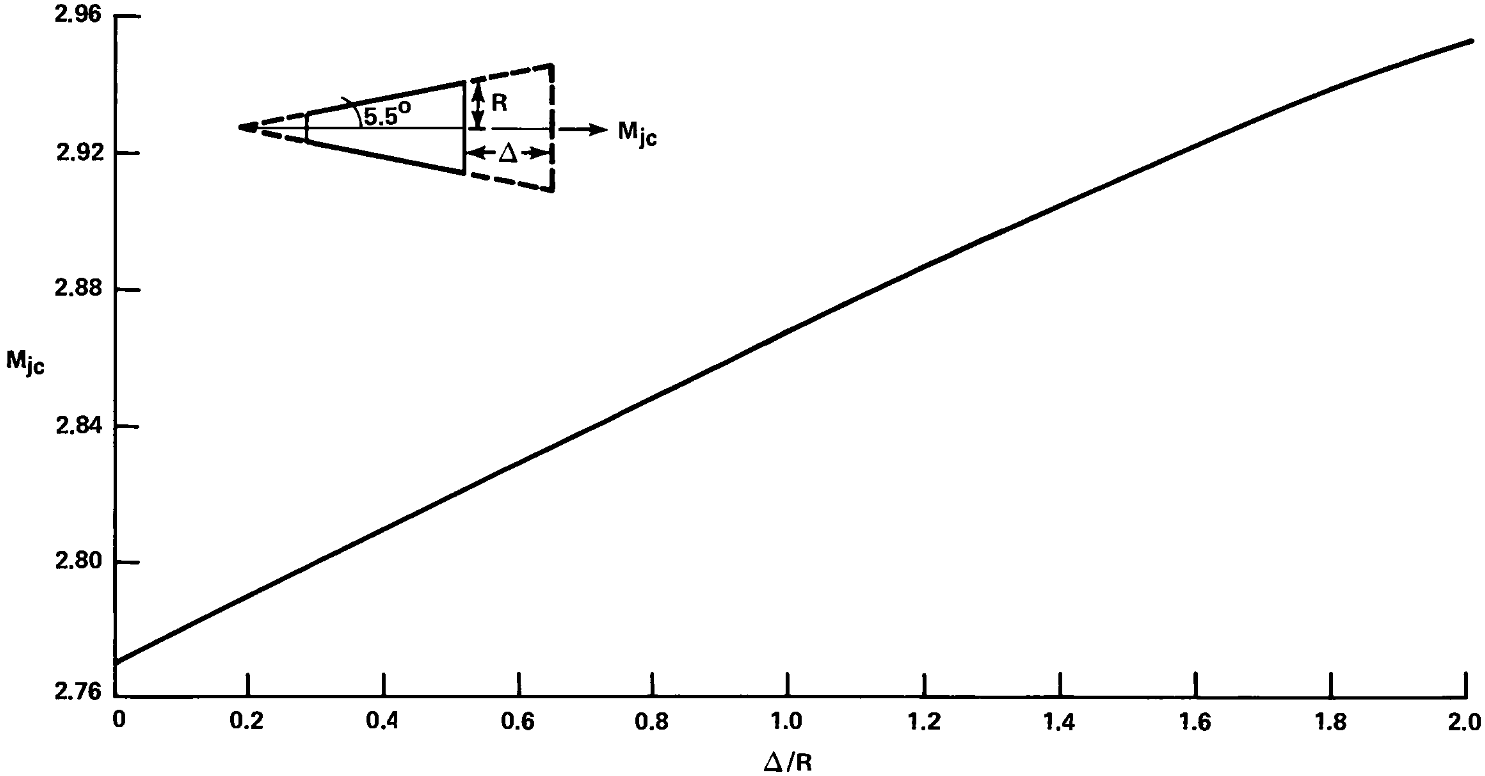

FIGURE 44 MACH NO. CORRECTION – NOZZLE NO. 2

REFERENCES

1. Edney, B., "Anomalous Heat Transfer and Pressure Distributions on Blunt Bodies at Hypersonic Speeds in the Presence of an Impinging Shock," FFA Report 115, The Aeronautical Research Institute of Sweden, Stockholm, 1968.

2. Hains, F. D. and Keyes, J. W., "Shock Interference Heating in Hypersonic Flows," AIAA Journal, Vol. 10, No. 11, Nov 1972, pp. 1441-1447.

3. Heirs, R. S. and Loubsky, W. J., "Effects of Shock-Wave Impingement on the Heat Transfer on a Cylindrical Leading Edge," NASA TN D-3859, Ames Research Center, Moffet Field, Calif., 1967.

4. Kaufman, L. G., III, Karkegi, R. H. and Morton, L. C., "Shock Impingement Caused by Boundary Layer Separation Ahead of Blunt Fins," ARL TR 72-0118, Aerospace Research Laboratories, WPAFB, Ohio, 1972.

5. Gillerlain, J. D., Jr., "Experimental Investigation of a Fin-Cone Interface Flow Field at Mach 5," NSWC/WOL/TR 75-63, Naval Surface Weapons Center, White Oak Laboratory, Silver Spring, Md., 1976.

6. Chien, K.-Y., "Normal Impingement of a Supersonic Jet on a Plane--A Basic Study of Shock-Interference Heating," NSWC/WOL/TR 75-195, Naval Surface Weapons Center, White Oak Laboratory, Silver Spring, Md., 1975.

7. Gummer, J. H. and Hunt, B. L., "The Impingement of a Uniform, Axisymmetric, Supersonic Jet on a Perpendicular Flat Plate," The Aeronautical Quarterly, Vol. 22, Pt. 4, Nov 1971, pp. 403-420.

8. Carling, J. C. and Hunt, B. L., "The Near Wall Jet of a Normally Impinging, Uniform, Axisymmetric, Supersonic Jet," Journal of Fluid Mechanics, Vol. 66, Pt. 1, 1974, pp. 159-176.

9. Pollard, D. J. and Bradbury, L. J. S., "Impingement of a Two-Dimensional Supersonic Jet upon a Normal Ground Surface," AIAA Journal, Vol. 14, No. 8, Aug 1976, pp. 1095-1098.

10. Zien, T. F., Chien, K.-Y. and Driftmyer, R. T., "Two-Dimensional Supersonic Jet Impingement on a Flat Plate," AIAA Paper 78-208, AIAA 16th Aerospace Sciences Meeting, Huntsville, Alabama, Jan 1978. Also, AIAA Journal, Vol. 17, No. 1, Jan 1979, pp. 4-5.

11. Ames Research Staff, "Equations, Tables, and Charts for Compressible Flow," NACA Report 1135, 1953.

12. Gummer, J. H. and Hunt, B. L., "The Impingement of Non-Uniform, Axisymmetric, Supersonic Jets on a Perpendicular Flat Plate," Israel Journal of Technology, Vol. 12, 1974, pp. 221-235.

DISTRIBUTION

Commander
Naval Sea Systems Command
Attn: SEA-05121 (Chief Technical Analyst)
SEA-033
SEA-031
SEA-09G32 2
Department of the Navy
Washington, DC 20362

Commander
Naval Air Systems Command
Attn: AIR-03B
AIR-03C
AIR-320
AIR-320C (William C. Volz)
AIR-310 (Dr. H. J. Mueller)
AIR-50174 2
Department of the Navy
Washington, DC 20361

Office of Naval Research
Attn: ONR-430B (Morton Cooper) 2
CDR R. D. Matulka
800 N. Quincy Street
Arlington, VA 22203

Commander
David W. Taylor Naval Ship Research and Development Center
Attn: 5641 (Central Library Branch)
5643 (Aerodynamics Laboratory)
Dr. T. C. Tai
Dr. C. von Kerczek
Bethesda, MD 20034

Commander
Naval Weapons Center
Attn: 3161 (Bertha Ryan, W. R. Compton, C. F. Markarian, Ray Van Aken)
533 (Technical Library)
406
4063 (R. E. Meeker)
China Lake, CA 93555

Director
Naval Research Laboratory
Attn: Library
6503
Washington, DC 20390

DISTRIBUTION (Cont.)

NASA
Langley Station
Attn: MS/185 (Technical Library)
Aero & Space Mech Div.
Dennis Bushwell
Ivan Beckwith
R. Trimpi
MS/164 (J. B. Anders)
Hampton, VA 23665

NASA
Lewis Research Center
Attn: 60-3 (Library)
Chief, Wind Tunnel and Flight Division
21000 Brookpart Road
Cleveland, OH 44135

NASA
George C. Marshall Space Flight Center
Attn: R-AERO-AU (T. Reed)
ED31 (W. K. Dahm)
Huntsville, AL 35812

NASA
Attn: RR (Dr. H. H. Kurzweg)
600 Independence Avenue S.W.
Washington, DC 20546

Technical Library
Director Defense Research and
Engineering (DDR&E)
Attn: Stop 103
Room 3E-1063, The Pentagon
Washington, DC 20301

Defense Documentation Center
Cameron Station
Alexandria, VA 22314 12

Commander
Naval Missile Center
Attn: Technical Library
Point Mugu, CA 93041

DISTRIBUTION (Cont.)

Commanding Officer
USA Aberdeen Research and Development Center
Attn: STEAP-TL (Technical Library Division)
AMXRD-XSE
Aberdeen Proving Ground, MD 21005

Director
Strategic Systems Project Office
Attn: NSP-2722 2
Department of the Navy
Washington, DC 20390

Director of Intelligence
Attn: AFOIN-3B
Headquarters, USAF (AFNINDE)
Washington, DC 20330

Commander
Space and Missile Systems Organization
Attn: SMTTM (LT C. Lee)
Air Force Unit Post Office
Los Angeles Air Force Station, CA 90045

Headquarters
Arnold Engineering Development Center
Attn: Library/Documents (Joe Ashley, Jr.)
R. W. Henzel, TD
DYR (CAPT C. Tirres)
Library/Documents
Arnold Air Force Station, TN 37389

von Karman Gas Dynamics Facility
ARO, Inc.
Attn: Dr. J. D. Whitfield, Chief
Arnold Air Force Station, TN 37389

Commanding Officer
Harry Diamond Laboratories
Attn: Library
Adelphi, MD 20783

Commanding General
U.S. Army Missile Command
Attn: AMSMI-RR
Chief, Document Section 2
AMSMI-RDK (R. A. Deep)
AMSMI-RDK (T. R. Street)
Redstone Arsenal, AL 35809

DISTRIBUTION (Cont.)

Department of the Army
Office of the Chief of Research and Development
ABMDA, The Pentagon
Washington, DC 20350

U.S. Army Cold Region Research and Engineering
Laboratory
Attn: Dr. Y. C. Yen
Hanover, NH 03755

Commanding Officer
Picatinny Arsenal
Attn: SMUPA-VC-3 (A. A. Loeb)
Dover, NJ 07801

Commander (ADL)
Naval Air Development Center
Warminster, PA 18974

Air Force Weapons Laboratory
Technical Library (SUL)
Kirtland Air Force Base
Albuquerque, NM 87117

U.S. Army Ballistic Missile Defense Agency
Attn: Dr. Sidney Alexander
1300 Wilson Boulevard
Arlington, VA 22209

Applied Physics Laboratory
Attn: Document Library 2
Dr. F. Hill
Dr. L. L. Cronvich
J. D. Randall
Johns Hopkins University
Johns Hopkins Road
Laurel, MD 20810

Commanding Officer
Naval Intelligence Support Center
4301 Suitland Road
Washington, DC 20390

DISTRIBUTION (Cont.)

Department of Aeronautics
Attn: COL D. H. Daley, Prof. & Head
DFAN
USAF Academy, CO 80840

Chief of Naval Research
Attn: ONR 100
Arlington, VA 22217

Air Force Armament Test Laboratory
Attn: C. B. Butler
Eglin Air Force Base, FL 32542

Headquarters, Edgewood Arsenal
Attn: A. Flateau
Edgewood Arsenal, MD 21010

Fluid Mechanics Research Laboratory
Wright-Patterson Air Force Base
Attn: E. G. Johnson, Director 5
Dayton, OH 45433

Commander
U.S. Army
Natick Research & Development Command
Attn: G. A. Barnard
DRDNA-UAS
Natick, MA 01760

NASA Ames Research Center
Attn: Dr. M. Horstman
Mr. W. C. Davy
Moffett Field, CA 94035

Fluid Dynamics Laboratory
Wright-Patterson Air Force Base
Attn: Dr. D. J. Harney
Dayton, OH 45433

Energetics Laboratory
Wright-Patterson Air Force Base
Attn: Dr. A. W. Fiore
Dayton, OH 45433

Naval Postgraduate School
Attn: Prof. D. J. Collins
Department of Aeronautics
Monterey, CA 93940

DISTRIBUTION (Cont.)

University of Akron
Attn: Prof. B. T. F. Chung
Mechanical Engineering Department
Akron, OH 44325

Aerospace Engineering Program
University of Alabama
Attn: Prof. W. K. Roy, Chm.
P.O. Box 6307
Tuscaloosa, AL 35486

AME Department
University of Arizona
Attn: Dr. L. B. Scott
Tucson, AZ 85721

Polytechnic Institute of Brooklyn
Attn: Dr. J. Polczynski
Graduate Center Library
Route 110, Farmingdale
Long Island, NY 11735

Polytechnic Institute of Brooklyn
Attn: Reference Department
Spicer Library
333 Jay Street
Brooklyn, NY 11201

Brown University
Division of Engineering
Attn: Dr. M. Sibulkin
Library
Providence, RI 02912

California Institute of Technology
Attn: Graduate Aeronautical Laboratories
Aero. Librarian
Karman Lab-301 (Dr. H. Liepmann)
Firestone Flight Sciences Lab.
(Prof. L. Lees)
Guggenheim Lab. (Prof. D. Coles, 321)
Dr. A. Roshko
Pasadena, CA 91109

University of California
Attn: Dr. M. Holt
Dept. of Mechanical Engineering
Berkeley, CA 94720

DISTRIBUTION (Cont.)

University of California - Los Angeles
Attn: Prof. J. D. Cole
Dept. of Mechanics and Structures
Los Angeles, CA 90024

GASDYNAMICS
University of California
Attn: A. K. Oppenheim
Richmond Field Station
1301 South 46th Street
Richmond, CA 94804

Department of Aerospace Engineering
University of Southern California
Attn: Dr. John Laufer
University Park
Los Angeles, CA 90007

University of California - San Diego
Attn: Dr. P. A. Libby
Dr. H. K. Cheng
Department of Aerospace and Mechanical Engineering Sciences
LaJolla, CA 92037

Case Western Reserve University
Attn: Dr. Eli Reshotko, Chairman
Department of Mechanical and Aerospace Engineering
Cleveland, OH 44106

The Catholic University of America
Attn: Dr. C. C. Chang
Dr. Paul K. Chang, Mechanical Engineering Dept.
Dr. M. J. Casarella, Mechanical Engineering Dept.
Washington, DC 20017

University of Cincinnati
Attn: Department of Aerospace Engineering
Dr. Arnold Polak
Cincinnati, OH 45221

Department of Aerospace Engineering Sciences
University of Colorado
Boulder, CO 80302

DISTRIBUTION (Cont.)

Cornell University
Attn: Dr. S. F. Shen
Prof. F. K. Moore, Head
Thermal Engineering
Dept., 208 Upson Hall
Graduate School of Aero. Engineering
Ithaca, NY 14850

University of Delaware
Attn: Dr. James E. Danberg
Mechanical and Aeronautical Engineering Dept.
Newark, DE 19711

George Washington University
Attn: Prof. A. B. Cambel
Prof. R. Goulard
School of Engineering
Washington, DC 20052

Georgia Institute of Technology
Attn: Dr. Arnold L. Ducoffe
225 North Avenue, N.W.
Atlanta, GA 30332

Technical Reports Collection
Gordon McKay Library
Harvard University
Division of Engineering and Applied Physics
Pierce Hall
Oxford Street
Cambridge, MA 02138

Illinois Institute of Technology
Attn: Dr. M. V. Morkovin
Prof. A. A. Fejer, M.A.E. Dept.
3300 South Federal
Chicago, IL 60616

University of Illinois
Aeronautical and Astronautical Engineering
Department
101 Transportation Bldg.
Urbana, IL 61801

Iowa State University
Aerospace Engineering Dept.
Ames, Iowa 50010

DISTRIBUTION (Cont.)

The Johns Hopkins University
Attn: Professor S. Corrsin
Baltimore, MD 21218

University of Kentucky
Attn: C. F. Knapp
Wenner-Gren Aero. Lab.
Lexington, KY 40506

Department of Aero. Engineering, ME 106
Louisianna State University
Attn: Dr. P. H. Miller
Baton Rouge, LA 70803

University of Maryland
Attn: Prof. A. Wiley Sherwood,
Department of Aerospace Engineering
Prof. Charles A. Shreeve
Department of Mechanical Engineering
Dr. S. I. Pai, Institute for Fluid
Dynamics and Applied Mathematics
Dr. Redfield W. Allen, Department
of Mechanical Engineering
Dr. W. L. Melnik, Department of
Aerospace Engineering
Dr. John D. Anderson, Jr.
Department of Aerospace Engineering
College Park, MD 20740

Michigan State University
Attn: Library, Documents Department
East Lansing, MI 48823

Massachusetts Institute of Technology
Attn: Mr. J. R. Martucelli, Rm. 33-211
Prof. M. Finston
Prof. J. Baron, Dept. of Aero. and
Astro., Rm. 37-461
Prof. A. H. Shapiro, Head, Mech.
Engr. Dept.
Aero. Engineering Library
Prof. Ronald F. Probestein
Dr. E. E. Covert
Aerophysics Laboratory
Cambridge, MA 02139

DISTRIBUTION (Cont.)

University of Michigan
Attn: Dr. M. Sichel, Dept. of Aero. Engr.
Engineering Library
Aerospace Engineering Lib.
Mr. C. Cousineau, Engin-Trans Lib.
Dr. C. M. Vest, Dept. of Mech. Engr.
Ann Arbor, MI 48104

Serials and Documents Section
General Library
University of Michigan
Ann Arbor, MI 48104

Mississippi State University
Attn: Mr. Charles B. Cliett
Department of Aerophysics and
Aerospace Engineering
P.O. Drawer A
State College, MS 39762

U.S. Naval Academy
Engineering Department, Aerospace Division
Annapolis, MD 21402

U.S. Naval Postgraduate School
Library, Code 2124
Attn: Technical Reports Section
Monterey, CA 93940

New York University
Attn: Director of
Guggenheim Aerospace Laboratories
Prof. V. Zakkay
Engineering and Science Library
University Heights
New York, NY 10453

North Carolina State College
Attn: Dr. F. R. DeJarnette, Dept. Mech.
and Aero. Engineering
Dr. H. A. Hassan, Dept. of Mech.
and Aero. Engineering
Raleigh, NC 27607

North Carolina State University
Attn: D. H. Hill Library
P.O. Box 5007
Raleigh, NC 27607

DISTRIBUTION (Cont.)

University of North Carolina
Attn: Department of Aero. Engineering
Library, Documents Section
APROTC Det 590
Chapel Hill, NC 27514

Northwestern University
Technological Institute
Attn: Department of Mechanical Engineering
Library
Evanston, IL 60201

Notre Dame University
Attn: Dr. J. D. Nicolaides, Dept. of
Aero. Engineering
College of Engineering Library
South Bend, IN 46556

Department of Aero-Astro Engineering
Ohio State University
Attn: Engineering Library
Prof. J. D. Lee
Prof. G. L. Von Eschen
2036 Neil Avenue
Columbus, OH 43210

Ohio State University Libraries
Documents Division
1858 Neil Avenue
Columbus, OH 43210

The Pennsylvania State University
Attn: Dept. of Aero Engr., Hammond Bldg.
Library, Documents Section
University Park, PA 18602

Bevier Engineering Library
126 Benedum Hall
University of Pittsburgh
Pittsburgh, PA 15261

Princeton University
Attn: Prof. S. Bogdonoff
Dr. I. E. Vas
Aerospace & Mechanical Science Dept.
D-214 Engrg. Quadrangle
Princeton, NJ 08540

DISTRIBUTION (Cont.)

Purdue University
School of Aeronautical and Engineering
Sciences
Attn: Library
Dr. P. S. Lykoudis, Dept. of Aero.
Engineering
Lafayette, IN 47907

Rensselaer Polytechnic Institute
Attn: Dept. of Aeronautical Engineering
and Astronautics
Troy, NY 12181

Rutgers - The State University
Attn: Dr. R. H. Page
Dr. C. F. Chen
Department of Mechanical Industrial and
Aerospace Engineering
New Brunswick, NJ 08903

Stanford University
Attn: Librarian, Dept. of Aeronautics and
Astronautics
Stanford, CA 94305

Stevens Institute of Technology
Attn: Mechanical Engineering Department
Library
Hoboken, NJ 07030

The University of Texas at Austin
Attn: Engr S.B.114B, Dr. Friedrich
Applied Research Laboratories
P.O. Box 8029
Austin, TX 78712

University of Toledo
Attn: Dept. of Aero. Engineering
Dept. of Mech. Engineering
2801 W. Bancroft
Toledo, OH 43606

University of Virginia
School of Engineering and Applied Science
Attn: Dr. I. D. Jacobson
Dr. G. Matthews
Dr. R. N. Zapata
Charlottesville, VA 22901

DISTRIBUTION (Cont.)

University of Washington
Attn: Engineering Library
Dept. of Aeronautics and Astronautics
Prof. R. E. Street, Dept. of Aero. and Astro.
Prof. A. Hertzberg, Aero. and Astro., Guggeheim Hall
Seattle, WA 98105

West Virginia University
Attn: Library
Morgantown, WV 26506

Federal Reports Center
University of Wisconsin
Attn: S. Reilly
Mechanical Engineering Building
Madison, WI 53706

Los Alamos Scientific Laboratory
Attn: Report Library
P.O. Box 1663
Los Alamos, NM 87544

University of Maryland
Attn: Dr. R. C. Roberts, Mathematics Department
Baltimore County (UMBC)
5401 Wilkens Avenue
Baltimore, MD 21228

Institute for Defense Analyses
Attn: Classified Library
400 Army-Navy Drive
Arlington, VA 22202

Kaman Sciences Corporation
Attn: Library
P.O. Box 7463
Colorado Springs, CO 80933

Kaman Science Corporation
Attn: Dr. J. R. Ruetenik
Avidyne Division
83 Second Avenue
Burlington, MA 01803

DISTRIBUTION (Cont.)

Rockwell International
B-1 Division
Technical Information Center (BA08)
International Airport
Los Angeles, CA 90009

Rockwell International Corporation
Technical Information Center
4300 E. Fifth Avenue
Columbus, OH 43216

M.I.T. Lincoln Laboratory
Attn: Library A-082
P.O. Box 73
Lexington, MA 02173

The RAND Corporation
Attn: Library - D
Dr. William S. King
1700 Main Street
Santa Monica, CA 90406

Aerojet Electrosystems Co.
Attn: Engineering Library
1100 W. Hollyvale Avenue
Azusa, CA 91702

The Boeing Company
Attn: 87-67
P.O. Box 3999
Seattle, WA 98124

United Aircraft
Research Laboratories
Attn: Dr. William M. Foley
East Hartford, CT 06108

United Aircraft Corporation
Attn: Library
400 Main Street
East Hartford, CT 06108

Hughes Aircraft Company
Attn: Company Tech. Doc. Center
6/E11, B. W. Campbell
Centinela at Teale
Culver City, CA 90230

DISTRIBUTION (Cont.)

Lockheed Missiles and Space Company, Inc.
Attn: Mr. G. M. Laden, Dept. 81-25,
Bldg. 154
Mr. Murl Culp
P.O. Box 504
Sunnyvale, CA 94086

Lockheed Missiles and Space Company
Attn: Technical Information Center
3251 Hanover Street
Palo Alto, CA 94304

Lockheed-California Company
Attn: Central Library, Dept. 84-40,
Bldg. 170
PLT. B-1
Burbank, CA 91503

Vice President and Chief Scientist
Dept. 03-10
Lockheed Aircraft Corporation
P.O. Box 551
Burbank, CA 91503

Martin Marietta Corporation
Martin Marietta Labs
Attn: Science-Technology Library
1450 S. Rolling Road
Baltimore, MD 21227

Martin Marietta Corporation
Orlando Division
P.O. Box 5837
Orlando, FL 32855

General Dynamics
Attn: Research Library 2246
George Kaler, Mail Zone 2880
P.O. Box 748
Fort Worth, TX 76101

Calspan Corporation
Attn: Library
4455 Genesee Street
Buffalo, NY 14221

Air University Library
(SE) 63-578
Maxwell Air Force Base, AL 36112

DISTRIBUTION (Cont.)

McDonnell Company
Attn: R. D. Detrich, Dept. 209,
Bldg. 33
P.O. Box 516
St. Louis, MO 63166

McDonnell-Douglas Aircraft Corporation
Missile and Space Systems Division
Attn: A2-260 Library
Dr. J. S. Murphy, A-830
Mr. W. H. Branch, Director
300 Ocean Park Boulevard
Santa Monica, CA 90405

Fairchild Industries, Inc.
Fairchild Republic Co.
Attn: Engineering Library
Conklin Street
Farmingdale, NY 11735

General Applied Science Laboratories, Inc.
Attn: Dr. F. Lane
Merrick and Stewart Avenues
Westbury, Long Island, NY 11590

General Electric Company
Attn: Dr. H. T. Nagamatsu
Research and Development Lab. (Comb. Bldg.)
Schenectady, NY 12301

The Whitney Library
General Electric Research and Development Center
Attn: M. F. Orr, Manager
The Knolls, K-1
P.O. Box 8
Schenectady, NY 12301

General Electric Company
Missile and Space Division
Attn: MSD Library
Larry Chasen, Mgr.
Dr. J. D. Stewart, Mgr.
Research and Engineering
P.O. Box 8555
Philadelphia, PA 19101

General Electric Company
AEG Technical Information Center, N-32
Cincinnati, OH 45215

DISTRIBUTION (Cont.)

General Electric Company
Missile and Space Division
Attn: Dr. S. M. Scala
Dr. H. Lew
Mr. J. W. Faust
A. Martellucci
W. Daskin
J. D. Cresswell
J. B. Arnaiz
L. A. Marshall
J. Cassanto
R. Hobbs
C. Harris
F. George
P.O. Box 8555
Philadelphia, PA 19101

AVCO-Everett Research Laboratory
Attn: Library 2
Dr. George Sutton
2385 Revere Beach Parkway
Everett, MA 02149

Vought Corporation
P.O. Box 225907
Dallas, TX 75265

Northrop Corp.
Electronic Division
2301 W. 120th Street
Hawthorne, CA 90250

Government Documents
The Foundren Library
Rice Institute
P.O. Box 1892
Houston, TX 77001

Grumman Aerospace Corporation
Attn: Mr. R. A. Scheuing
Mr. H. B. Hopkins
Mr. H. R. Reed
South Oyster Bay Road
Bethpage, Long Island, NY 11714

The Marquardt Company
P.O. Box 2013
Van Nuys, CA 91409

DISTRIBUTION (Cont.)

ARDE Associates
Attn: Librarian
P.O. Box 286
580 Winters Avenue
Paramus, NJ 07652

Aerophysics Company
Attn: Mr. G. D. Boehler
3500 Connecticut Avenue, N.W.
Washington, DC 20003

Aeronautical Research Associates
of Princeton
Attn: Dr. C. duP. Donaldson
50 Washington Road
Princeton, NJ 08540

General Research Corporation
Attn: Technical Information Office
5383 Hollister Avenue
P.O. Box 3587
Santa Barbara, CA 93105

Sandia Laboratories
Attn: Mr. K. Goin, Div. 5642
Mrs. B. R. Allen, 3421
Mr. W. H. Curry, 5625
Mr. A. M. Torneby, 3141
Dr. C. Peterson
Box 5800
Albuquerque, NM 87115

Hercules Incorporated
Attn: Library
Allegany Ballistics Laboratory
P.O. Box 210
Cumberland, MD 21502

General Electric Company
Attn: Dave Hovis, Rm. 4109
P.O. Box 2500
Daytona Beach, FL 32015

TRW Defense & Space Systems Group
Attn: Technical Libr/Doc Acquisitions
Dr. A. B. Witte
One Space Park
Redondo Beach, CA 90278

DISTRIBUTION (Cont.)

Stanford Research Institute
Attn: Dr. G. Abrahamson
333 Ravenswood Avenue
Menlo Park, CA 94025

Hughes Aircraft Company
Attn: Technical Library, 600-C222
P.O. Box 3310
Fullerton, CA 92634

Westinghouse Electric Corporation
Astronuclear Laboratory
Attn: Library
P.O. Box 10864
Pittsburgh, PA 15236

University of Tennessee
Space Institute
Attn: Prof. J. M. Wu
Tullahoma, TN 37388

CONVAIR Division of General Dynamics
Library and Information Services
P.O. Box 12009
San Diego, CA 92112

CONVAIR Division of General Dynamics
Attn: Dr. J. Raat, Mail Zone 640-02
P.O. Box 80847
San Diego, CA 92138

AVCO Missiles Systems Division
Attn: E. E. H. Schurmann
J. Otis
201 Lowell Street
Wilmington, MA 01887

Chrysler Corporation
Space Division
Attn: G. T. Boyd, Dept. 2781
E. A. Rawk, Dept. 2920
P.O. Box 29200
New Orleans, LA 70129

General Dynamics
Pomona Division
Attn: Tech. Doc. Center, Mail Zone 6-20
P.O. Box 2507
Pomona, CA 91766

DISTRIBUTION (Cont.)

General Electric Company
Attn: W. Danskin
Larry Chasen
Dr. H. Lew
3198 Chesnut Street
Philadelphia, PA 19101

Ford Aerospace & Communication Corporation
Attn: Dr. A. Demetriades
Ford and Jamboree Roads
Newport Beach, CA 92663

Raytheon Company
Attn: D. P. Forsmo
Missile Systems Division
Hartwell Road
Bedford, MA 01730

TRW Systems Group
Attn: M. W. Sweeney, Jr.
Space Park Drive
Houston, TX 77058

Marine Bioscience Laboratory
Attn: Dr. A. C. Charters
513 Sydnor Street
Ridgecrest, CA 93555

University of Wyoming
Attn: Head, Dept. Mech. Eng.
University Station
P.O. Box 3295
Laramie, WY 82070

Applied Mechanics Review
Southwest Research Institute
8500 Culebra Road
San Antonio, TX 78228

American Institute of Aeronautics
and Astronautics
Attn: J. Newbauer
1290 Sixth Avenue
New York, NY 10019

DISTRIBUTION (Cont.)

Technical Information Service
American Institute of Aeronautics and
Astronautics
Attn: Miss P. Marshall
750 Third Avenue
New York, NY 10017

Faculty of Aeronautical Systems
University of West Florida
Attn: Dr. R. Fledderman
Pensacola, FL 32504

Saber Industries, Inc.
Attn: J. A. Finkel
Library
P.O. Box 60
North Troy, VT 05859

Pratt and Whitney Aircraft
Attn: W. G. Alwang, EB-1M5
East Hartford, CT 06108

Science Applications, Inc.
Attn: Dr. J. D. Trolinger
P.O. Box 861
Tullahoma, TN 37388

The Aerospace Corporation
Attn: J. M. Lyons, Bldg. 82
P.O. Box 92957
Los Angeles, CA 90009

NDW-NSWC(W)-5605/1 (Rev. 5-78)

TO AID IN UPDATING THE DISTRIBUTION LIST FOR NAVAL SURFACE WEAPONS CENTER, WHITE OAK TECHNICAL REPORTS PLEASE COMPLETE THE FORM BELOW:

TO ALL HOLDERS OF NSWC/WOL/TR 79-289
by T. F. Zien and R. T. Driftmyer
DO NOT RETURN THIS FORM IF ALL INFORMATION IS CURRENT

A. FACILITY NAME AND ADDRESS *(OLD) (Show Zip Code)*

NEW ADDRESS *(Show Zip Code)*

B. ATTENTION LINE ADDRESSES:

C.

☐ REMOVE THIS FACILITY FROM THE DISTRIBUTION LIST FOR TECHNICAL REPORTS ON THIS SUBJECT.

D.

NUMBER OF COPIES DESIRED ______________________

GPO 930-764

DEPARTMENT OF THE NAVY
NAVAL SURFACE WEAPONS CENTER
WHITE OAK, SILVER SPRING, MD. 20910

OFFICIAL BUSINESS
PENALTY FOR PRIVATE USE, $300

POSTAGE AND FEES PAID
DEPARTMENT OF THE NAVY
DOD 316

U.S.MAIL

COMMANDER
NAVAL SURFACE WEAPONS CENTER
WHITE OAK, SILVER SPRING, MARYLAND 20910

ATTENTION: CODE R 44

DEPARTMENT OF THE NAVY
SURFACE WEAPONS CENTER